Supporting Information (SI)

Switching Dual Catalysis without Molecular Switch: Using A Multi-Component Information System for Reversible Reconfiguration of Catalytic Machinery

Abir Goswami,[a] Thomas Paululat,[b] and Michael Schmittel[a,*]

[a] *Organische Chemie I,* [b] *Organische Chemie II. Center of Micro- and Nanochemistry and Engineering, University of Siegen, Adolf–Reichwein–Str. 2, D-57068 Siegen, Germany.*

E-mail: schmittel@chemie.uni-siegen.de

Fax: (+49) 271-740-14357

Table of Contents

1. Synthesis

General Remarks

All solvents were dried by distillation prior to use while commercial reagents (**1**, **3**, **6**, **7**, **A2**, **B1**, **14**, hexacyclen) were used without any further purification. Bruker Avance (400 MHz) and Varian VNMR-S 600 (600 MHz) spectrometers were used to measure ^{1}H and ^{13}C NMR spectra using a deuterated solvent as the lock and residual protiated solvent as internal reference ($CDCl_3$: δ_H 7.26 ppm, δ_C 77.0 ppm; CD_2Cl_2: δ_H 5.32 ppm, δ_C 53.8 ppm, THF-d_8: δ_H 1.72 ppm, 3.58 ppm, δ_C 25.3 ppm, 67.2 ppm). The following abbreviations were used to define NMR peak pattern: s = singlet, d = doublet, t = triplet, dd = doublet of doublets, ddd = doublet of doublets of doublets, td = triplet of doublets, br = broad, m= multiplet. Coupling constant values are given in Hertz (Hz) and, wherever possible, assignment of protons is provided. The numbering of different carbons in different molecular skeletons does not necessarily follow IUPAC nomenclature rules; it was exclusively implemented for assigning NMR signals. All electrospray ionization (ESI-MS) spectra were recorded on a Thermo-Quest LCQ deca and theoretical isotopic distributions of the mass signals were calculated using IsoPro 3.0 software. Melting points of compounds were measured on a BÜCHI 510 instrument and are not corrected. Infrared spectra were recorded on a Varian 1000 FT-IR instrument. Elemental analysis was performed using the EA-3000 CHNS analyzer. UV-vis spectra were recorded on a Cary Win 50 (298 K) spectrometer. Binding constants were determined through UV-vis titrations in combination with a 1:1 binding formula of two ligands or with SPECFIT/32TM global analysis system by Spectrum Software Associates (Marlborough, MA). Column chromatography was performed either on silica gel (60-400 mesh) or neutral alumina (Fluka, 0.05-0.15 mm, Brockmann Activity 1). Merck silica gel (60 F254) or neutral alumina (150 F254) sheets were used for thin layer chromatography (TLC). All rotor preparations were performed directly in the NMR tube using CD_2Cl_2 as solvent. Compounds **2**,[1] **4**,[1] **A1**,[2] **B2**,[3] **8**,[4] **9**,[1] **12**,[1] **13**,[5] **S**[1] were synthesized according to literature known procedures.

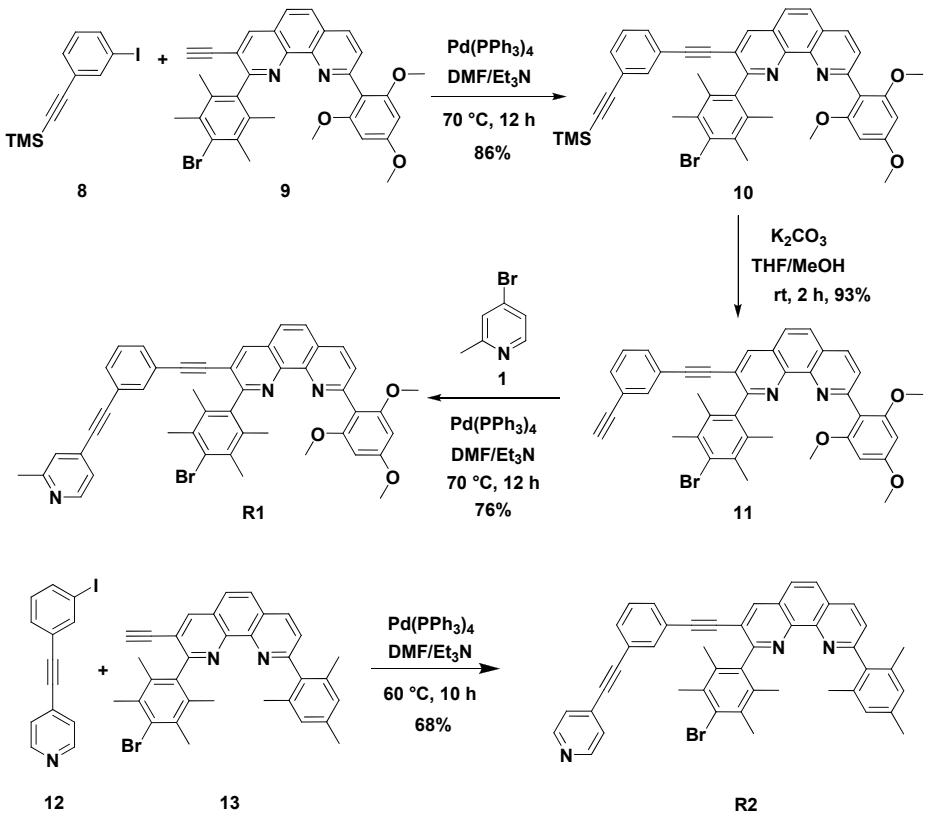

Scheme 1. Synthesis of rotators **R1** and **R2**.

2-(4-Bromo-2,3,5,6-tetramethylphenyl)-9-(2,4,6-trimethoxyphenyl)-3-((3-((trimethylsilyl)-ethynyl)phenyl)ethynyl)-1,10-phenanthroline (10)

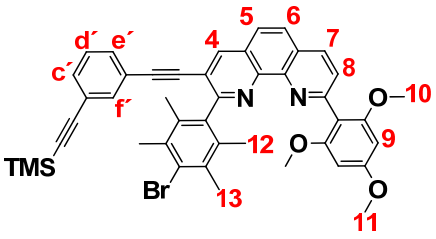

In an oven-dried 100 mL sealed tube, a mixture of ((3-iodophenyl)ethynyl)trimethylsilane (**8**) (207 mg, 0.690 mmol) and 2-(4-bromo-2,3,5,6-tetramethylphenyl)-3-ethynyl-9-(2,4,6-trimethoxyphenyl)-1,10-phenanthroline (**9**) (200 mg, 0.344 mmol) were dissolved in dry DMF (20 mL) and Et_3N (20 mL) and degassed thoroughly. Then $Pd(PPh_3)_4$ (20.0 mg, 17.3 µmol) was added and the mixture was refluxed at 70 °C for 12 h for completion of the coupling reaction. The reaction mixture was cooled down to room temperature and the solvents were removed. The residue was subjected to column chromatography (silica gel, ethyl acetate/hexane = 3:7, R_f = 0.3) to afford 223 mg of compound **10** as brown solid (0.30 mmol, 86%). **Melting point** = 186 °C. **IR (KBr):** $\tilde{\nu}$= 530, 612, 645, 665, 684, 722, 758, 794, 810, 845, 895, 924, 948, 989, 993, 1015, 1038, 1052, 1073,

1130, 1155, 1204, 1224, 1249, 1335, 1384, 1414, 1457, 1491, 1535, 1586, 1608, 2157, 2203, 2225, 2836, 2955 cm^{-1}. **^{1}H NMR (400 MHz, CD_2Cl_2):** δ = 0.27 (s, 9H, TMS-H), 2.00 (s, 6H, 13-H), 2.49 (s, 6H, 12-H), 3.69 (s, 6H, 10-H), 3.87 (s, 3H, 11-H), 6.26 (s, 2H, 9-H), 7.09 (ddd, ^3J = 7.8 Hz, ^4J = 1.6 Hz, ^4J = 1.2 Hz, 1H, e′/c′-H), 7.13 (t, ^3J = 1.2 Hz, 1H, f′-H), 7.24 (t, ^3J = 7.8 Hz, 1H, d′-H), 7.37 (ddd, ^3J = 7.8 Hz, ^4J = 1.6 Hz, ^4J = 1.2 Hz, 1H, c′/e′-H), 7.58 (d, ^3J = 8.0 Hz, 1H, 8-H), 7.86 (d, ^3J = 8.8 Hz, 1H, 5/6-H), 7.90 (d, ^3J = 8.8 Hz, 1H, 6/5-H), 8.27 (d, ^3J = 8.0 Hz, 1H, 7-H), 8.49 (s, 1H, 4-H) ppm. **^{13}C NMR (100 MHz, $CDCl_3$):** δ = 0.4, 19.0, 21.5, 56.2, 56.7, 88.0, 91.7, 95.1, 96.0, 104.4, 113,4, 120.2, 123.7, 123.4, 126.3, 127.5, 127.7, 128.1, 128.8, 129.3, 129.8, 131.9, 132.6, 134.2, 134.6, 135.6, 136.2, 139.3, 140.1, 145.9, 146.7, 156.6, 159.7, 162.4, 163.1 ppm. **ESI-MS:** *m/z* (%) 753.9 (100) [**10** + H]$^+$. **Elemental analysis:** Calculated for $C_{44}H_{41}BrN_2O_3Si$: C, 70.11; H, 5.48; N, 3.72. Found: C, 69.88; H, 5.39; N, 3.46.

2-(4-Bromo-2,3,5,6-tetramethylphenyl)-3-((3-ethynylphenyl)ethynyl)-9-(2,4,6-trimethoxyphenyl)-1,10-phenanthroline (11)

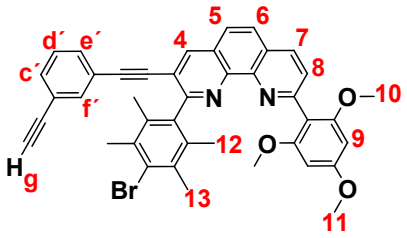

Compound **10** (200 mg, 0.265 mmol) was dissolved in THF (20 mL) and MeOH (20 mL). Thereafter, aqueous K_2CO_3 (149 mg, 1.08 mmol in 10 mL of deionized H_2O) was added and the mixture was allowed to stir at rt for 2 h. The solvent was evaporated and the product was extracted in DCM (25 mL). After washing the organic layer with deionized water (50 mL), the organic layer was removed and dried over anhydrous $MgSO_4$. The evaporation of solvent afforded compound **11** as colorless solid (168 mg, 0.246 mmol, 93%). **Melting point** = 211 °C. **IR (KBr):** $\tilde{\nu}$ = 533, 568, 614, 641, 665, 689, 722, 769, 734, 805, 818, 843, 892, 906, 947, 988, 1015, 1039, 1052, 1072, 1129, 1158, 1184, 1204, 1225, 1277, 1334, 1384, 1413, 1435, 1464, 1492, 1537, 1586, 1608, 2099, 2213, 2838, 2932, 2991, 3162 cm^{-1}. **^{1}H NMR (400 MHz, CD_2Cl_2):** δ = 2.01 (s, 6H, 13-H), 2.49 (s, 6H, 12-H), 3.18 (s, 1H, g-H), 3.69 (s, 6H, 10-H), 3.87 (s, 3H, 11-H), 6.26 (s, 2H, 9-H), 7.10 (ddd, ^3J = 7.8 Hz, ^4J = 1.6 Hz, ^4J = 1.2 Hz, 1H, e′/c′-H), 7.21 (t, ^4J = 1.2 Hz, 1H, f′-H), 7.26 (t, ^3J = 7.8 Hz, 1H, d′-H), 7.42 (ddd, ^3J = 7.8 Hz, ^4J = 1.6 Hz, ^4J = 1.2 Hz, 1H, c′/e′-H), 7.59 (d, ^3J = 8.0 Hz, 1H, 8-H), 7.86 (d, ^3J = 8.8 Hz, 1H, 5/6-H), 7.91 (d, ^3J = 8.8 Hz, 1H, 6/5-H), 8.27 (d, ^3J = 8.0 Hz, 1H, 7-H), 8.50 (s, 1H, 4-H) ppm. **^{13}C NMR (100 MHz, $CDCl_3$):** δ = 18.6, 21.1, 55.9, 56.3, 78.3, 82.8, 87.7, 91.3, 94.5, 119.7, 122.9, 123.5, 126.0, 127.2, 127.3, 127.7, 128.4, 129.0, 129.4, 132.0, 132.5,

133.8, 134.3, 135.4, 135.8, 139.0, 139.7, 145.2, 145.6, 146.4, 156.2, 159.3, 162.1, 162.7 ppm. **ESI-MS:** *m/z* (%) 681.7 (100) [**11** + H]$^+$. **Elemental analysis:** Calcd. for $C_{41}H_{33}BrN_2O_3 \bullet H_2O$: C, 70.39; H, 5.04; N, 4.0. Found: C, 70.39; H, 4.69; N, 3.93.

2-(4-Bromo-2,3,5,6-tetramethylphenyl)-3-((3-((2-methylpyridin-4-yl)ethynyl)phenyl)ethynyl)-9-(2,4,6-trimethoxyphenyl)-1,10-phenanthroline (R1)

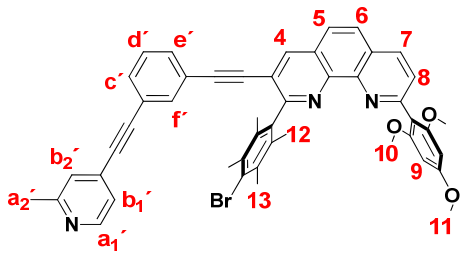

In an oven-dried 100 mL tube, compounds **11** (70.0 mg, 103 µmol) and **1** (145 mg, 843 µmol) were dissolved in dry DMF (20 mL) and Et_3N (20 mL) and degassed thoroughly. Then $Pd(PPh_3)_4$ (20.0 mg, 17.3 µmol) was added and the mixture was refluxed at 70 °C for 12 h. The reaction mixture was cooled down to rt and the solvents were removed. The residue was subjected to column chromatography (silica gel, ethyl acetate/CH_2Cl_2 = 3:7, R_f = 0.2) to afford 60 mg of compound **R1** as colorless solid (77.6 µmol, 76%). **Melting point** = 184 °C. **IR (KBr):** $\tilde{\nu}$ = 528, 566, 579, 684, 753, 791, 857, 893, 1087, 1128, 1157, 1205, 1226, 1335, 1384, 1414, 1458, 1466, 1602, 2025, 2219, 2841, 2932, 3007 cm^{-1}. **^{1}H NMR (400 MHz, CD_2Cl_2):** δ = 2.02 (s, 6H, 13-H), 2.50 (s, 6H, 12-H), 2.57 (s, 3H, a_2´-H), 3.71 (s, 6H, 10-H), 3.87 (s, 3H, 11-H), 6.26 (s, 2H, 9-H), 7.17 (ddd, ^3J = 7.8 Hz, ^4J = 1.6 Hz, ^4J = 1.2 Hz, 1H, e´/c´-H), 7.21 (t, ^4J = 1.2 Hz, 1H, f´-H), 7.27 (d, ^3J = 5.6 Hz, 1H, b_1´-H), 7.32 (t, ^3J = 7.8 Hz, 1H, d´-H), 7.34 (s, 1H, b_2´-H), 7.49 (ddd, ^3J = 7.8 Hz, ^4J = 1.6 Hz, ^4J = 1.2 Hz, 1H, c´/e´-H), 7.67 (d, ^3J = 8.0 Hz, 1H, 8-H), 7.89 (d, ^3J = 8.8 Hz, 1H, 5/6-H), 7.94 (d, ^3J = 8.8 Hz, 1H, 6/5-H), 8.34 (d, ^3J = 8.0 Hz, 1H, 7-H), 8.49 (d, ^3J = 5.6 Hz, 1H, a_1´-H), 8.52 (s, 1H, 4-H) ppm. **^{13}C NMR (100 MHz, $CDCl_3$):** δ = 18.6, 21.1, 24.2, 55.9, 56.4, 87.8, 87.8, 88.0, 91.4, 92.7, 94.7, 120.0, 123.1, 123.6, 125.6, 126.1, 127.2, 127.4, 127.7, 128.4, 129.2, 129.4, 131.9, 132.1, 132.3, 133.8, 134.3, 135.2, 136.4, 139.0, 139.6, 139.7, 144.9, 145.6, 149.0, 155.8, 158.9, 159.5, 162.3, 162.8 ppm. **ESI-MS:** *m/z* (%) 774.5 (100) [**R1** + H]$^+$. **Elemental analysis:** Calcd. for $C_{47}H_{38}BrN_3O_3 \bullet H_2O$: C, 71.39; H, 5.10; N, 5.31. Found: C, 71.05; H, 4.86; N, 5.31.

2-(4-Bromo-2,3,5,6-tetramethylphenyl)-9-mesityl-3-((3-(pyridin-4-ylethynyl)phenyl)ethynyl)-1,10-phenanthroline (R2)

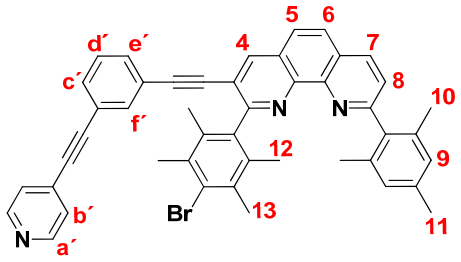

A mixture of 4-((3-iodophenyl)ethynyl)pyridine (**12**) (120 mg, 0.393 mmol), 2-(4-bromo-2,3,5,6-tetramethylphenyl)-3-ethynyl-9-mesityl-1,10-phenanthroline (**13**) (70.0 mg, 0.131 mmol) were taken in oven-dried 100 mL tube and dissolved in dry DMF (20 mL) and Et_3N (20 mL). The solution was degassed thoroughly and refluxed for 10 h at 60 °C and then evaporated to dryness. The crude product was purified by column chromatography (silica gel, CH_2Cl_2, $R_f = 0.3$) providing 63.0 mg of **R2** as colorless solid (88.6 µmol, 68%). **Melting point** = 197 °C; **IR (KBr):** $\tilde{\nu}$ = 533, 639, 685, 795, 818, 850, 895, 921, 988, 1144, 1166, 1213, 1384, 1458, 1475, 1536, 1595, 1938, 2212, 2918, 3052 cm^{-1}. **^{1}H NMR (400 MHz, CD_2Cl_2):** δ = 2.01 (s, 6H, 13-H), 2.04 (s, 6H, 10-H), 2.34 (s, 3H, 11-H), 2.50 (s, 6H, 12-H), 6.96 (s, 2H, 9-H), 7.17 (ddd, ^3J = 7.8 Hz, ^4J = 1.6 Hz, ^4J = 1.2 Hz, 1H, e´/c´-H), 7.22 (t, ^4J = 1.2 Hz, 1H, f´-H), 7.33 (t, ^3J = 7.8 Hz, 1H, d´-H), 7.44 (d, ^3J = 6.0 Hz, 2H, b´-H), 7.50 (ddd, ^3J = 7.8 Hz, ^4J = 1.6 Hz, ^4J = 1.2 Hz, 1H, c´/e´-H), 7.58 (d, ^3J = 8.0 Hz, 1H, 8-H), 7.89 (d, ^3J = 8.8 Hz, 1H, 5/6-H), 7.94 (d, ^3J = 8.8 Hz, 1H, 6/5-H), 8.34 (d, ^3J = 8.0 Hz, 1H, 7-H), 8.52 (s, 1H, 4-H), 8.62 (d, ^3J = 6.0 Hz, 2H, a´-H) ppm. **^{13}C NMR (100 MHz, $CDCl_3$):** δ = 18.6, 21.5, 21.2, 21.3, 87.7, 88.0, 92.8, 94.6, 119.8, 123.0, 123.6, 125.3, 125.9, 126.0, 127.3, 127.6, 128.1, 128.7, 129.2, 129.4, 131.3, 132.1, 132.2, 133.9, 134.2, 135.2, 136.1, 136.5, 138.0, 138.4, 138.8, 139.7, 145.5, 146.4, 150.3, 161.0, 162.8 ppm. **ESI-MS:** *m/z* (%) 712.5 (100) [**R2** + H]$^+$. **Elemental analysis:** Calcd. for $C_{46}H_{36}BrN_3$: C, 77.74; H, 5.11; N, 5.91. Found: C, 77.52; H, 4.74; N, 5.83.

Characterization of Stator (S) [1]**:**

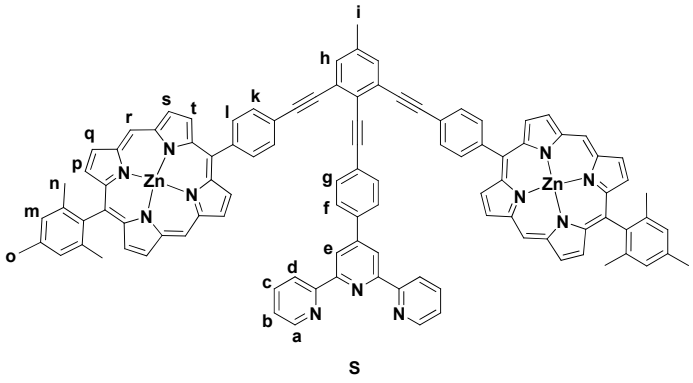

S

Melting point: > 250 °C. **IR (KBr):** $\tilde{\nu}$ = 564, 608, 634, 702, 720, 734, 785, 813, 833, 858, 906, 995, 1059, 1142, 1212, 1287, 1315, 1391, 1439, 1496, 1521, 1608, 2227, 2915 cm^{-1}. **^{1}H NMR (400 MHz, CD_2Cl_2):** δ = 1.82 (s, 12H, n-H), 2.62 (s, 3H, i-H), 2.70 (s, 6H, o-H), 7.11 (ddd, ^3J = 8.0 Hz, ^3J = 5.0 Hz, ^4J = 1.2 Hz, 2H, b-H), 7.38 (s, 4H, m-H), 7.70 (td, ^3J = 8.0 Hz, ^4J = 1.2 Hz, 2H, c-H), 7.73 (s, 2H, h-H), 8.11 (d, ^3J = 8.4 Hz, 2H, g/f-H), 8.15 (d, ^3J = 8.4 Hz, 2H, f/g-H), 8.19 (d, ^3J = 8.0 Hz, 4H, k-H), 8.33 (ddd, ^3J = 5.0 Hz, ^4J = 1.2 Hz, ^5J = 0.8 Hz, 2H, a-H), 8.38 (d, ^3J = 8.0 Hz, 4H, l-H), 8.47 (ddd, ^3J = 8.0 Hz, ^4J = 1.2 Hz, ^5J = 0.8 Hz, 2H, d-H), 8.75 (s, 2H, e-H), 8.95 (d, ^3J = 4.4 Hz, 4H, p-H), 9.23 (d, ^3J = 4.4 Hz, 4H, t-H), 9.43 (d, ^3J = 4.4 Hz, 4H, q-H), 9.51 (d, ^3J = 4.4 Hz, 4H, s-H), 10.28 (s, 4H, r-H). **^{13}C NMR (100 MHz, d_8-THF:CD_2Cl_2 = 8:2):** δ = 20.6, 21.0, 21.5, 89.2, 89.5, 94.3, 97.3, 105.6, 117.7, 118.4, 118.6, 120.9, 122.5, 124.0, 125.0, 125.6, 126.8, 127.7, 127.9, 130.1, 130.7, 131.7, 131.9, 132.1, 132.7, 132.7, 135.3, 136.7, 137.5, 138.9, 139.0, 139.3, 139.8, 144.5, 149.2, 149.3, 149.8, 149.8, 149.9, 149.9, 156.1, 156.4 ppm. **ESI-MS:** *m/z* (%) 1604.7 (100) $[S + H]^+$. **Elemental analysis:** Calcd. for $C_{104}H_{69}N_{11}Zn_2 \bullet H_2O$: C, 77.03; H, 4.41; N, 9.50.Found: C, 77.04; H, 4.15; N, 9.40.

2. Synthesis and characterization of complexes

a) Model Complex **C1** = [**3**→**4**]

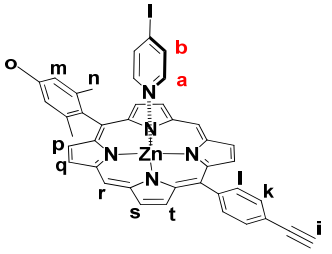

In an NMR tube, zinc porphyrin **4** (0.456 mg, 0.770 µmol) and 4-iodopyridine (**3**) (0.158 mg, 0.771 µmol) were dissolved in 500 µL of CD_2Cl_2 and NMR spectra were recorded. Yield: quantitative.

Melting point: > 200 °C; **IR (KBr):** $\tilde{\nu}$ = 558, 614, 697, 721, 787, 809, 838, 886, 909, 995, 1057, 1121, 1143,1158, 1182, 1209, 1228, 1288, 1313, 1374, 1395, 1437, 1522, 1559, 1612, 2137, 2915, 3051, 3079 cm^{-1}. **^{1}H NMR (400 MHz, CD_2Cl_2):** δ = 1.77 (s, 6H, n-H), 2.66 (s, 3H, o-H), 3.02 (brs, 2H, a-H), 3.40 (s, 1H, i-H), 6.12 (d, ^3J = 5.6 Hz, 2H, b-H), 7.33 (s, 2H, m-H), 7.93 (d, ^3J = 8.0 Hz, 2H, k-H), 8.25 (d, ^3J = 8.0 Hz, 2H, l-H), 8.88 (d, ^3J = 4.5 Hz, 2H, p-H), 9.06 (d, ^3J = 4.5 Hz, 2H, t-H), 9.36 (d, ^3J = 4.5 Hz, 2H, q-H), 9.41 (d, ^3J = 4.5 Hz, 2H, s-H), 10.21 (s, 2H, r-H) ppm.

b) Model complex **C2** = $[Cu(\mathbf{1})(\mathbf{2})]^+$

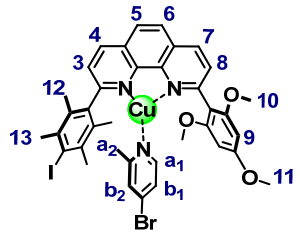

C2 = [Cu(1)(2)]$^+$

In an NMR tube, $[Cu(CH_3CN)_4]PF_6$ (0.868 mg, 2.33 µmol), ligands **2** (1.41 mg, 2.33 µmol) and 4-bromo-2-methylpyridine (**1**) (0.401 mg, 2.33 µmol) were dissolved in 500 µL of CD_2Cl_2. Yield by NMR: quantitative. **^{1}H NMR (CD_2Cl_2, 400 MHz):** δ 1.95 (s, 6H, 13-H), 2.07 (s, 3H, a_2-H), 2.37 (s, 6H, 12-H), 3.61 (s, 6H, 10-H), 3.75 (s, 3H, 11-H), 6.01 (s, 2H, 9-H), 7.22 (dd, ^3J = 6.0 Hz, ^4J = 2.0 Hz, 1H, b_1-H), 7.35 (d, ^4J = 2.0 Hz, 1H, b_2-H), 7.55 (d, ^3J = 6.0 Hz, 1H, a_1-H), 7.87 (d, ^3J = 8.4 Hz, 1H, 8-H), 7.96 (d, ^3J = 8.4 Hz, 1H, 3-H), 8.13 (s, 2H, 5 + 6-H), 8.59 (d, ^3J = 8.4 Hz, 1H, 7-H), 8.68 (d, ^3J = 8.4 Hz, 1H, 4-H) ppm. **ESI-MS**: *m/z* (%) = 839.7 (100) $[Cu(\mathbf{1})(\mathbf{2})]^+$].

c) Model complex **C3** = [**1**→**4**]

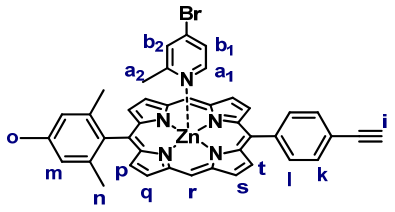

C3 = [(2)(4)]

In an NMR tube, zinc porphyrin **4** (0.456 mg, 0.770 µmol) and **1** (0.133 mg, 0.771 µmol) were dissolved in 500 µL of CD_2Cl_2 and NMR spectra were recorded. Yield: quantitative. **^{1}H NMR (400 MHz, CD_2Cl_2):** δ = 1.81 (s, 6H, n-H), 1.93 (s, 3H, a_2-H)*, 2.66 (s, 3H, m2-H), 3.40 (s, 1H, i-H), 7.04 (dd, ^3J = 4.0 Hz, ^4J = 1.2 Hz, 1H, b_1-H), 7.04 (d, ^4J = 1.2 Hz, 1H, b_2-H), 7.34 (s, 2H, m-H), 7.39 (d, ^3J = 4.0 Hz, 1H, a_1-H), 7.95 (d, ^3J = 8.0 Hz, 2H, k-H), 8.25 (d, ^3J = 8.0 Hz, 2H, l-H),

8.94 (d, ^3J = 4.5 Hz, 2H, p-H), 9.11 (d, ^3J = 4.5 Hz, 2H, t-H), 9.42 (d, ^3J = 4.5 Hz, 2H, q-H), 9.47 (d, ^3J = 4.5 Hz, 2H, s-H), 10.30 (s, 2H, r-H) ppm. * Shift depends on concentration.

d) Model complex **C4** = $[Cu(\mathbf{2})(\mathbf{3})]^+$

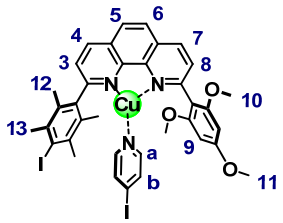

C4 = [Cu(2)(3)]$^+$

In an NMR tube, ligands **2** (1.41 mg, 2.33 µmol) and **3** (0.478 mg, 2.33 µmol) as well as $[Cu(CH_3CN)_4]PF_6$ (0.422 mg, 2.33 µmol) were dissolved in 500 µL of CD_2Cl_2. Yield by NMR: quantitative. **^{1}H NMR (CD_2Cl_2, 400 MHz):** δ 1.97 (s, 6H, 13-H), 2.47 (s, 6H, 12-H), 3.63 (s, 6H, 10-H), 3.83 (s, 3H, 11-H), 6.13 (s, 2H, 9-H), 7.11 (brs, 2H, b-H), 7.63 (brs, 2H, a-H), 7.86 (d, ^3J = 8.4 Hz, 1H, 8-H), 7.97 (d, ^3J = 8.4 Hz, 1H, 3-H), 8.12 (s, 2H, 5 + 6-H), 8.58 (d, ^3J = 8.4 Hz, 1H, 7-H), 8.68 (d, ^3J = 8.4 Hz, 1H, 4-H) ppm. **ESI-MS**: *m/z* (%) = 871.7 (100) $[[Cu(\mathbf{2})(\mathbf{3})]^+]$.

e) Model complex **C5** = $[Zn(\mathbf{2})(\mathbf{6})]^{2+}$

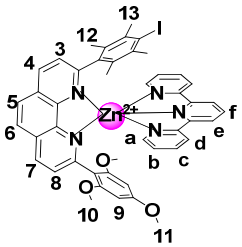

In an NMR tube, phenanthroline **2** (0.469 mg, 0.776 µmol), terpyridine (**6**) (0.181 mg, 0.776 µmol), and $Zn(OTf)_2$ (0.282 mg, 0.776 µmol) were dissolved in 500 µL of CD_2Cl_2:CD_3CN = 10:1. After heating the sample at 50 °C for 2 h, NMR spectra were recorded showing exclusive formation of the zinc HETTAP complex (> 95%). **IR (KBr):** $\tilde{\nu}$ = 580, 613, 637, 779, 1031, 1129, 1159, 1227, 1268, 1382, 1430, 1460, 1560, 1603, 2221, 2853, 2924 cm^{-1}. **^{1}H NMR (400 MHz, CD_2Cl_2:CD_3CN = 10:1):** δ = 0.86 (s, 6H, 13-H), 1.94 (s, 6H, 12-H), 2.91 (s, 6H, 10-H), 3.48 (s, 3H, 11-H), 5.58 (s, 2H, 9-H), 7.49 (ddd, ^3J = 7.6 Hz, ^3J = 5.6 Hz, ^4J = 1.6 Hz, 2H, b-H), 7.59 (ddd, ^3J = 5.6 Hz, ^4J = 1.6 Hz, ^5J = 0.8 Hz, 2H, a-H), 7.87 (d, ^3J = 8.4 Hz, 1H, 8-H), 8.08 (d, ^3J = 8.4 Hz, 1H, 3-H), 8.25 (td, ^3J = 7.6 Hz, ^4J = 1.6 Hz, 2H, c-H), 8.41 – 8.49 (m, 6H, d-, e-, 5- & 6-H), 8.59 (t, ^3J = 8.2 Hz, 1H, f-H), 8.97 (d, ^3J = 8.4 Hz, 1H, 7-H), 9.00 (d, ^3J = 8.4 Hz, 1H, 4-H) ppm. **ESI-MS:** *m/z* (%) 450.8 (20) [**C5**], 1049.8 (100) [**C5** + OTf^-]. **Elemental analysis:** Calculated for

$C_{48}H_{40}F_6IN_5O_9S_2Zn$•$0.7CH_2Cl_2$: C, 46.39; H, 3.31; N, 5.55; S, 5.09. Found: C, 46.74; H, 2.92; N, 5.64; S, 5.27.

f) Model complex **C6** = $[Cu(\mathbf{2})(\mathbf{6})]^+$

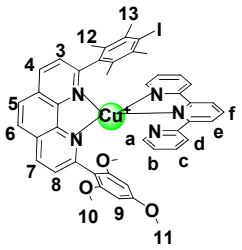

In an NMR tube, phenanthroline **2** (0.469 mg, 0.776 µmol), terpyridine **6** (0.181 mg, 0.776 µmol), and $[Cu(CH_3CN)_4)]PF_6$ (0.289 mg, 0.776 µmol) were dissolved in 500 of µL CD_2Cl_2. NMR spectra were recorded showing quantitative formation of the copper(I) HETTAP complex. **Melting point:** 150 °C. **IR (KBr):** $\tilde{\nu}$ = 558, 610, 651, 768, 843, 949, 992, 1031, 1067, 1128, 1158, 1184, 1206, 1228, 1338, 1384, 1429, 1456, 1486, 1585, 1608, 2931 cm^{-1}. **^{1}H NMR (400 MHz, CD_2Cl_2):** δ = 1.39 (s, 6H, 13-H), 1.93 (s, 6H, 12-H), 3.21 (s, 6H, 10-H), 3.56 (s, 3H, 11-H), 5.65 (s, 2H, 9-H), 7.08 (ddd, ^3J = 7.4 Hz, ^3J = 5.6 Hz, ^4J = 1.6 Hz, 2H, b-H), 7.32 (td, ^3J = 7.4 Hz, ^4J = 1.6 Hz, 2H, c-H), 7.62 (d, ^3J = 8.4 Hz, 1H, 8-H), 7.90 (d, ^3J = 8.4 Hz, 1H, 3-H), 8.01 (ddd, ^3J = 5.6 Hz, ^4J = 1.6 Hz, ^5J = 0.8 Hz, 2H, a-H), 8.04 – 8.18 (m, 7H, d-, e-, f-, 5- & 6-H), 8.49 (d, ^3J = 8.4 Hz, 1H, 7-H), 8.62 (d, ^3J = 8.4 Hz, 1H, 4-H) ppm. **^{13}C NMR (400 MHz, CD_2Cl_2):** δ = 19.5, 27.2, 55.4, 55.7, 90.0, 110.0, 112.4, 121.5, 122.9, 124.8, 126.7, 126.7, 127.2, 127.8, 128.5, 129.5, 131.9, 136.5, 136.7, 137.0, 137.3, 137.9, 140.6, 143.8, 143.9, 148.6, 152.7, 152.8, 155.2, 158.6, 158.9, 162.4. **ESI-MS:** *m/z* (%) 900.1 (100) [**C6**]. **Elemental analysis:** Calculated for $C_{46}H_{40}CuF_6IN_5O_3P$•$0.5CH_2Cl_2$: C, 51.30; H, 3.80; N, 6.43. Found: C, 51.29; H, 3.63; N, 6.35.

Synthesis of nanorotor C7= $[Zn(\mathbf{S})(\mathbf{R1})]^{2+}$

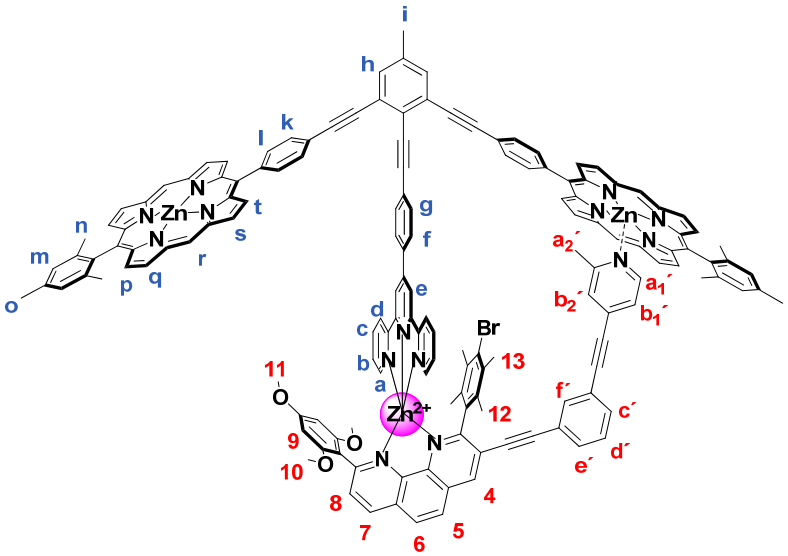

In an NMR tube, stator **S** (0.662 mg, 0.413 µmol) and rotator **R1** (0.319 mg, 0.413 µmol) were dissolved in 500 µL of CD_2Cl_2. After addition of $Zn(OTf)_2$ (0.150 mg, 0.413 µmol) as a standard solution in CD_3CN, NMR spectra were measured immediately. Yield: quantitative. **Melting point:** > 250 °C. **IR (KBr):** $\tilde{\nu}$ = 535, 571, 638, 712, 724, 737, 781, 817, 1026, 1031, 1056, 1227, 1262, 1340, 1397, 1465, 1451, 1510, 1517, 1613, 1653, 2013, 2208, 2854, 2937 cm^{-1}. **^{1}H NMR (600 MHz, CD_2Cl_2):** δ = −1.80 (s, 3H, a_2'-H), 0.70 (s, 6H, 13-H), 1.59 (s, 6H, 12-H), 1.68 (merged with H_2O, 1H, a_1'-H), 1.79 (s, 12H, n-H), 2.55 (s, 3H, i-H), 2.59 (s, 6H, o-H), 2.61 (s, 3H, 11-H), 2.64 (s, 6H, 10-H), 5.03 (s, 2H, 9-H), 5.22 (dd, ^3J = 5.6 Hz, ^4J = 1.2 Hz, 1H, b_1'-H), 5.31 (merged with $CDHCl_2$, 1H, b_2'-H), 6.00 (s, 1H, f'-H), 6.99 (ddd, ^3J = 7.8 Hz, ^4J = 1.4 Hz, ^4J = 1.2 Hz, 1H, e'/c'-H), 7.07 (t, ^3J = 7.8 Hz, 1H, d'-H), 7.22 (ddd, ^3J = 7.8 Hz, ^4J = 1.4 Hz, ^4J = 1.2 Hz, 1H, c'/e'-H), 7.32 (s, 4H, m-H), 7.38 (ddd, ^3J = 8.0 Hz, ^3J = 5.2 Hz, ^4J = 1.2 Hz, 2H, b-H), 7.50 (dd, ^3J = 5.2 Hz, ^4J = 1.2 Hz, 2H, a-H), 7.73 (s, 2H, h-H), 7.85 (d, ^3J = 8.4 Hz, 1H, 8-H), 8.11 (td, ^3J = 8.0 Hz, ^4J = 1.2 Hz, 2H, c-H), 8.13 (d, ^3J = 8.0 Hz, 4H, k-H), 8.13 (d, merged with k-H, 2H, f/g-H), 8.22 (br, 2H, g/f-H), 8.29 (d, ^3J = 8.8 Hz, 1H, 6/5-H), 8.34 (d, ^3J = 8.0 Hz, 4H, l-H), 8.37 (d, ^3J = 8.8 Hz, 1H, 5/6-H), 8.49 (dd, ^3J = 8.0 Hz, ^4J = 1.2 Hz, 2H, d-H), 8.50 (s, 2H, e-H), 8.84 (d, ^3J = 8.4 Hz, 1H, 7-H),8.86 (s, 1H, 4-H), 8.88 (d, ^3J = 4.4 Hz, 4H, p-H), 9.15 (d, ^3J = 4.4 Hz, 4H, t-H), 9.35 (d, ^3J = 4.4 Hz, 4H, q-H), 9.45 (d, ^3J = 4.4 Hz, 4H, s-H), 10.22 (s, 4H, r-H) ppm. **ESI-MS:** *m/z* (%) 1221.3 (100) $[[Zn(\mathbf{S})(\mathbf{R1})]^{2+}]$. **Elemental analysis:** Calculated for $C_{153}H_{107}BrF_6N_{14}O_9S_2Zn_3 \bullet CH_2Cl_2 \bullet H_2O$: C, 65.06; H, 3.94; N, 6.90; S, 2.26. Found: C, 65.01; H, 3.69; N, 6.57; S, 1.98.

Synthesis of nanorotor C8= $[Cu(\mathbf{S})(\mathbf{R1})]^+$

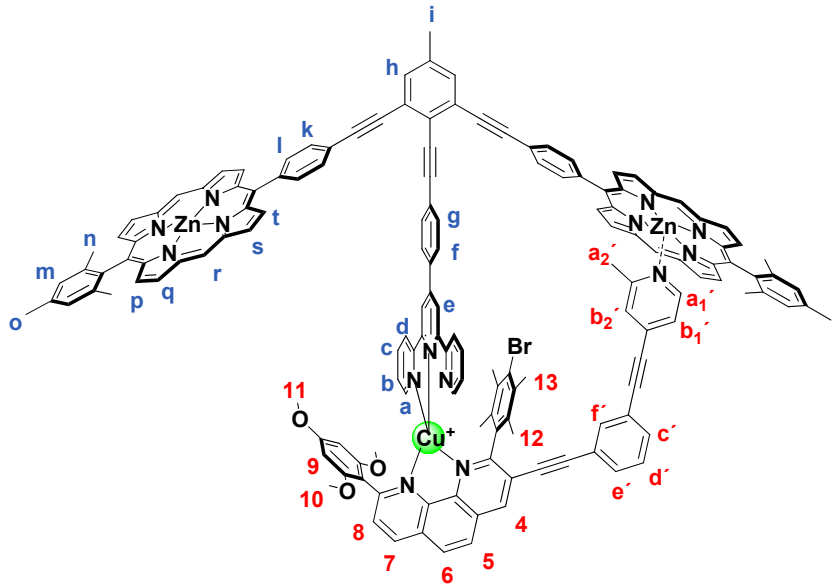

In an NMR tube, stator **S** (0.680 mg, 0.424 µmol), rotator **R1** (0.327 mg, 0.424 µmol) and $[Cu(CH_3CN)_4)]PF_6$ (0.159 mg, 0.424 µmol) were dissolved in 500 µL of CD_2Cl_2 and ^{1}H NMR spectra were measured immediately. NMR and ESI-MS spectra confirm the quantitative formation of nanorotor $[Cu(\mathbf{S})(\mathbf{R1})]^+$. **Melting point** > 250 °C. **IR (KBr):** $\tilde{\nu}$ = 558, 683, 702, 720, 734, 786, 812, 845, 994, 1057, 1129, 1158, 1206, 1227, 1283, 1339, 1393, 1455, 1519, 1548, 1605, 2212, 2852, 2922 cm^{-1}. **^{1}H NMR (600 MHz, CD_2Cl_2):** δ = −1.79 (s, 3H, a_2´-H), 1.08 (s, 6H, 13-H), 1.54 (s, 6H, 12-H), 1.69 (d, ^3J = 6.4 Hz, 1H, a_1´-H), 1.80 (s, 12H, n-H), 2.61 (s, 3H, i-H), 2.66 (s, 6H, o-H), 2.84 (s, 6H, 10-H), 2.90 (s, 3H, 11-H), 5.16 (s, 2H, 9-H), 5.27 (merged with $CDHCl_2$, 1H, b_1´-H), 5.41 (brs, 1H, b_2´-H), 6.04 (t, ^4J = 1.2 Hz, 1H, f´-H), 6.97 (ddd, ^3J = 7.8 Hz, ^4J = 1.4 Hz, ^4J = 1.2 Hz, 1H, e´/c´-H), 6.99 (ddd, ^3J = 7.8 Hz, ^3J = 4.8 Hz, ^4J = 1.2 Hz, 2H, b-H), 7.05 (t, ^3J = 7.8 Hz, 1H, d´-H), 7.17 (ddd, ^3J = 7.8 Hz, ^4J = 1.4 Hz, ^4J = 1.2 Hz, 1H, c´/e´-H), 7.26 (td, ^3J = 7.8 Hz, ^4J = 1.2 Hz, 2H, c-H), 7.34 (s, 4H, m-H), 7.71 (d, ^3J = 8.8 Hz, 1H, 8-H), 7.73 (s, 2H, h-H), 7.86 (dd, ^3J = 4.8 Hz, ^4J = 1.2 Hz, 2H, a-H), 7.96 (d, ^3J = 8.8 Hz, 1H, 5/6-H), 7.97 (d, ^3J = 8.0 Hz, 2H, g/f-H), 8.01 (dd, ^3J = 7.8 Hz, ^4J = 1.2 Hz, 2H, d-H), 8.10 (d, ^3J = 8.8 Hz, 1H, 6/5-H), 8.15 (d, ^3J = 8.0 Hz, 4H, k-H), 8.18 (d, ^3J = 8.0 Hz, 2H, f/g -H), 8.26 (s, 2H, e-H), 8.35 (d, ^3J = 8.0 Hz, 2H, l-H), 8.48 (s, 1H, 4-H), 8.50 (d, ^3J = 8.8 Hz, 1H, 7-H), 8.92 (d, ^3J = 4.4 Hz, 4H, p-H), 9.17 (d, ^3J = 4.4 Hz, 4H, t-H), 9.38 (d, ^3J = 4.4 Hz, 4H, q-H), 9.46 (d, ^3J = 4.4 Hz, 4H, s-H), 10.24 (s, 4H, r-H) ppm. **ESI-MS:** *m/z* (%) 2470.7 (100) $[Cu(\mathbf{S})(\mathbf{R1})(CH_3OH)]^+$. **Elemental analysis:** Calculated for $C_{151}H_{107}BrCuF_6N_{14}O_3PZn_2$•$3H_2O$: C, 68.73; H, 4.32; N, 7.43. Found: C, 68.80; H, 4.32; N, 7.11.

Synthesis of nanorotor C9= $[Zn(\mathbf{S})(\mathbf{R2})]^{2+}$

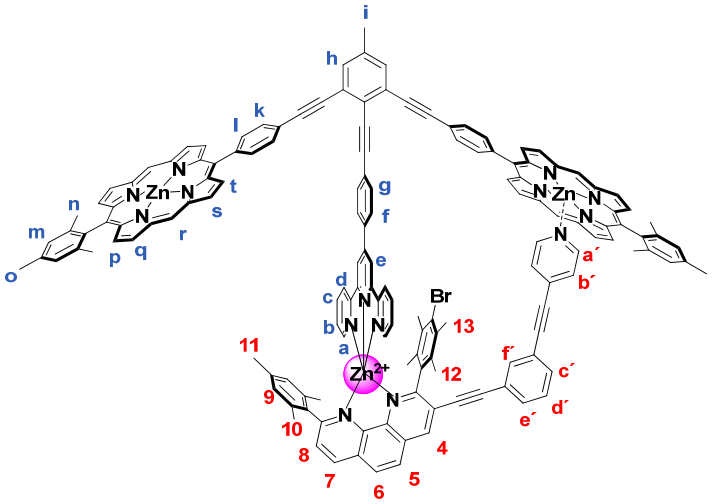

In an NMR tube, stator **S** (0.656 mg, 0.409 µmol) and rotator **R1** (0.291 mg, 0.409 µmol) were dissolved in 500 µL of CD_2Cl_2. After addition of $Zn(OTf)_2$ (0.149 mg, 0.409 µmol) as a standard solution in CD_3CN, NMR spectra were measured immediately. Yield: quantitative. **Melting point:** > 250 °C. **IR (KBr):** $\tilde{\nu}$ = 518, 573, 638, 703, 722, 734, 785, 812, 832, 852, 994, 1015, 1030, 1057, 1161, 1224, 1259, 1393, 1429, 1477, 1519, 1546, 1603, 2213, 2920 cm^{-1}. **^{1}H NMR (600 MHz, CD_2Cl_2):** δ = 0.80 (s, 6H, 13-H), 0.89 (s, 6H, 10-H), 1.07 (s, 3H, 11-H), 1.48 (s, 6H, 12-H), 1.78 (s, 12H, n-H), 2.19 (d, ^3J = 6.4 Hz, 2H, a´-H), 2.60 (s, 3H, i-H), 2.63 (s, 6H, o-H), 5.33 (d, ^3J = 6.4 Hz, 2H, b´-H), 5.63 (s, 2H, 9-H), 5.85 (s, 1H, f´-H), 6.96 (ddd, ^3J = 7.8 Hz, ^4J = 1.4 Hz, ^4J = 1.2 Hz, 1H, e´/c´-H), 7.06 (t, ^3J = 7.8 Hz, 1H, d´-H), 7.23 (ddd, ^3J = 7.8 Hz, ^4J = 1.4 Hz, ^4J = 1.2 Hz, 1H, c´/e´-H), 7.32 (s, 4H, m-H), 7.45 (ddd, ^3J = 7.8 Hz, ^3J = 5.2 Hz, ^4J = 1.2 Hz, 2H, b-H), 7.69 (dd, ^3J = 5.2 Hz, ^4J = 1.2 Hz, 2H, a-H), 7.73 (s, 2H, h-H), 7.86 (d, ^3J = 8.4 Hz, 1H, 8-H), 8.09 (d, ^3J = 8.0 Hz, 2H, g/f-H), 8.14 (d, ^3J = 8.0 Hz, 4H, k-H), 8.17 (td, ^3J = 7.8 Hz, ^4J = 1.2 Hz, 2H, c-H), 8.25 (d, ^3J = 8.0 Hz, 2H, f/g-H), 8.35 (d, ^3J = 8.8 Hz, 1H, 5/6-H), 8.37 (d, ^3J = 8.0 Hz, 4H, l-H), 8.39 (d, ^3J = 8.8 Hz, 1H, 6/5-H), 8.45 (s, 2H, e-H), 8.47 (d, ^3J = 7.8 Hz, ^4J = 1.2 Hz, ^5J = 0.8 Hz, 2H, d-H), 8.87 (d, ^3J = 4.4 Hz, 4H, p-H), 8.90 (s, 1H, 4-H), 8.94 (d, ^3J = 8.4 Hz, 1H, 7-H), 9.16 (d, ^3J = 4.4 Hz, 4H, t-H), 9.34 (d, ^3J = 4.4 Hz, 4H, q-H), 9.46 (d, ^3J = 4.4 Hz, 4H, s-H), 10.21 (s, 4H, r-H) ppm. **ESI-MS:** *m/z* (%) 1189.8 (100) $[[Zn(\mathbf{S})(\mathbf{R2})]^{2+}]$. **Elemental analysis:** Calculated for $C_{152}H_{105}BrF_6N_{14}O_6S_2Zn_3 \bullet CH_2Cl_2 \bullet H_2O$: C, 66.08; H, 3.95; N, 7.05; S, 2.31. Found: C, 65.83; H, 3.86; N, 6.74; S, 2.24.

Synthesis of nanorotor C10= $[Cu(\mathbf{S})(\mathbf{R2})]^+$

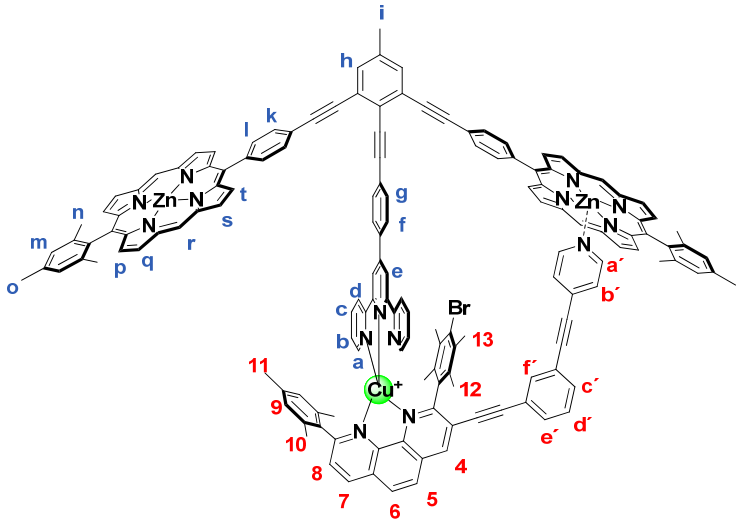

In an NMR tube, stator **S** (0.664 mg, 0.414 µmol), rotator **R2** (0.294 mg, 0.414 µmol) and $[Cu(CH_3CN)_4)]PF_6$ (0.154 mg, 0.414 µmol) were dissolved in 500 µL of CD_2Cl_2. NMR and ESI-MS spectra confirmed the quantitative formation of nanorotor $[Cu(\mathbf{S})(\mathbf{R2})]PF_6$. **Melting point** > 250 °C. **IR (KBr):** $\tilde{\nu}$ = 474, 523, 753, 662, 714, 726, 746, 787, 819, 834, 1022, 1039, 1159, 1236, 1346, 1384, 1436, 1538, 1605, 1687, 2216, 2931, 3012 cm^{-1}. **^{1}H NMR (600 MHz, CD_2Cl_2):** δ = 1.21 (s, 6H, 13-H), 1.29 (s, 6H, 10-H), 1.53 (s, 9H, 11+12-H), 1.81 (s, 12H, n-H), 2.19 (d, ^3J = 6.6 Hz, 2H, a´-H), 2.61 (s, 3H, i-H), 2.66 (s, 6H, o-H), 5.40 (d, ^3J = 6.6 Hz, 2H, b´-H), 5.97 (t, ^4J = 1.2 Hz, 1H, f´-H), 6.03 (s, 2H, 9-H), 6.94 (ddd, ^3J = 7.8 Hz, ^4J = 1.4 Hz, ^4J = 1.2 Hz, 1H, e´/c´-H), 6.96 (ddd, ^3J = 7.8 Hz, ^3J = 4.8 Hz, ^4J = 1.2 Hz, 2H, b-H), 7.03 (t, ^3J = 7.8 Hz, 1H, d´-H), 7.19 (ddd, ^3J = 7.8 Hz, ^4J = 1.4 Hz, ^4J = 1.2 Hz, 1H, c´/e´-H), 7.34 (s, 4H, m-H), 7.42 (td, ^3J = 7.8 Hz, ^4J = 1.2 Hz, 4H, c-H), 7.44 (ddd, ^3J = 4.8 Hz, ^4J = 1.2 Hz, ^5J = 0.8 Hz, 2H, a-H), 7.64 (d, ^3J = 8.8 Hz, 1H, 8-H), 7.74 (s, 2H, h-H), 7.78 (ddd, ^3J = 7.8 Hz, ^4J = 1.2 Hz, ^5J = 0.8 Hz, 2H, d-H), 7.97 (d, ^3J = 8.0 Hz, 2H, g/f-H), 8.07 (d, ^3J = 8.8 Hz, 1H, 5/6-H), 8.14 (s, 2H, e-H), 8.16 (d, ^3J = 8.0 Hz, 4H, k-H), 8.16 (d, ^3J = 8.0 Hz, 2H, f/g -H), 8.19 (d, ^3J = 8.8 Hz, 1H, 6/5-H), 8.39 (d, ^3J = 8.0 Hz, 4H, l-H), 8.54 (d, ^3J = 8.8 Hz, 1H, 7-H), 8.56 (s, 1H, 4-H), 8.92 (d, ^3J = 4.4 Hz, 4H, p-H), 9.19 (d, ^3J = 4.4 Hz, 4H, t-H), 9.37 (d, ^3J = 4.4 Hz, 4H, q-H), 9.47 (d, ^3J = 4.4 Hz, 4H, s-H), 10.24 (s, 4H, r-H) ppm. **ESI-MS:** *m/z* (%) 2409.8 (100) $[Cu(\mathbf{S})(\mathbf{R2})(CH_3OH)(H_2O)]^+$. **Elemental analysis:** Calculated for $C_{150}H_{105}BrCuF_6N_{14}PZn_2 \bullet CH_2Cl_2 \bullet H_2O$: C, 69.07; H, 4.18; N, 7.47. Found: C, 69.03; H, 3.81; N, 7.46.

C11= $[Cu_2(\mathbf{R2})_2]^{2+}$

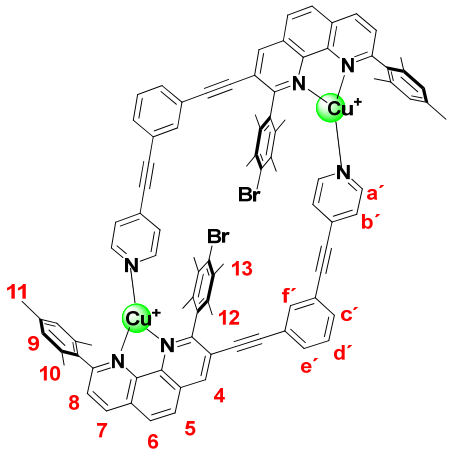

In an NMR tube, rotator **R2** (0.612 mg, 0.861 µmol) and $[Cu(CH_3CN)_4]PF_6$ (0.320 mg, 0.861 µmol) were dissolved in 500 µL of CD_2Cl_2. ^{1}H NMR and ESI-MS spectra confirm the quantitative formation of dimer $[Cu_2(\mathbf{R2})_2]^{2+}$. **Melting point:** 183 °C. **IR (KBr):** $\tilde{\nu}$ = 558, 684, 843, 948, 1016, 1084, 1128, 1158, 1206, 1227, 1336, 1384, 1417, 1463, 1491, 1610, 2215, 2925 cm^{-1}. **^{1}H NMR (400 MHz, CD_2Cl_2:CH_3CN = 4:1):** δ = 2.01 (s, 12H, 13-H), 2.07 (s, 12H, 12-H), 2.35 (s, 6H, 11-H), 2.51 (s, 12H, 10-H), 6.87 (brs, 4H, a´-H), 6.99 (s, 4H, 9-H), 7.05 (brs, 2H, f´-H), 7.21 (d, ^3J = 5.6 Hz, 4H, b´-H), 7.40 (t, ^3J = 7.8 Hz, 2H, d´-H), 7.45 (d, ^3J = 7.8 Hz, 2H, c´/e´-H), 7.56 (d, ^3J = 7.8 Hz, 2H, e´/c´-H), 7.98 (d, ^3J = 8.6 Hz, 2H, 8-H), 8.18 (d, ^3J = 8.8 Hz, 2H, 5/6-H), 8.22 (d, ^3J = 8.8 Hz, 2H, 6/5-H), 8.74 (d, ^3J = 8.6 Hz, 2H, 7-H), 8.84 (s, 2H, 4-H) ppm. **ESI-MS:** *m/z* (%) 774.5 (100) $[Cu_2(\mathbf{R2})_2]^{2+}$. **Elemental analysis:** Calculated for $C_{92}H_{72}Br_2Cu_2F_{12}N_6P_2$: C, 55.24; H, 3.90; N, 4.07. Found: C, 55.23; H, 3.59; N, 3.96.

C12= $[Cu_2(\mathbf{R1})_2]^{2+}$

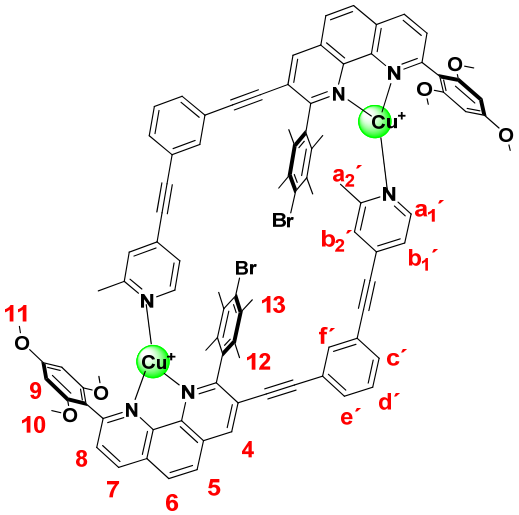

In an NMR tube, rotator **R1** (0.552 mg, 0.715 µmol) and $[Cu(CH_3CN)_4]PF_6$ (0.267 mg, 0.715 µmol) were dissolved in 500 µL of CD_2Cl_2. ^{1}H NMR and ESI-MS spectra confirm the quantitative formation of dimer $[Cu_2(\mathbf{R1})_2]^{2+}$. **Melting point:** 191 °C. **IR (KBr):** $\tilde{\nu}$ = 552, 617, 725, 817, 992, 1031, 1113, 1189, 1215, 1263, 1347, 1473, 1509, 1592, 1613, 2220, 2531, 2857, 2923 cm^{-1}. **^{1}H NMR (400 MHz, CD_2Cl_2):** δ = 1.97 (s, 12H, 13-H), 2.04 (s, 6H, a_2'-H), 2.33 (s, 12H, 12-H), 2.67 (s, 12H, 10-H), 2.77 (s, 6H, 11-H), 6.11 (s, 4H, 9-H), 7.11 (brs, 2H, a_1'-H), 7.14 (brs, 2H, f′-H), 7.20 (brs, 2H, b_2'-H), 7.45 (brs, 2H, b_1'-H), 7.46 (t, ^3J = 8.0 Hz, 2H, d′-H), 7.52 (brs, 2H, c′/e′-H), 7.65 (brs, 2H, e′/c′-H), 7.99 (d, ^3J = 8.6 Hz, 2H, 8-H), 8.14 (d, ^3J = 8.8 Hz, 2H, 5/6-H), 8.18 (d, ^3J = 8.8 Hz, 2H, 6/5-H), 8.63 (d, ^3J = 8.6 Hz, 2H, 7-H), 8.88 (s, 2H, 4-H) ppm. **ESI-MS:** *m*/*z* (%) 836.2 (100) $[Cu_2(\mathbf{R1})_2]^{2+}$. **Elemental analysis:** Calculated for $C_{94}H_{76}Br_2Cu_2F_{12}N_6O_6P_2 \bullet CH_2Cl_2 \bullet H_2O$: C, 55.24; H, 3.90; N, 4.07. Found: C, 55.23; H, 3.59; N, 3.96.

3. Model Study

In an NMR tube, 4-bromo-2-methylpyridine (**1**), 4-iodopyridine (**2**), phenanthroline **3**, zinc porphyrin **4**, and $[Cu(CH_3CN)_4]PF_6$ (1.13 μmol) were mixed in a ratio of 1:1:1:1:1. The mixture was dissolved in CD_2Cl_2. The subsequently measured ^1H NMR spectrum was compared with those of the individual complexes. Accordingly, the copper HETPYP complex $[Cu(\mathbf{1})(\mathbf{2})]^+$ and (**3**•**4**) were afforded selectively, as indicated by NMR.

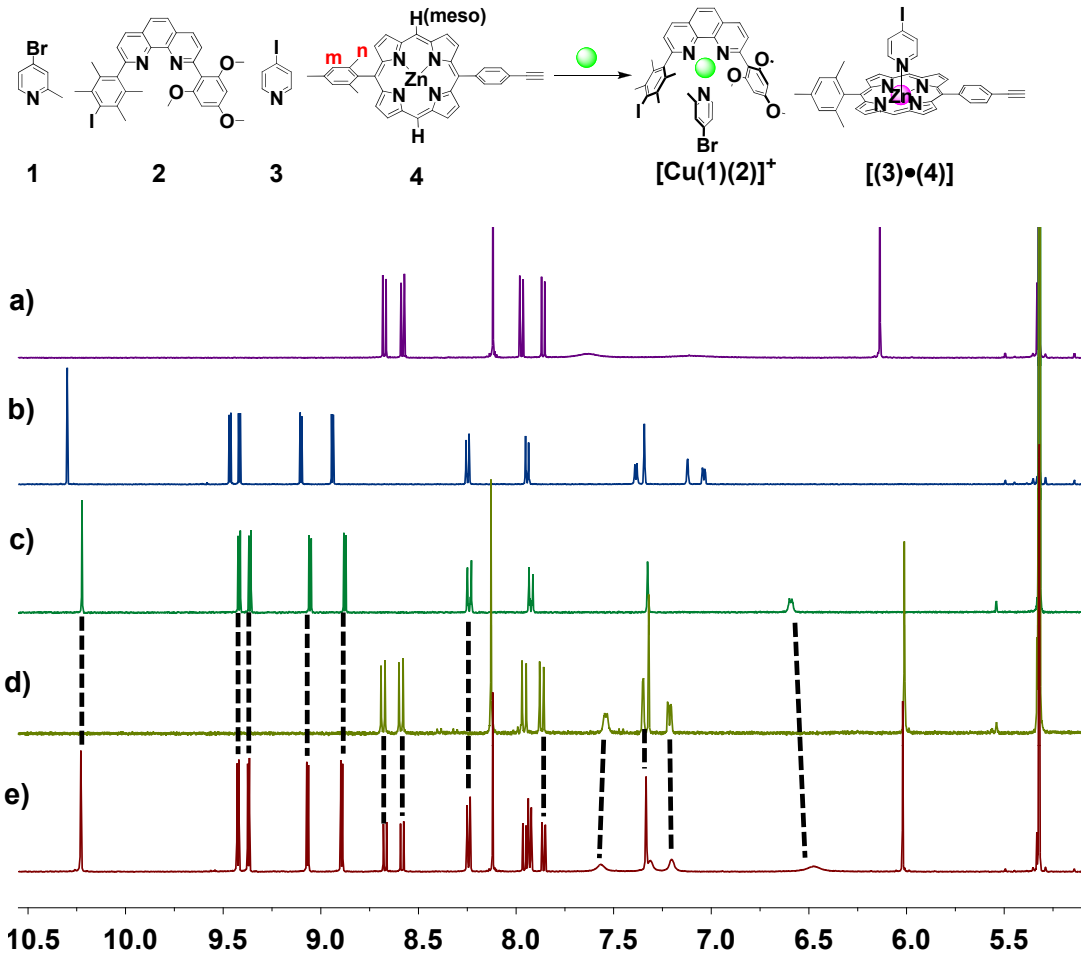

Figure S1. ^1H NMR (400 MHz, 298 K) of (a) $[Cu(\mathbf{2})(\mathbf{3})]^+$; (b) [(**1**)•(**4**)]; (c) [(**3**)•(**4**)]; (d) $[Cu(\mathbf{1})(\mathbf{2})]^+$; (e) after mixing of **1**, **2**, **3**, **4** and $[Cu(CH_3CN)_4]PF_6$ in a ratio of 1:1:1:1:1 in CD_2Cl_2 furnishing a mixture of $[Cu(\mathbf{1})(\mathbf{2})]^+$ and [(**3**)•(**4**)].

4. NMR Spectra

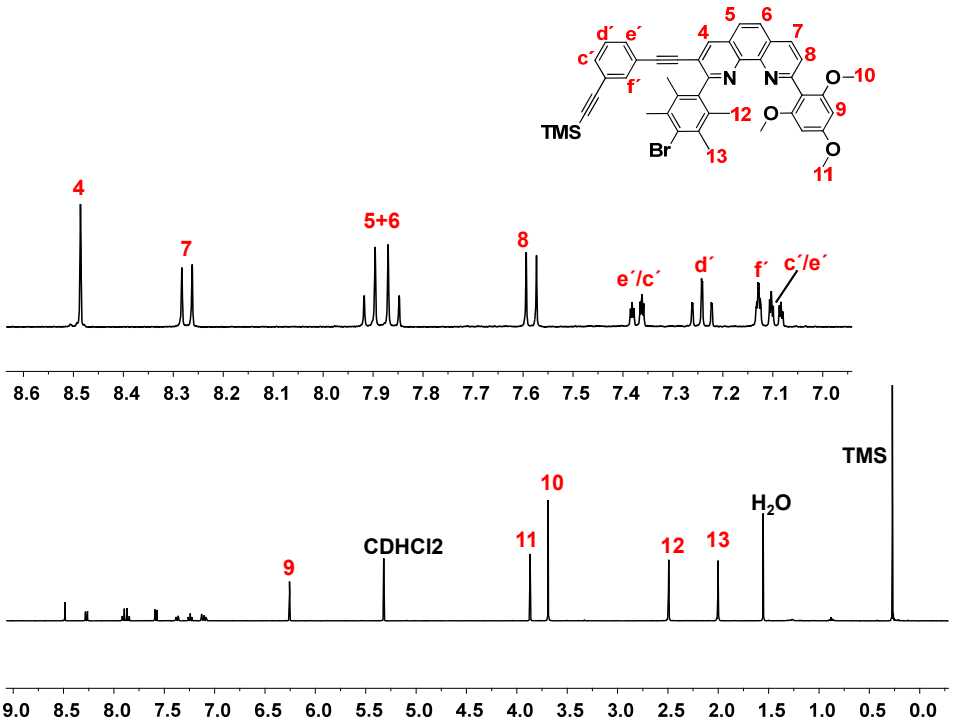

Figure S2. ^{1}H NMR spectrum of **10** in CD_2Cl_2 (400 MHz, 298 K).

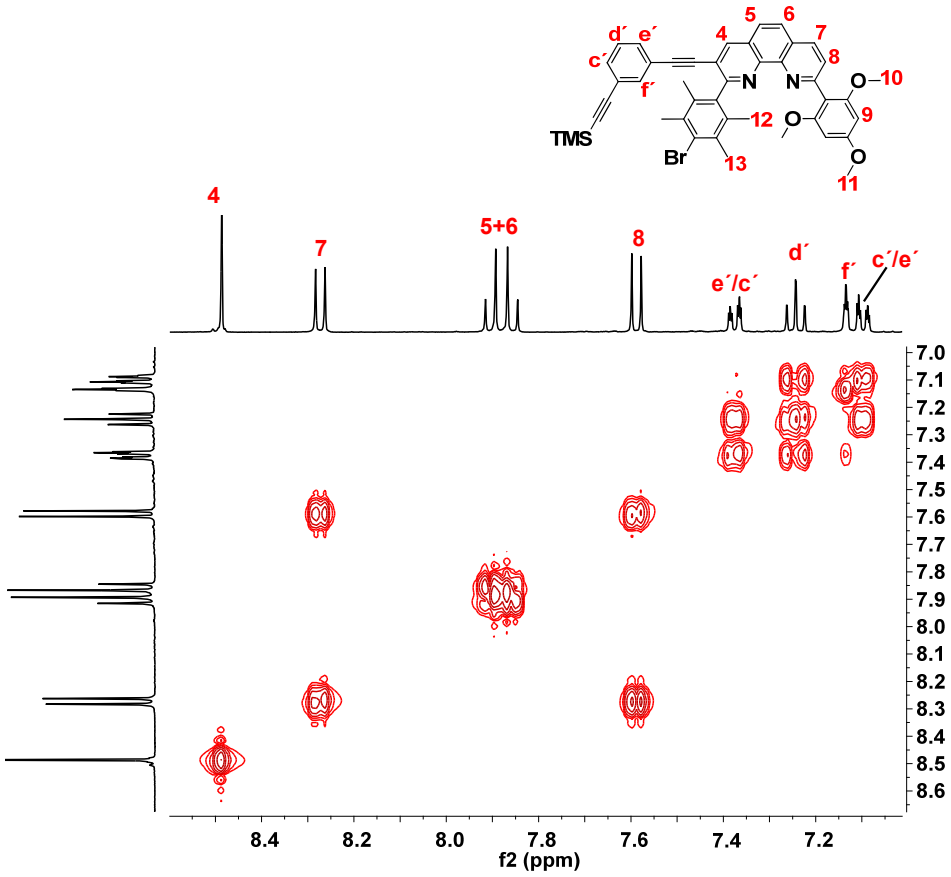

Figure S3. ^{1}H-^{1}H COSY spectrum of **10** in CD_2Cl_2 (400 MHz, 298 K).

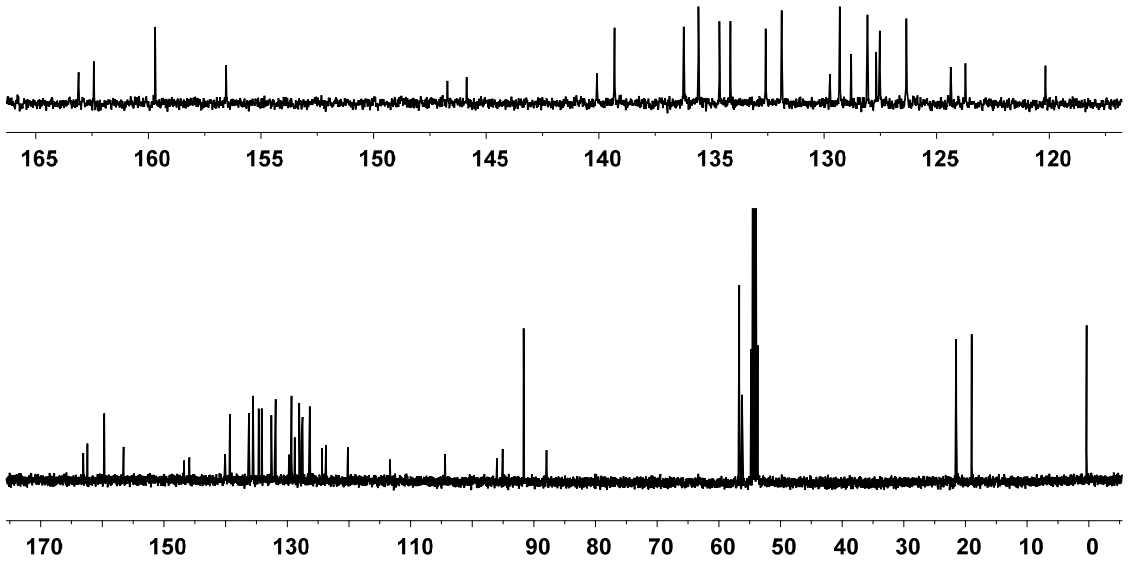

Figure S4. ^{13}C NMR spectrum of **10** in CD_2Cl_2 (100 MHz, 298 K).

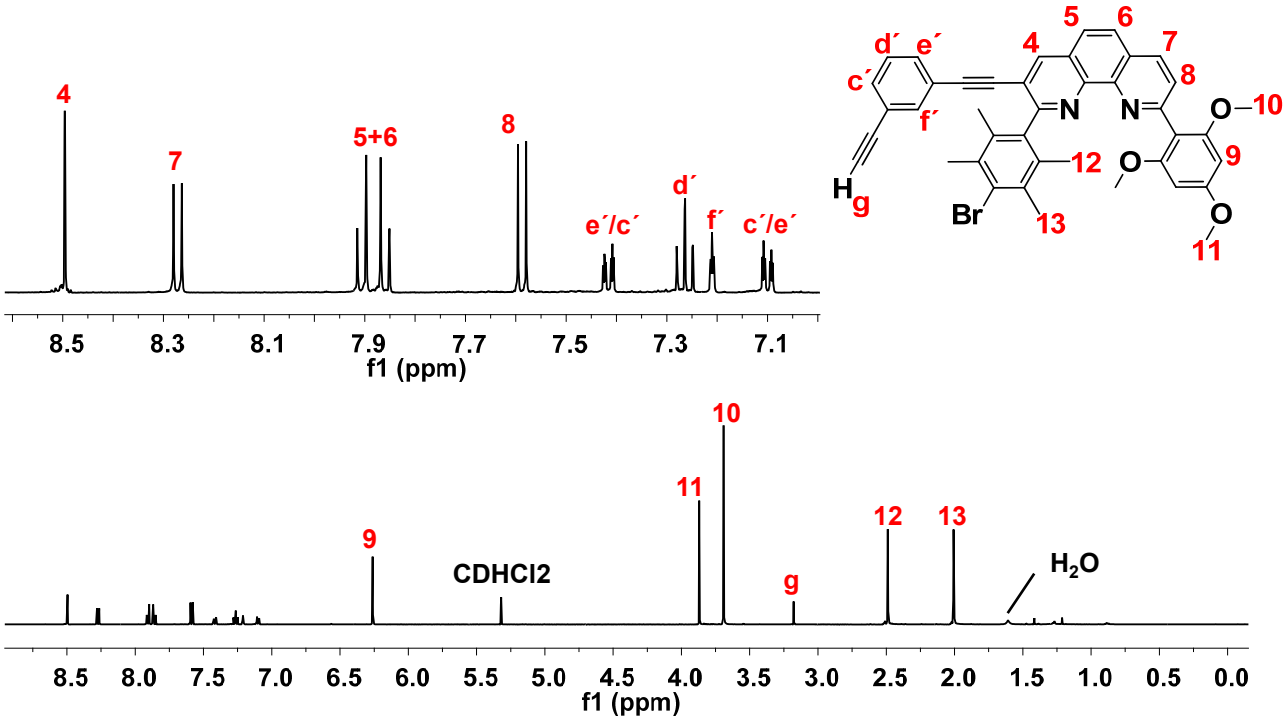

Figure S5. ^{1}H NMR spectrum of **11** in CD_2Cl_2 (400 MHz, 298 K).

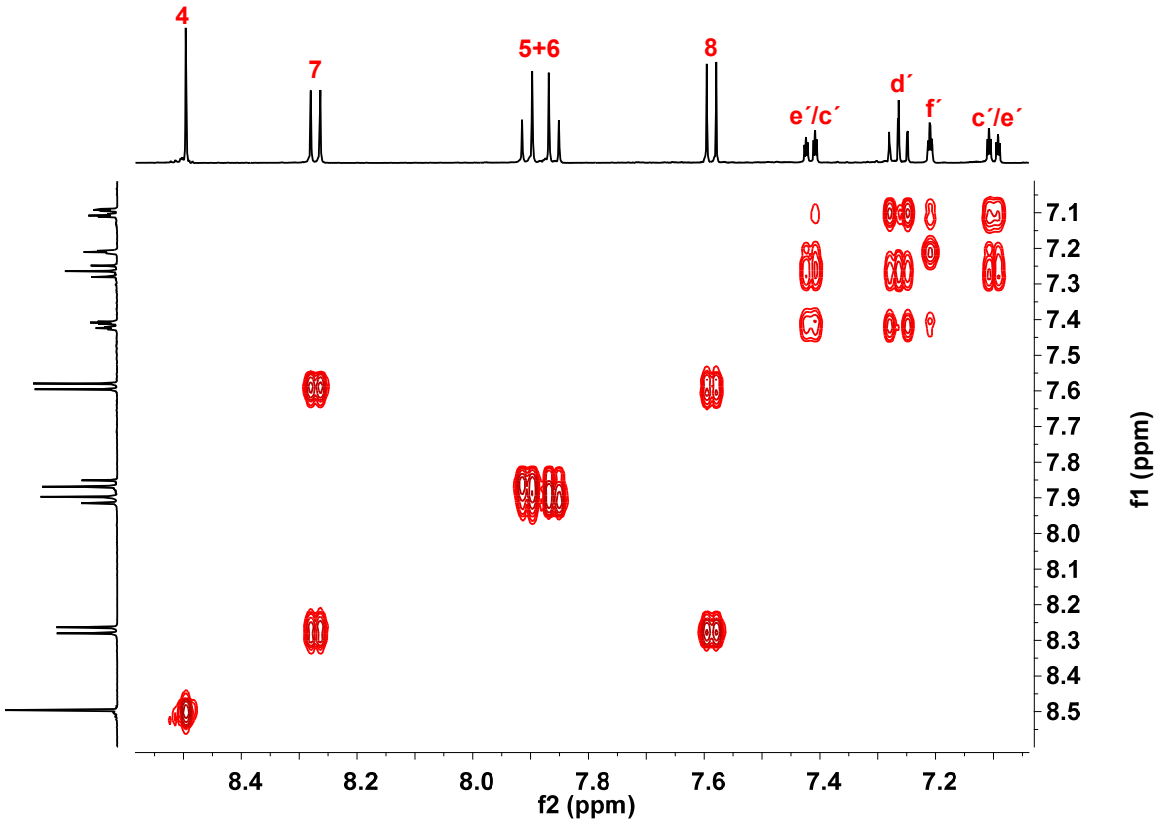

Figure S6. ^{1}H-^{1}H COSY spectrum of **11** in CD_2Cl_2 (400 MHz, 298 K).

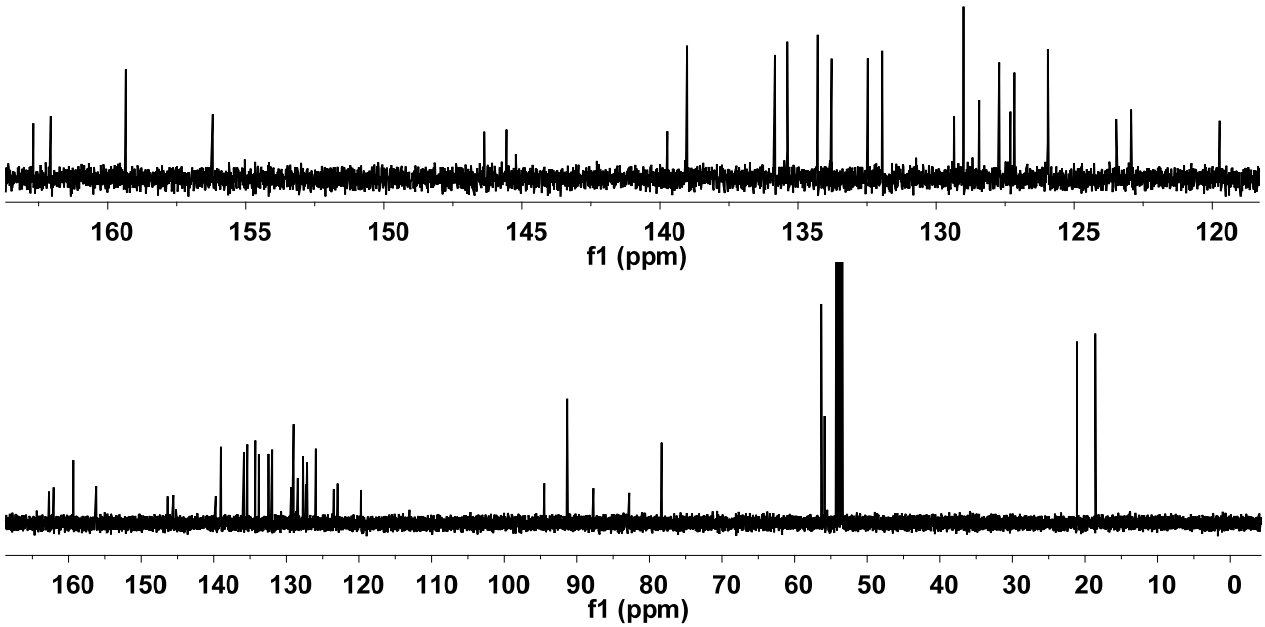

Figure S7. ^{13}C NMR spectrum of **11** in CD_2Cl_2 (100 MHz, 298 K).

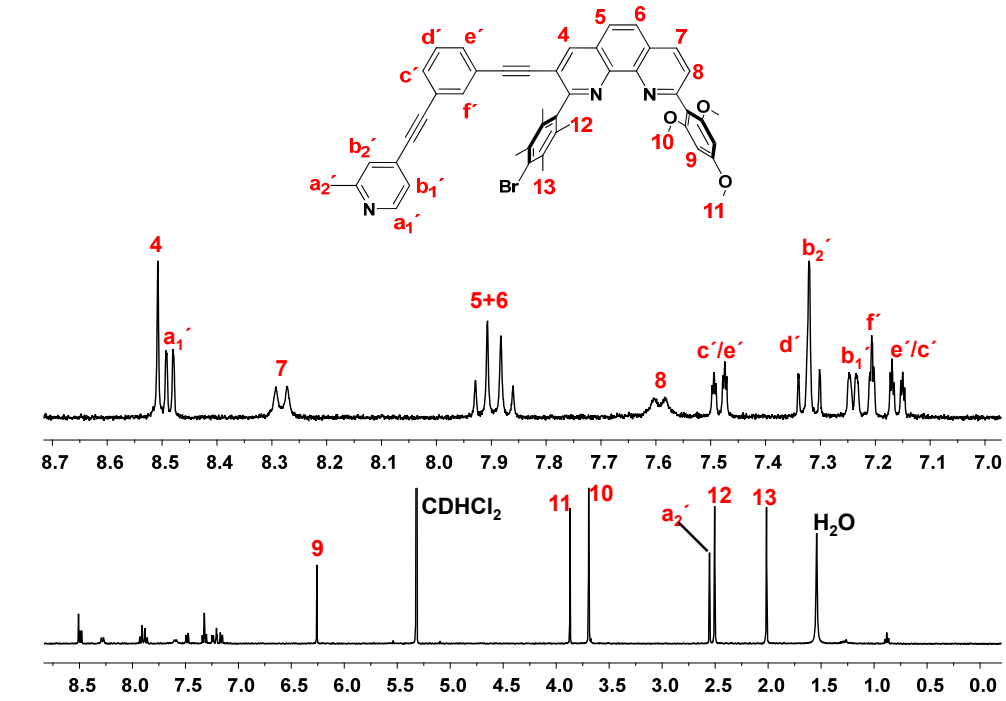

Figure S8. ^{1}H NMR spectrum of **R1** in CD_2Cl_2 (400 MHz, 298 K).

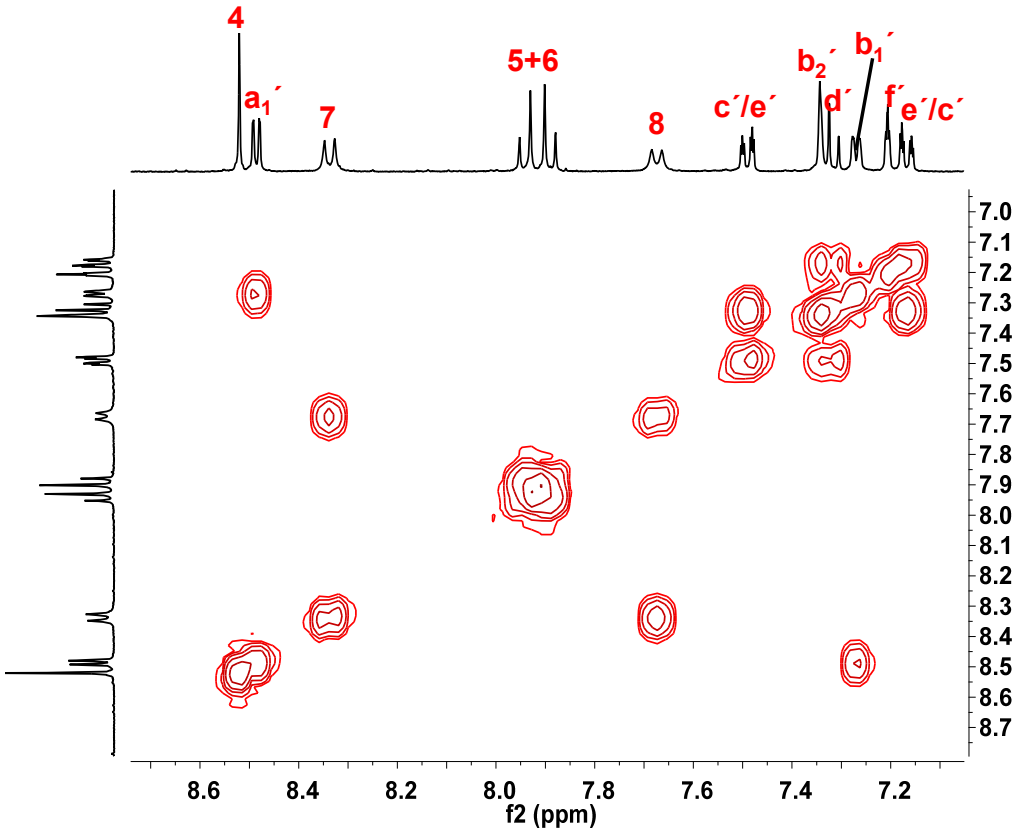

Figure S9. ^{1}H-^{1}H COSY spectrum of **R1** in CD_2Cl_2 (400 MHz, 298 K).

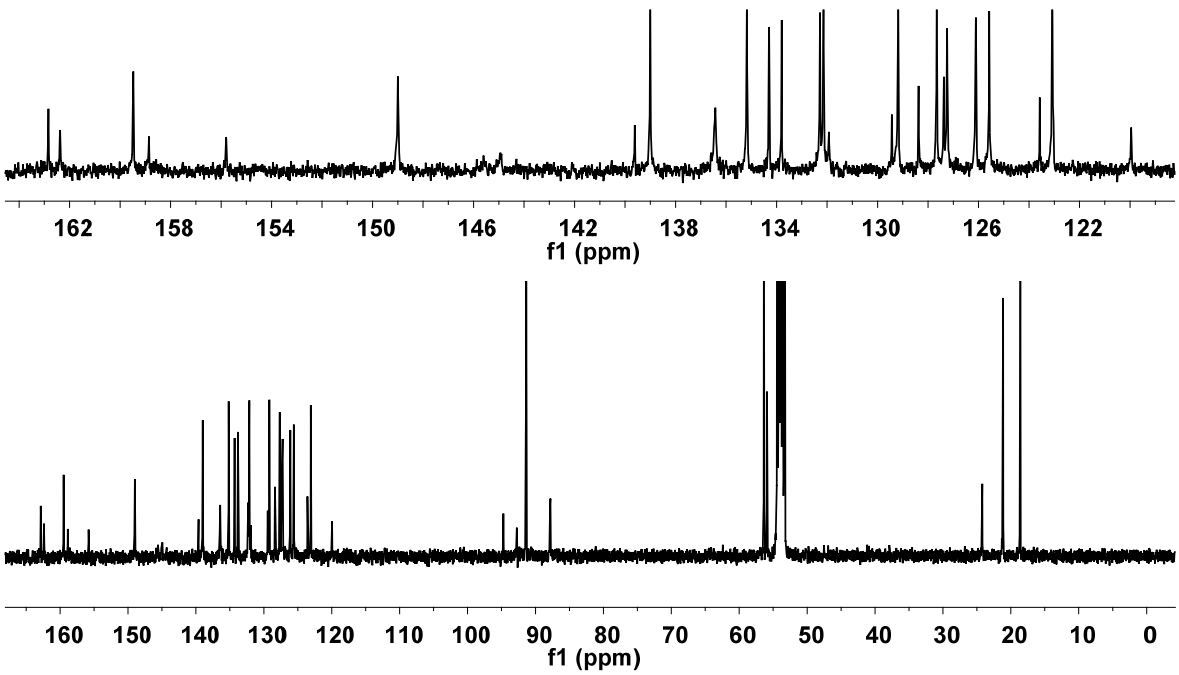

Figure S10. ^{13}C NMR spectrum of **R1** in CD_2Cl_2 (100 MHz, 298 K).

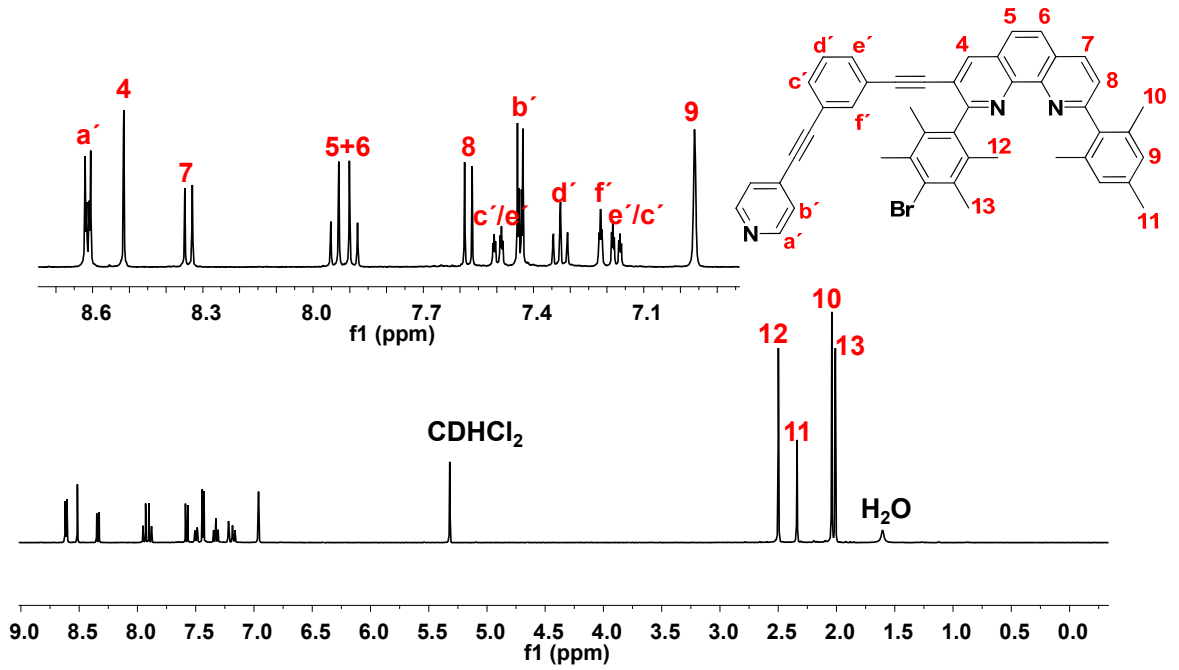

Figure S11. ^{1}H NMR spectrum of **R2** in CD_2Cl_2 (400 MHz, 298 K).

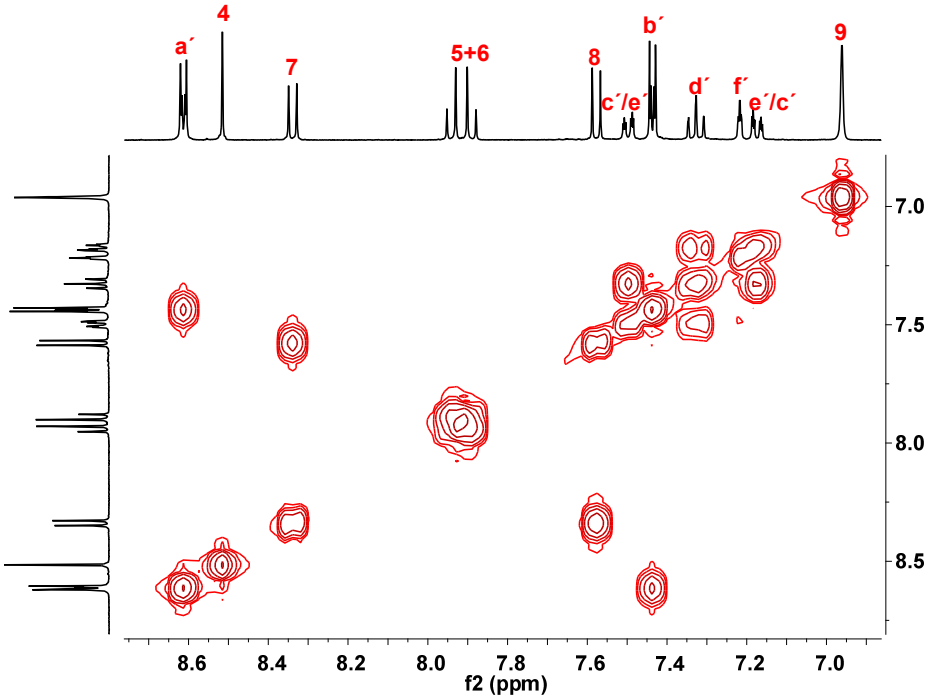

Figure S12. ^{1}H-^{1}H COSY spectrum of **R2** in CD_2Cl_2 (400 MHz, 298 K).

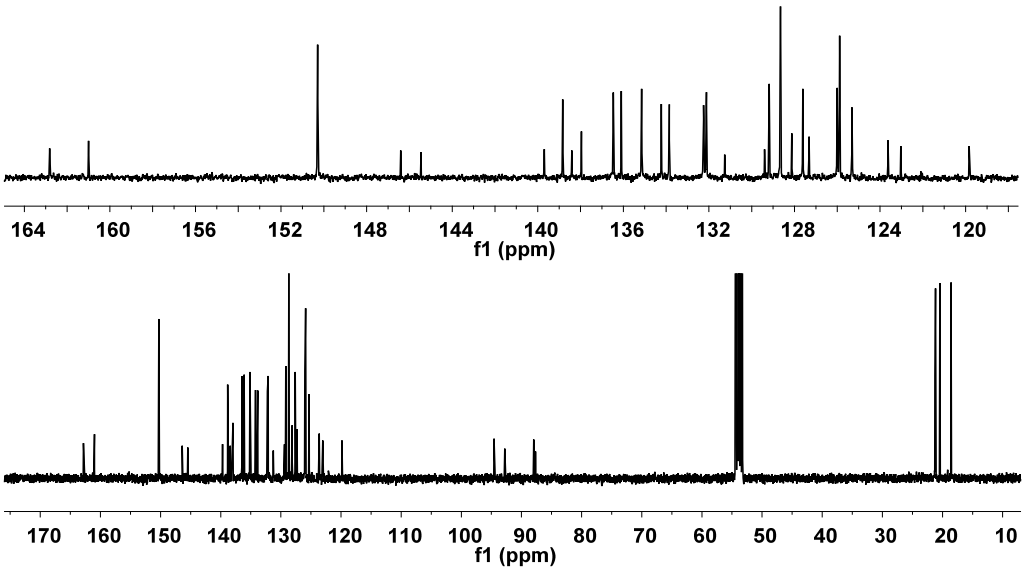

Figure S13. ^{13}C NMR spectrum of **R2** in CD_2Cl_2 (100 MHz, 298 K).

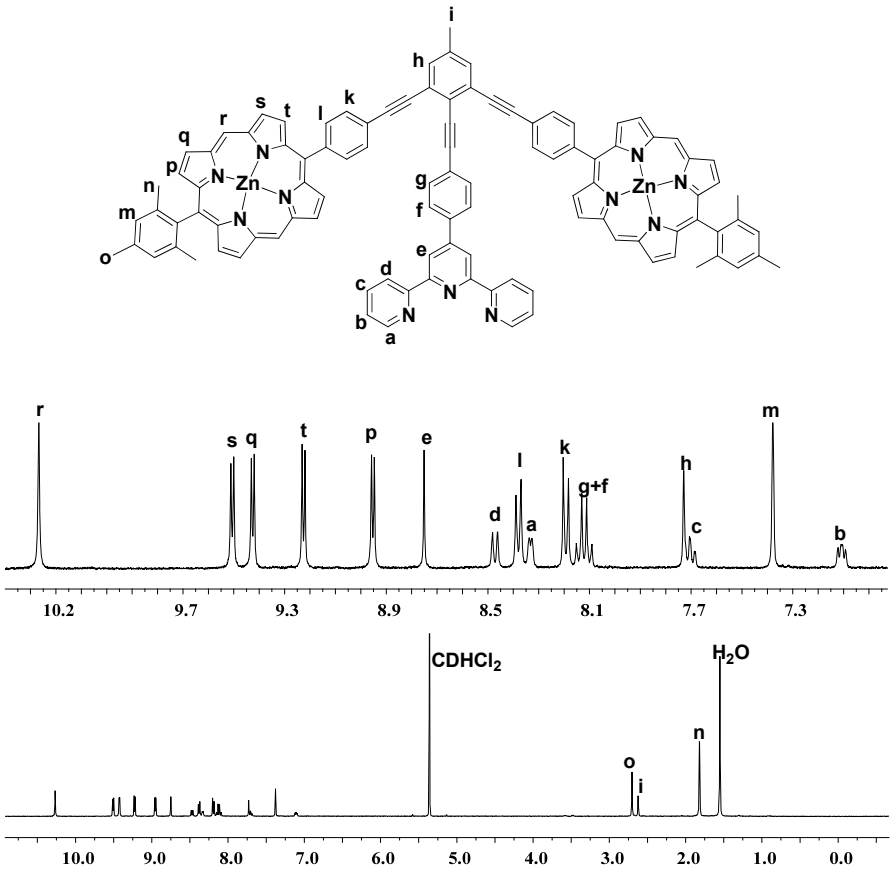

Figure S14. ^{1}H NMR spectrum of stator **S** in CD_2Cl_2 (400 MHz, 298 K).

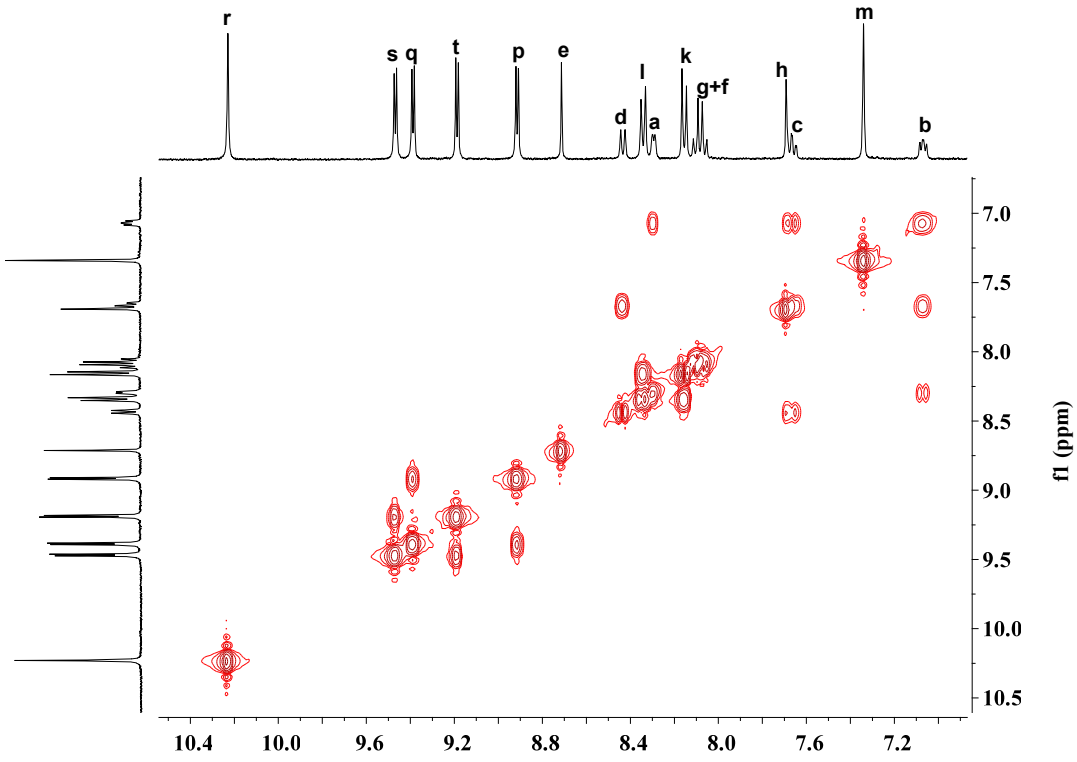

Figure S15. ^{1}H-^{1}H COSY spectrum of stator **S** in CD_2Cl_2 (400 MHz, 298 K).

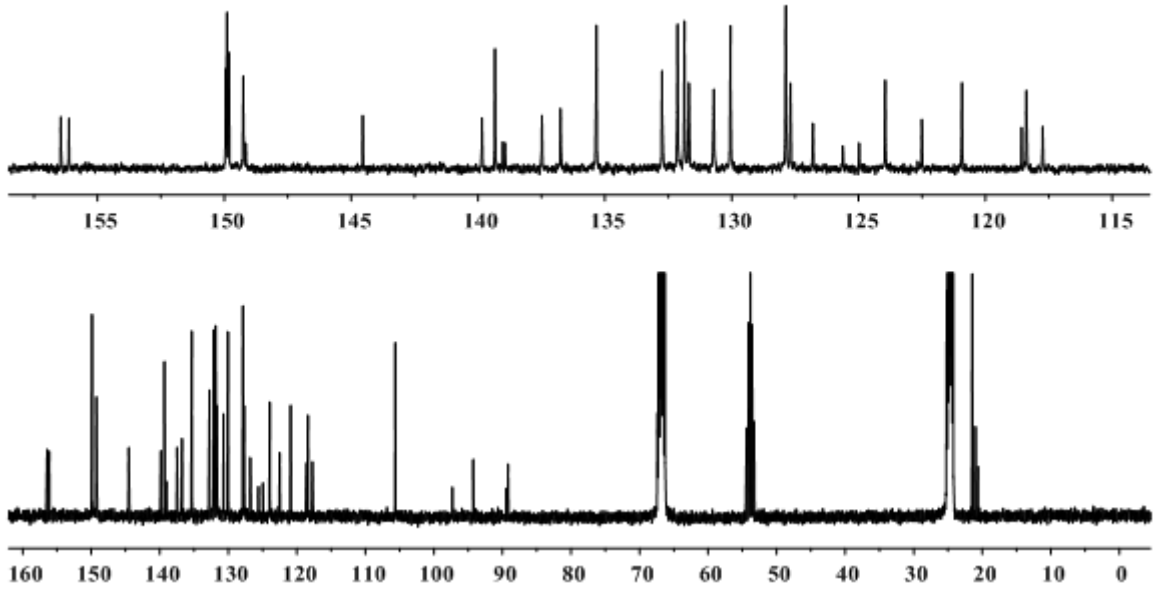

Figure S16. ^{13}C NMR spectrum of stator **S** in THF-d_8:CD_2Cl_2 (9:1) (100 MHz, 298 K).

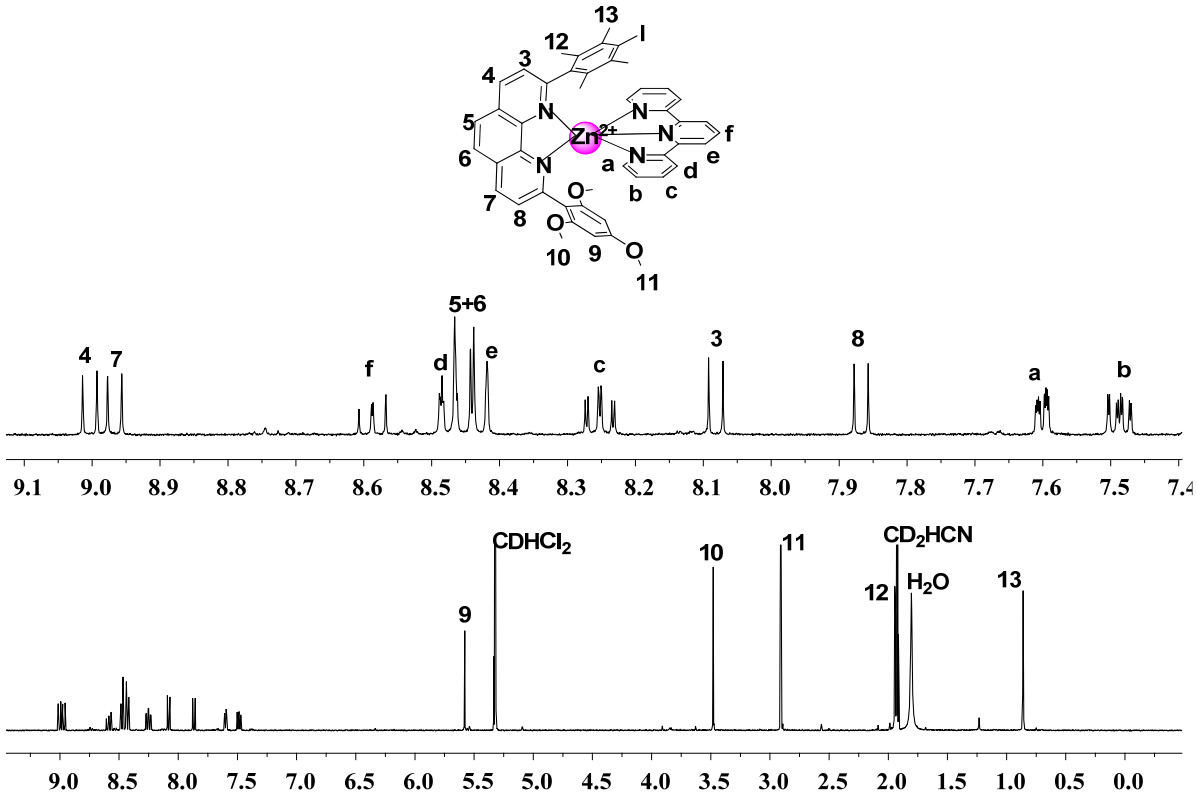

Figure S17. ^{1}H NMR spectrum of $[Zn(\mathbf{2})(\mathbf{6})]^{2+}$ in CD_2Cl_2:CD_3CN (10:1) (400 MHz, 298 K).

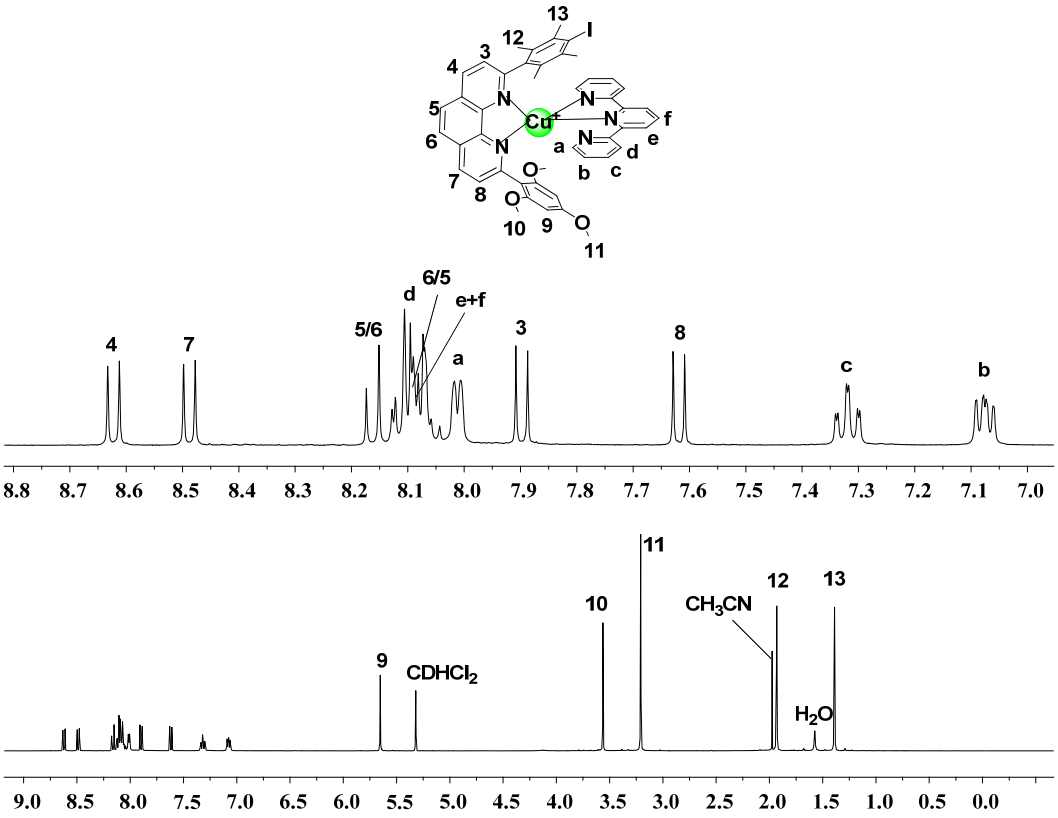

Figure S18. ^{1}H NMR spectrum of [Cu(**2**)(**6**)]$^{+}$ in CD_2Cl_2 (400 MHz, 298 K).

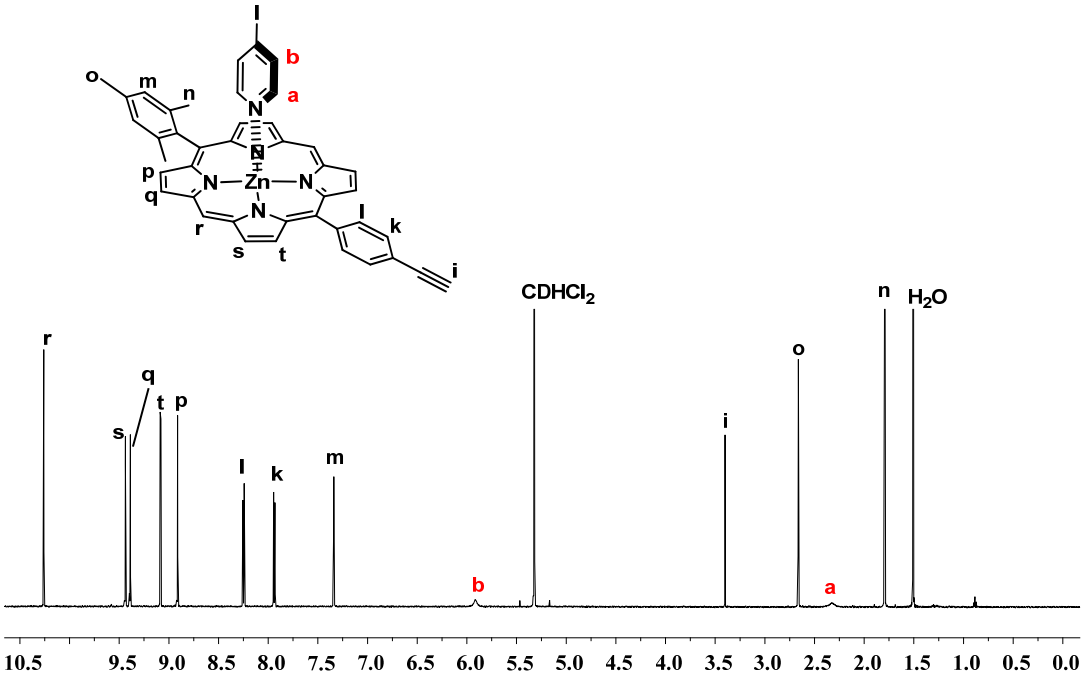

Figure S19. ^{1}H NMR spectrum of [(**3**)•(**4**)] in CD_2Cl_2 (400 MHz, 298 K).

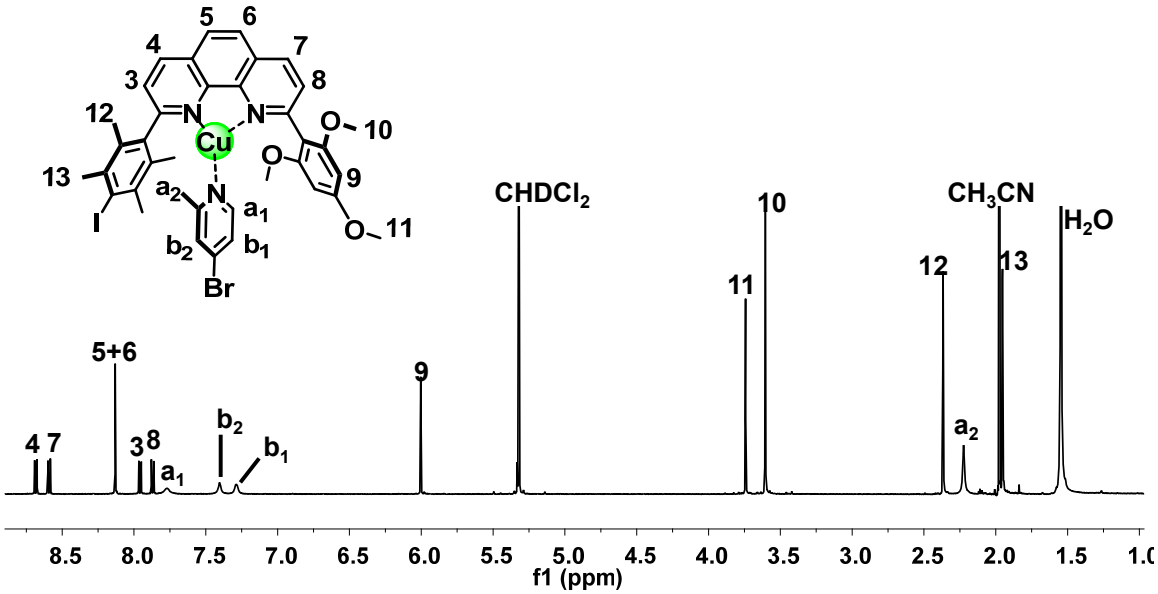

Figure S20. ^{1}H NMR spectrum of [Cu(**1**)(**2**)]$^{+}$ in CD_2Cl_2 (400 MHz, 298 K).

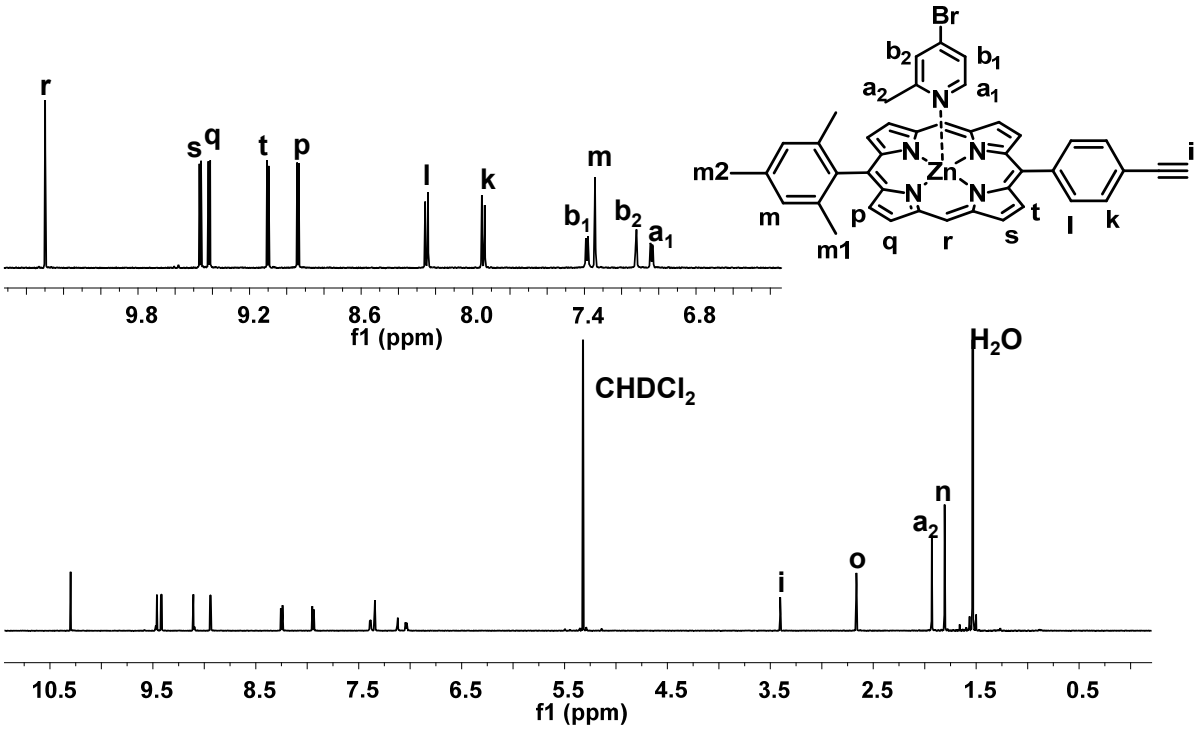

Figure S21. ^{1}H NMR spectrum of [(**1**)•(**4**)] in CD_2Cl_2 (400 MHz, 298 K).

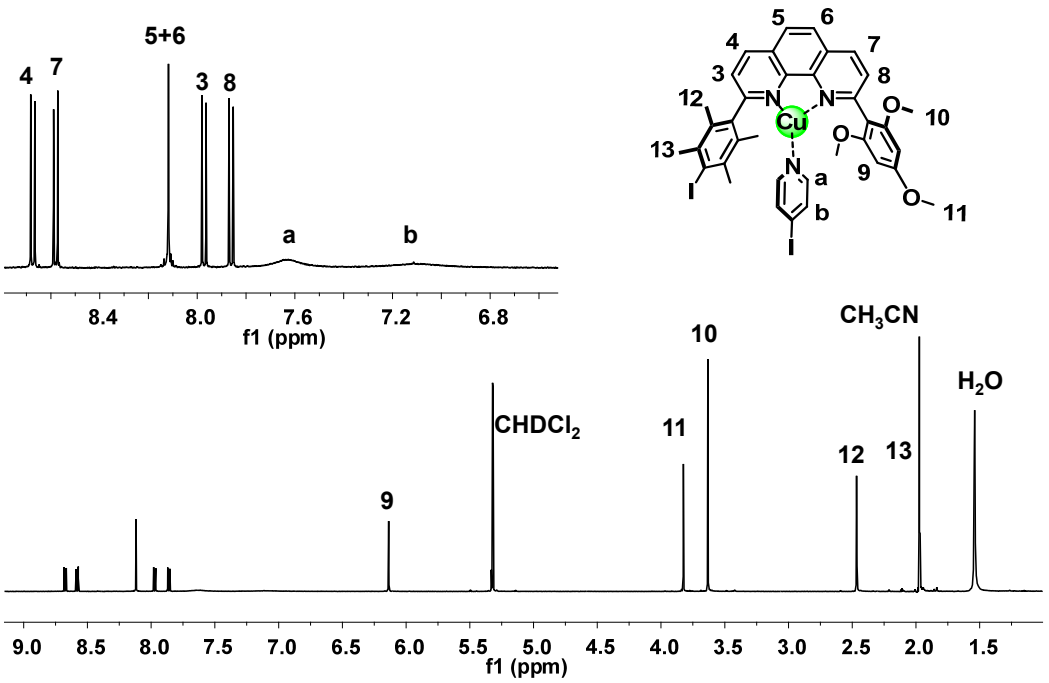

Figure S22. ^{1}H NMR spectrum of [Cu(**2**)(**3**)]$^{+}$ in CD_2Cl_2 (400 MHz, 298 K).

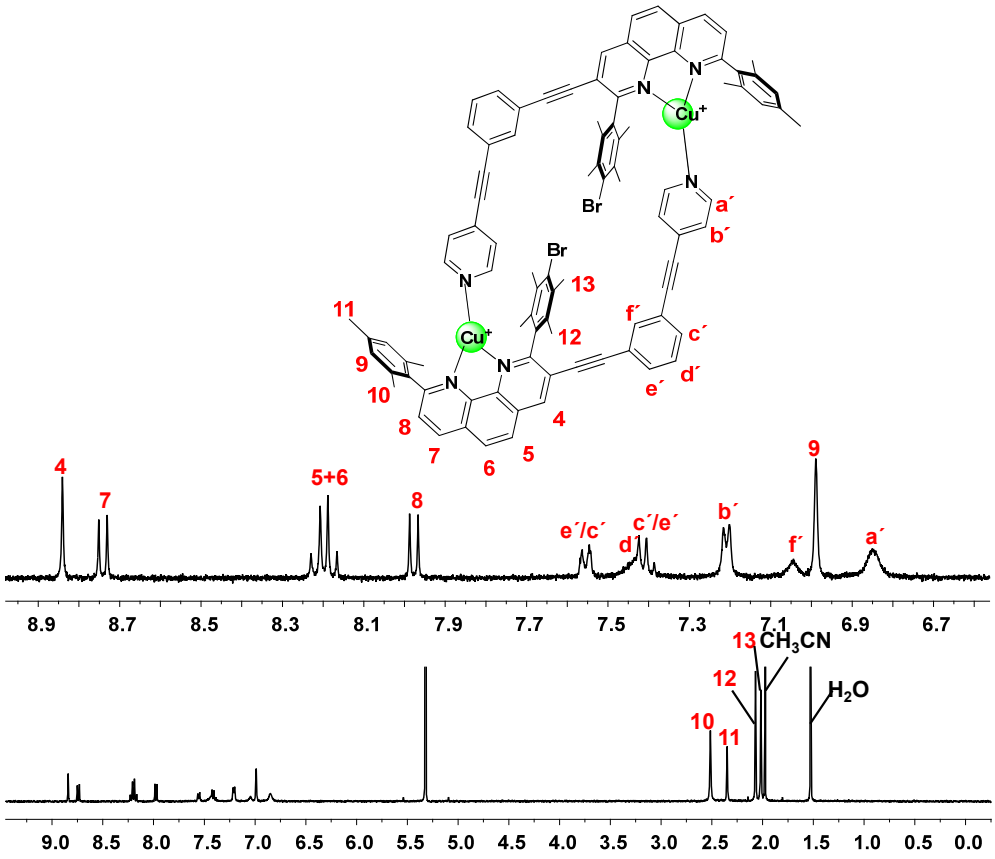

Figure S23. ^{1}H NMR spectrum of [Cu_2(**R2**)$_2$]$^{2+}$ in CD_2Cl_2 (400 MHz, 298 K).

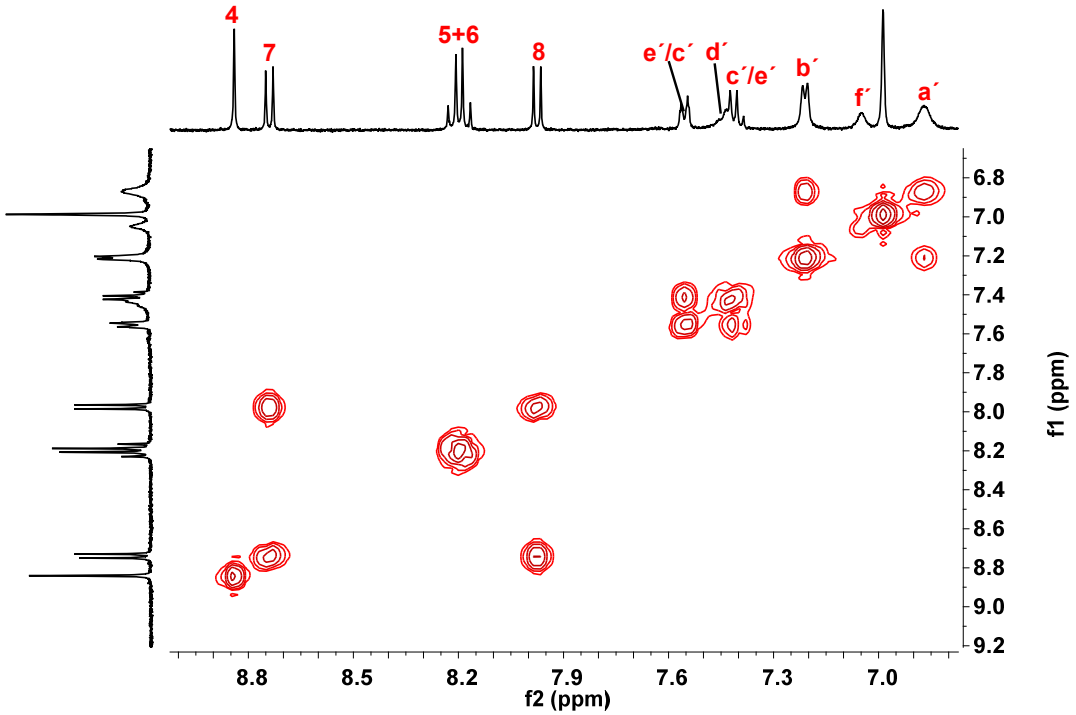

Figure S24. ^{1}H-^{1}H COSY spectrum of $[Cu_2(\mathbf{R2})_2]^{2+}$ in CD_2Cl_2 (400 MHz, 298 K).

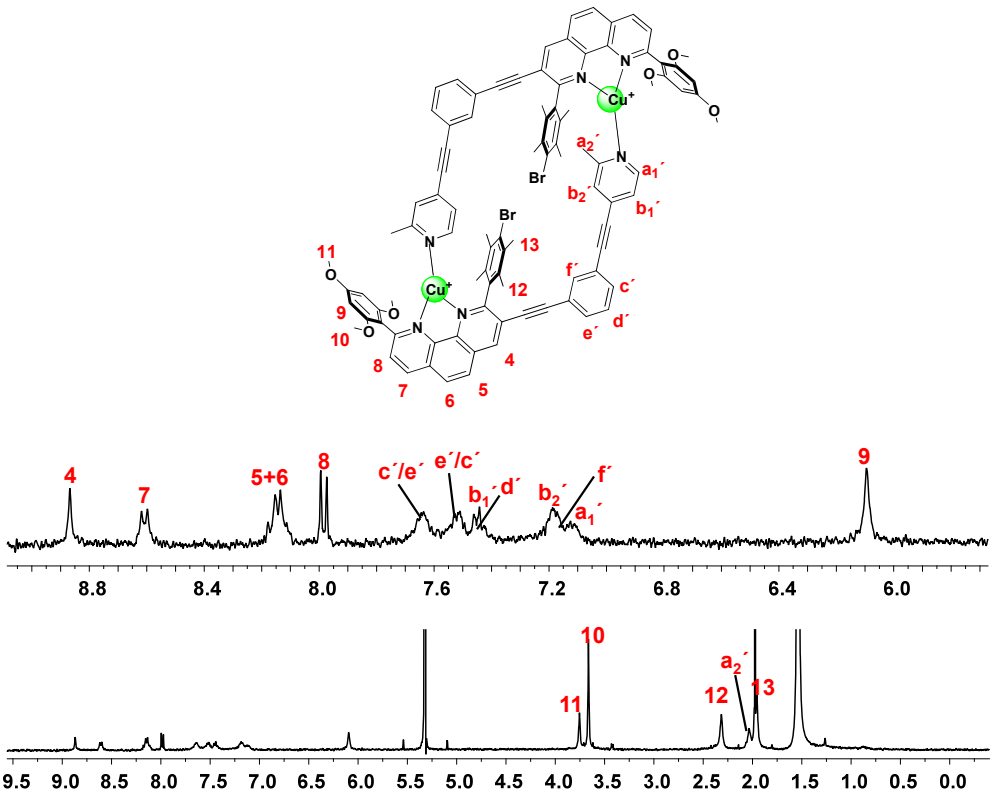

Figure S25. ^{1}H NMR spectrum of $[Cu_2(\mathbf{R1})_2]^{2+}$ in CD_2Cl_2 (400 MHz, 298 K).

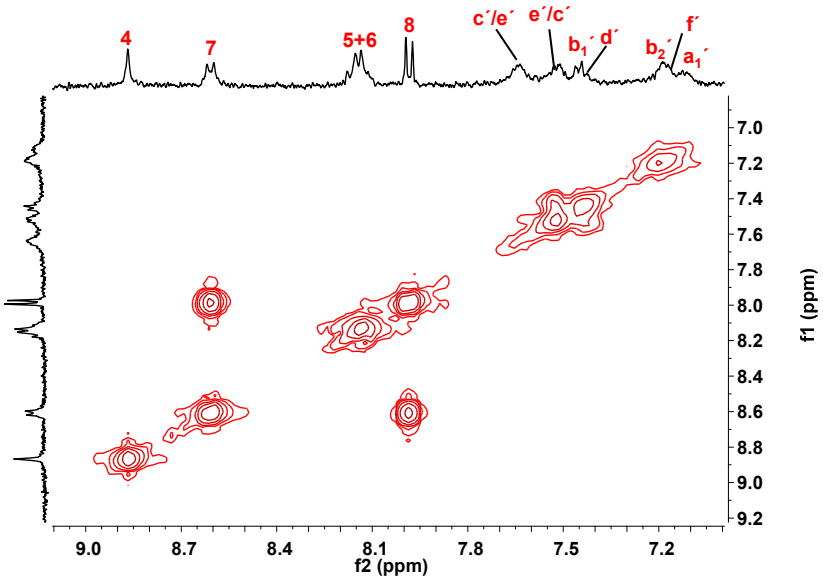

Figure S26. ^{1}H-^{1}H COSY spectrum of $[Cu_2(\mathbf{R1})_2]^{2+}$ in CD_2Cl_2 (400 MHz, 298 K).

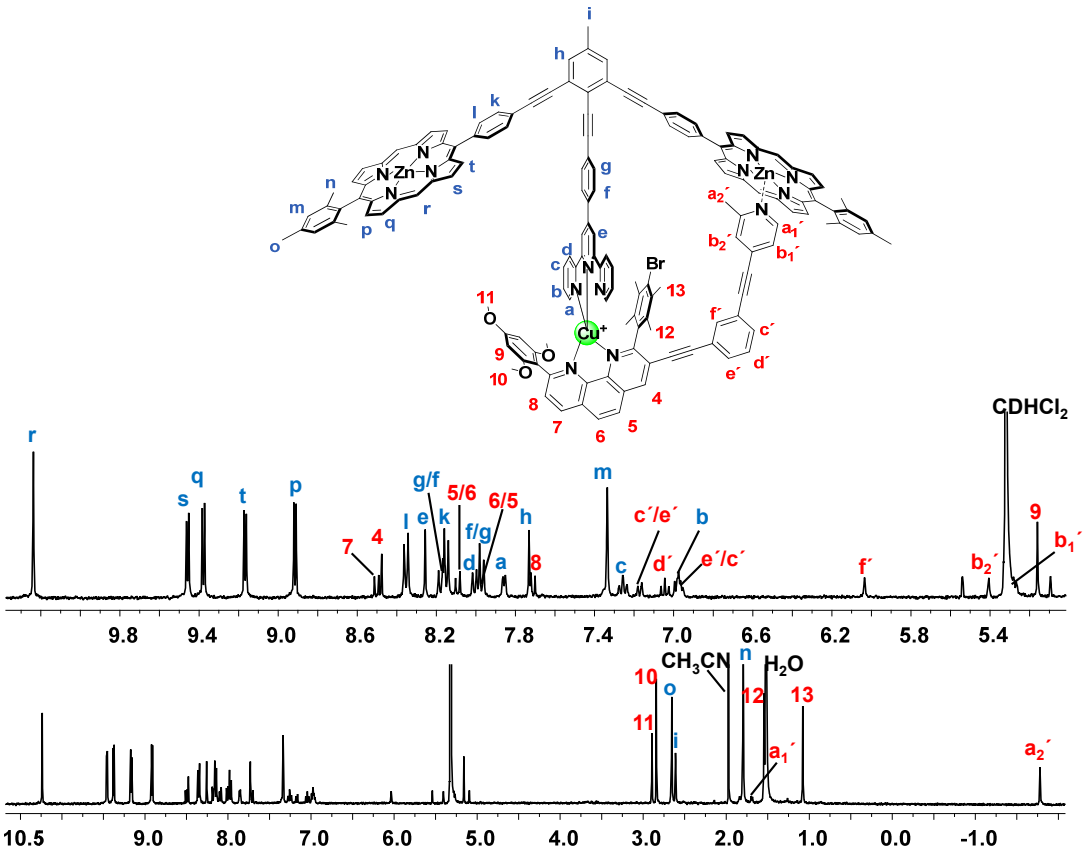

Figure S27. ^{1}H NMR spectrum of $[Cu(\mathbf{S})(\mathbf{R1})]^{+}$ in CD_2Cl_2 (400 MHz, 298 K).

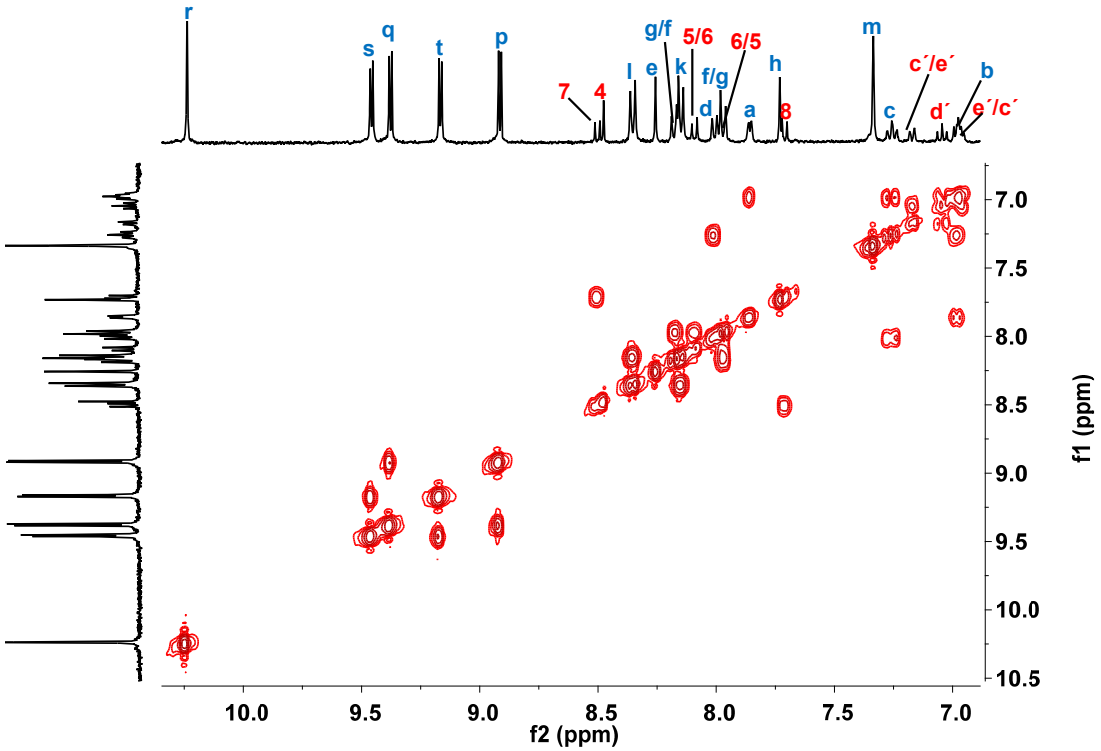

Figure S28. ^{1}H-^{1}H COSY spectrum of [Cu(**S**)(**R1**)]$^{+}$ in CD_2Cl_2 (400 MHz, 298 K)

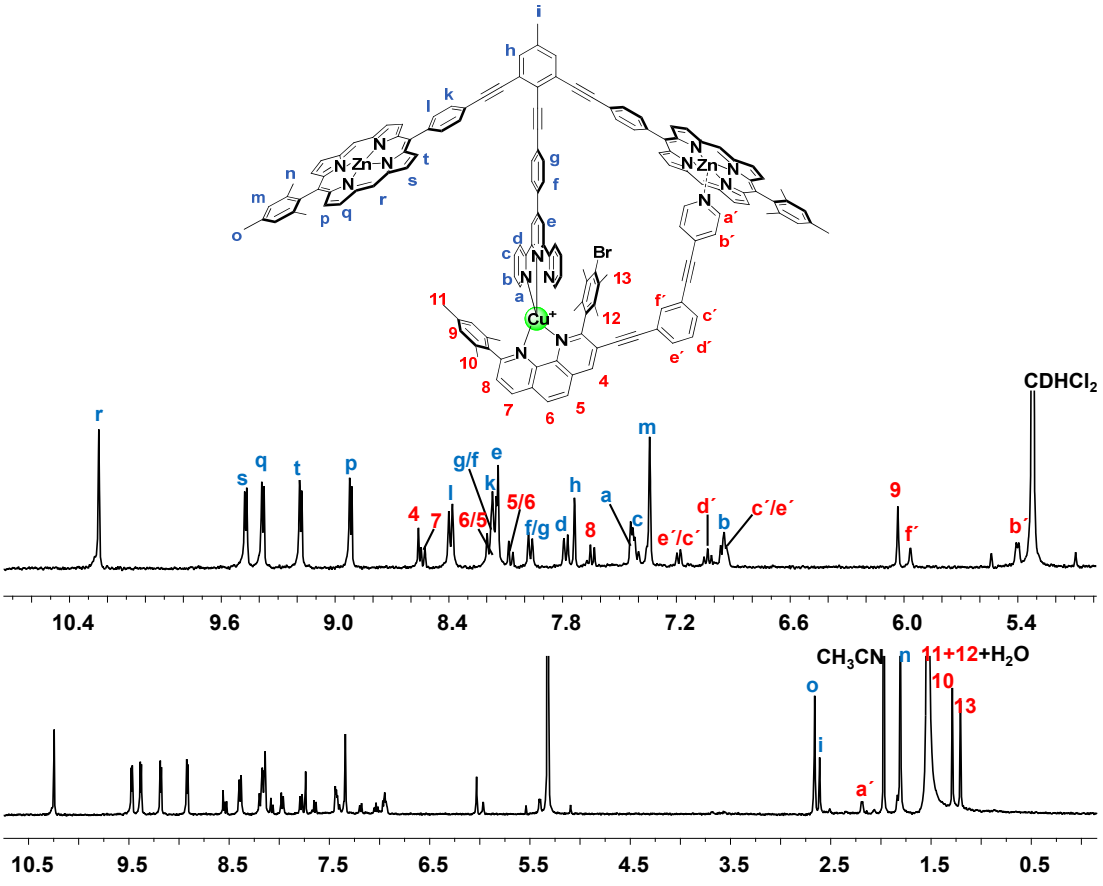

Figure S29. ^{1}H NMR spectrum of [Cu(**S**)(**R2**)]$^{+}$ in CD_2Cl_2 (400 MHz, 298 K).

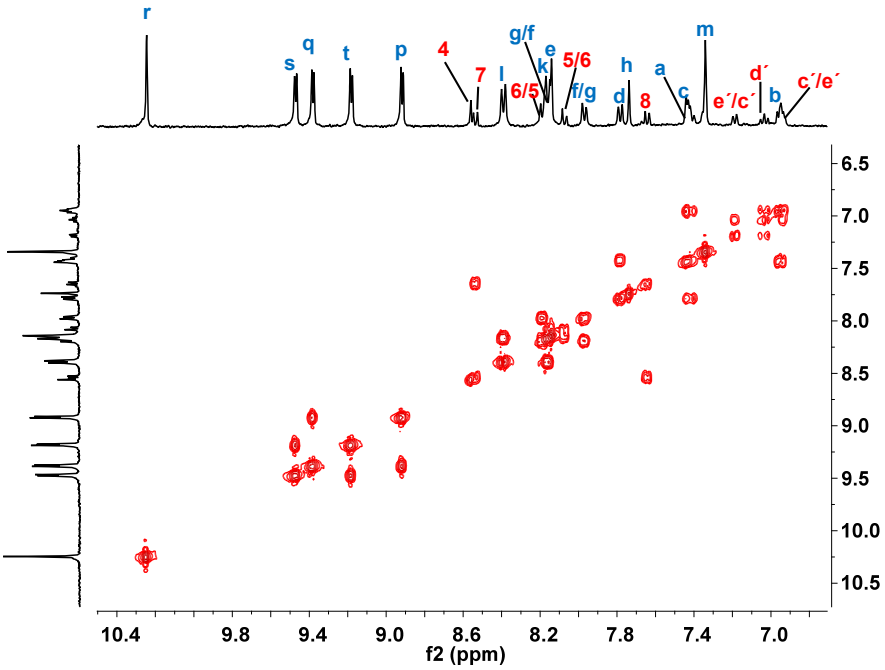

Figure S30. ^{1}H-^{1}H COSY spectrum of [Cu(**S**)(**R2**)]$^{+}$ in CD_2Cl_2 (400 MHz, 298 K).

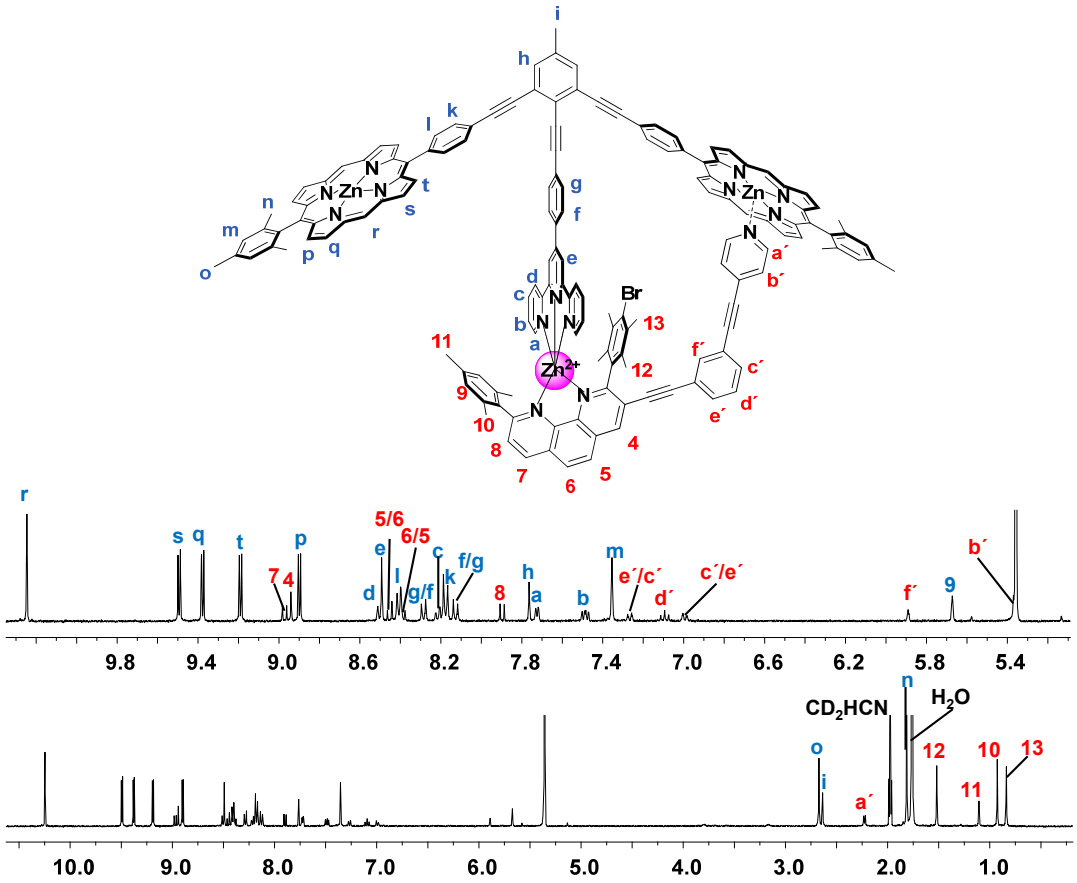

Figure S31. ^{1}H NMR spectrum of [Zn(**S**)(**R2**)]$^{2+}$ in CD_2Cl_2: CD_3CN (5:1) (400 MHz, 298 K).

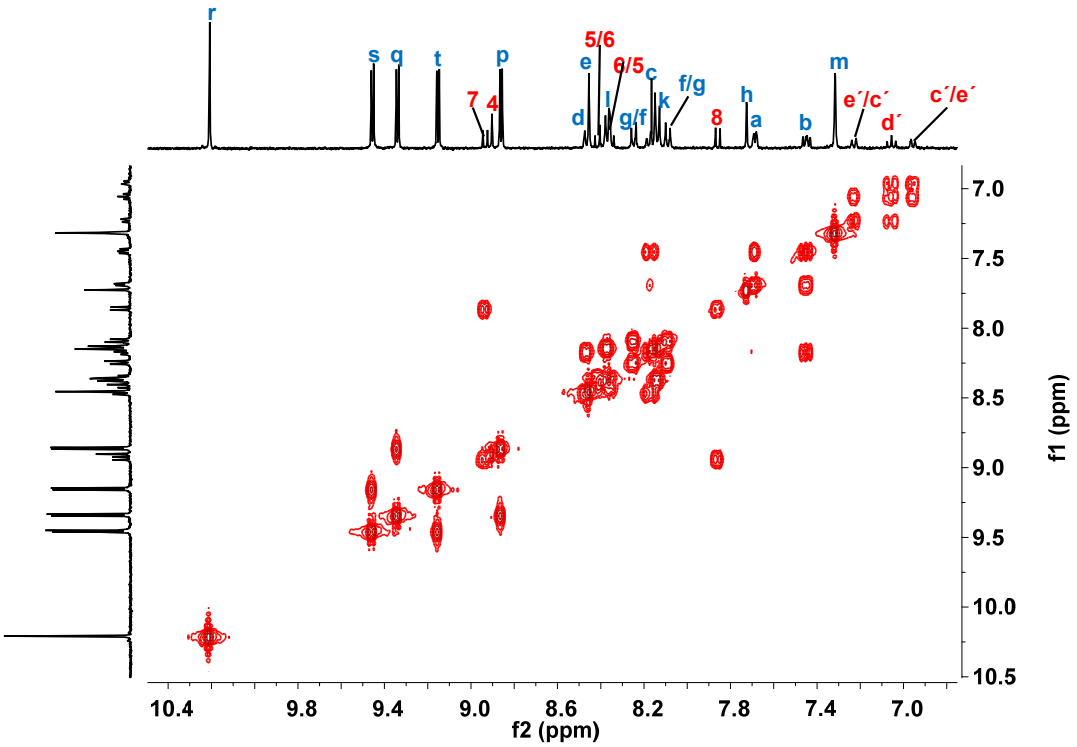

Figure S32. ^{1}H-^{1}H COSY NMR spectrum of $[Zn(\mathbf{S})(\mathbf{R2})]^{2+}$ in CD_2Cl_2: CD_3CN (5:1) (400 MHz, 298 K).

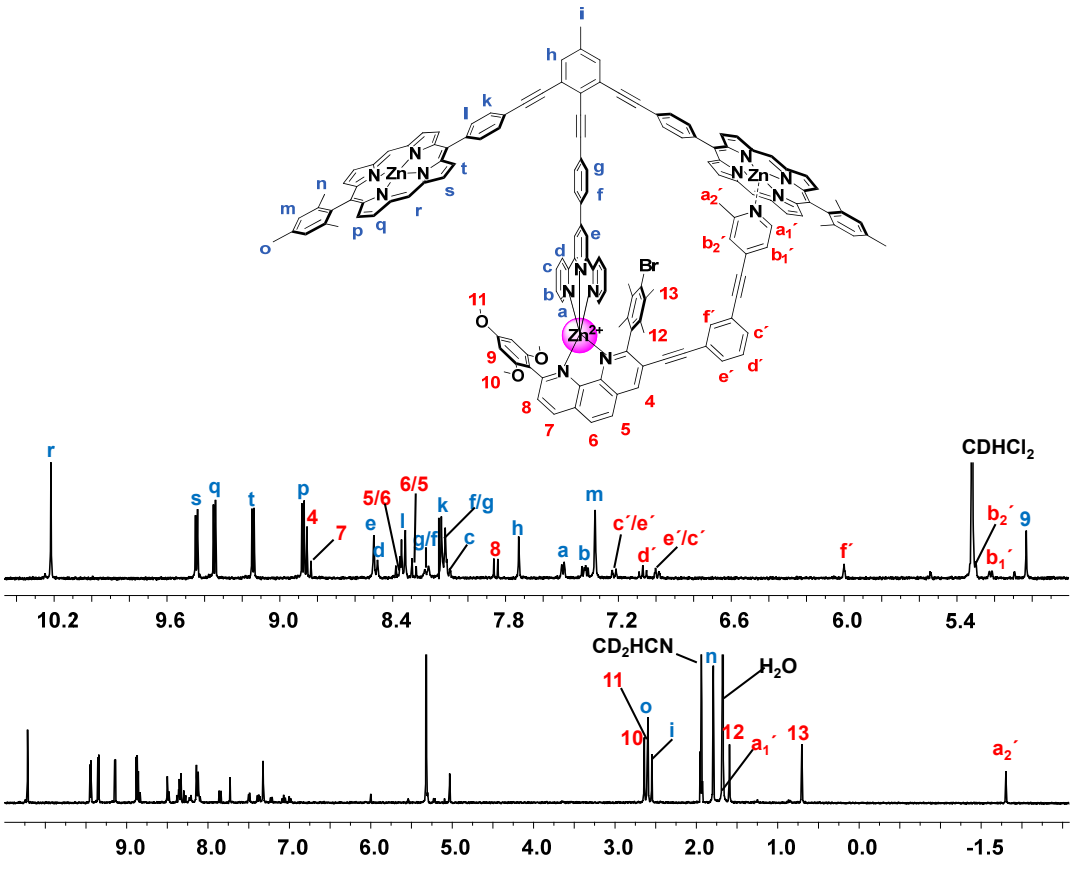

Figure S33. ^{1}H NMR spectrum of $[Zn(\mathbf{S})(\mathbf{R1})]^{2+}$ in CD_2Cl_2: CD_3CN (5:1) (400 MHz, 298 K).

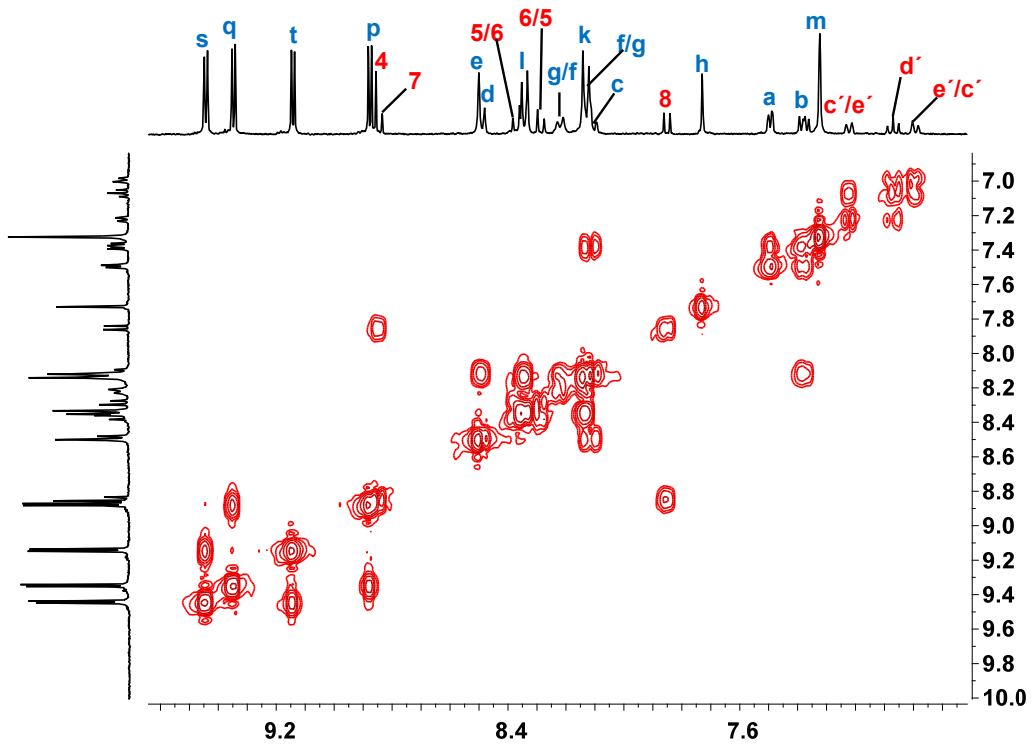

Figure S34. ^{1}H-^{1}H COSY NMR spectrum of $[Zn(\mathbf{S})(\mathbf{R1})]^{2+}$ in CD_2Cl_2: CD_3CN (5:1) (400 MHz, 298 K).

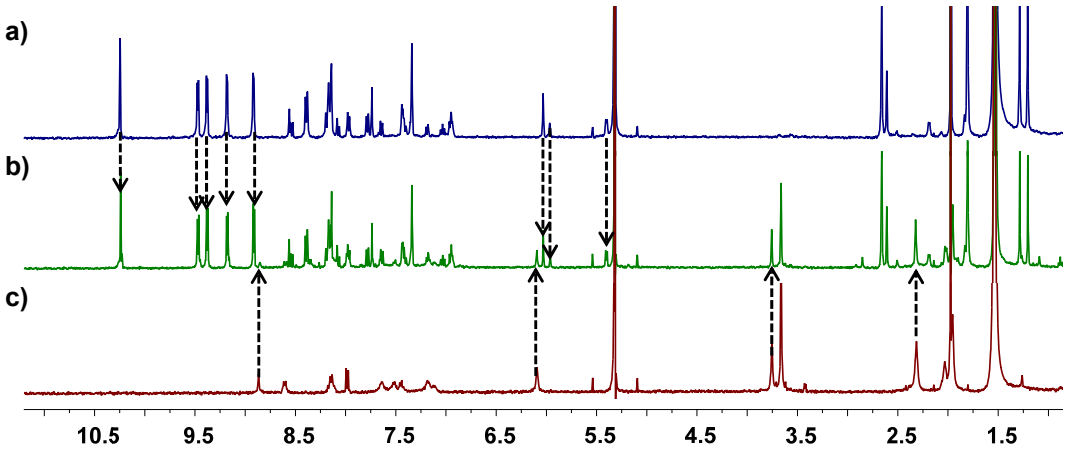

Figure S35. Partial ^{1}H NMR (400 MHz, in CD_2Cl_2) of (a) $[Cu(\mathbf{S})(\mathbf{R2})]^{+}$; (b) **NetState I**: mixture of $[Cu_2(\mathbf{R1})_2]^{2+}$ and $[Cu(\mathbf{S})(\mathbf{R2})]^{+}$; (c) $[Cu_2(\mathbf{R1})_2]^{2+}$.

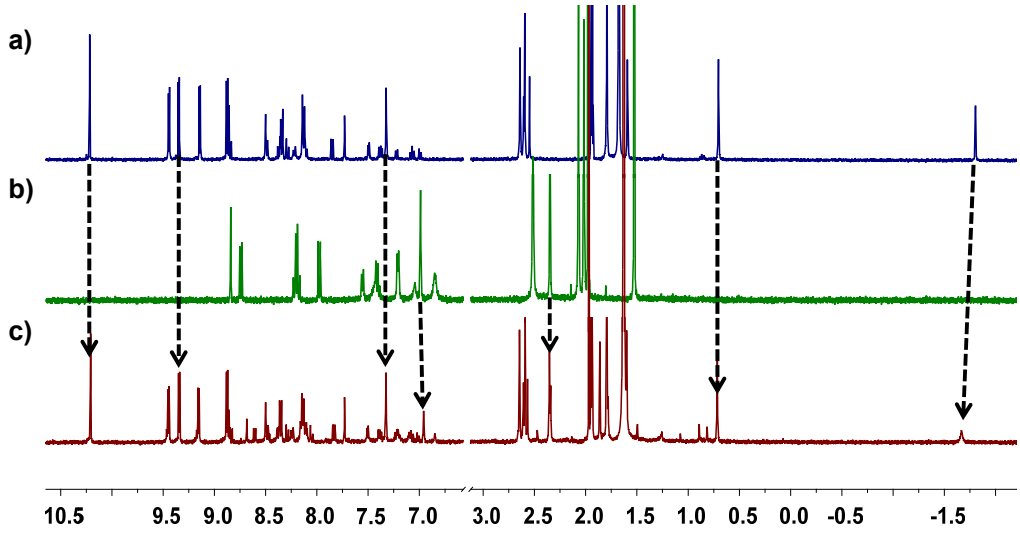

Figure S36. Partial ^{1}H NMR (400 MHz, CD_2Cl_2: CD_3CN (5:1)) of (a) $[Zn(\mathbf{S})(\mathbf{R1})]^{2+}$; (b) $[Cu_2(\mathbf{R2})_2]^{2+}$; (c) **NetState II**: mixture of $[Cu_2(\mathbf{R2})_2]^{2+}$ and $[Zn(\mathbf{S})(\mathbf{R1})]^{2+}$.

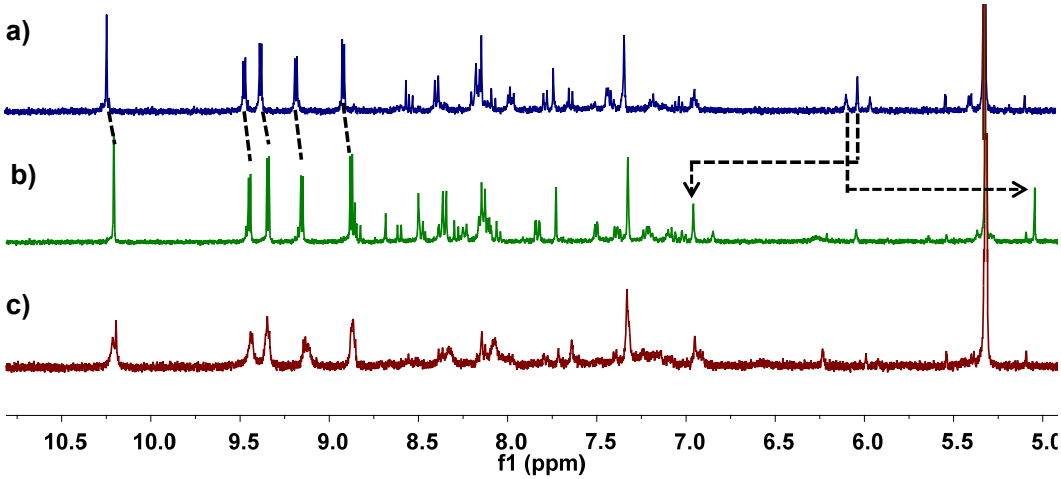

Figure S37. ^{1}H NMR spectra (400 MHz, CD_2Cl_2:CD_3CN = 5:1, 298 K) showing the reversible switching between NetState I and II. The different NMR traces represent: (a) NetState I formed (= mixture of 0.5 equiv. of $[Cu_2(\mathbf{R1})_2]^{2+}$ and 1.0 equiv. of $[Cu(\mathbf{S})(\mathbf{R2})]^{+}$) after mixing of **S**, **R1**, **R2** and $[Cu(CH_3CN)_4]PF_6$ (1.69×10^{-3} M) in 1:1:1:2 ratio; (b) NetState II (= mixture of 0.5 equiv. of $[Cu_2(\mathbf{R2})_2]^{2+}$ and 1.0 equiv. of $[Zn(S)(\mathbf{R1})]^{2+}$) is furnished after adding 1.0 equiv. of $Zn(OTf)_2$ as a standard solution in CD_3CN (36 µL) to (a); (c) NMR after addition of 1.0 equiv. of hexacyclen to NetState II. Reversibility (NetState II to NetState I) failed since the liberated copper(I) ions are unstable in solution.

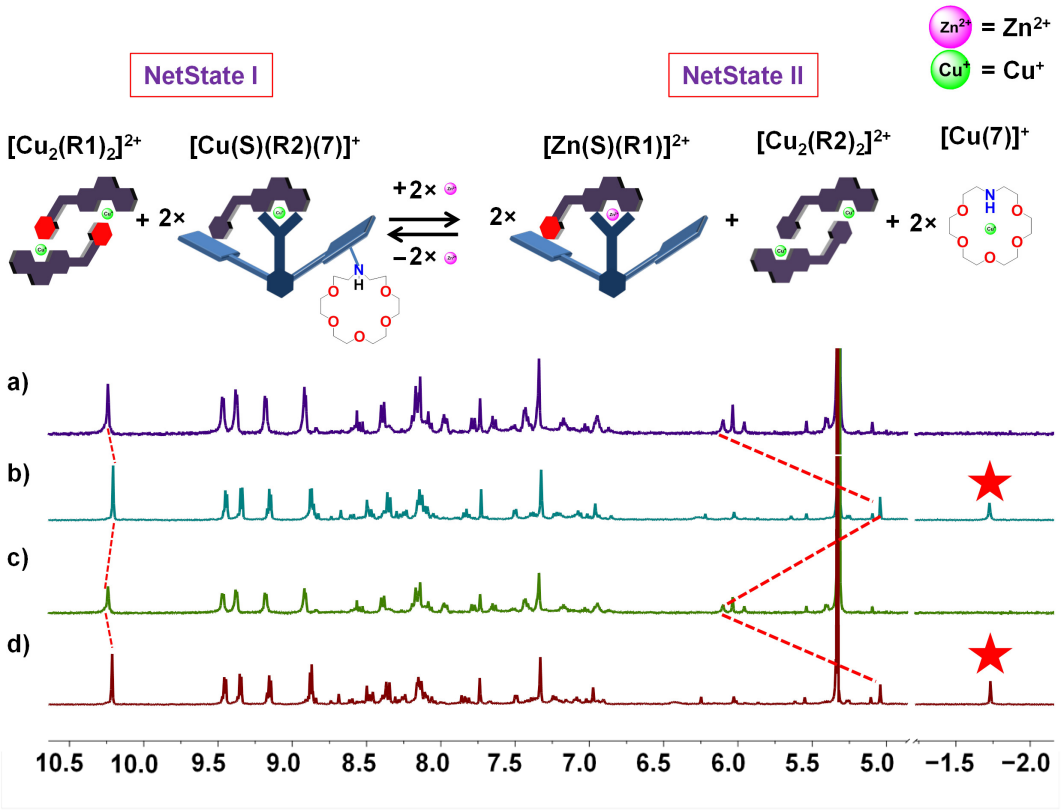

Figure S38. ^{1}H NMR spectra (400 MHz, CD_2Cl_2: CD_3CN (5:1), 298 K) showing the reversible switching between NetState I and II in presence of a receptor **7**. The different NMR traces represent: (a) NetState I (= mixture of 0.5 equiv. of $[Cu_2(\mathbf{R1})_2]^{2+}$ and 1.0 equiv. of $[Cu(\mathbf{S})(\mathbf{R2})]^{+}$) obtained after mixing of **S**, **R1**, **R2**, **7** and $[Cu(CH_3CN)_4]PF_6$ (1.67×10^{-3} M) in 1:1:1:1:2 ratio; (b) NetState II (= mixture of 0.5 equiv. of $[Cu_2(\mathbf{R2})_2]^{2+}$ and 1.0 equiv. of $[Zn(\mathbf{S})(\mathbf{R1})]^{2+}$) furnished after adding 1.0 equiv. of $Zn(OTf)_2$ as a standard solution in CD_3CN (47 μL) to (a); (c) NMR of NetState I received after addition of 1.0 equiv. of hexacyclen; (d) NetState II after adding another 1.0 equiv. of $Zn(OTf)_2$. Red asterisk marked signals arise from the α-methyl group of **R1** in nanorotor $[Zn(\mathbf{S})(\mathbf{R1})]^{2+}$, indicating the formation of NetState II.

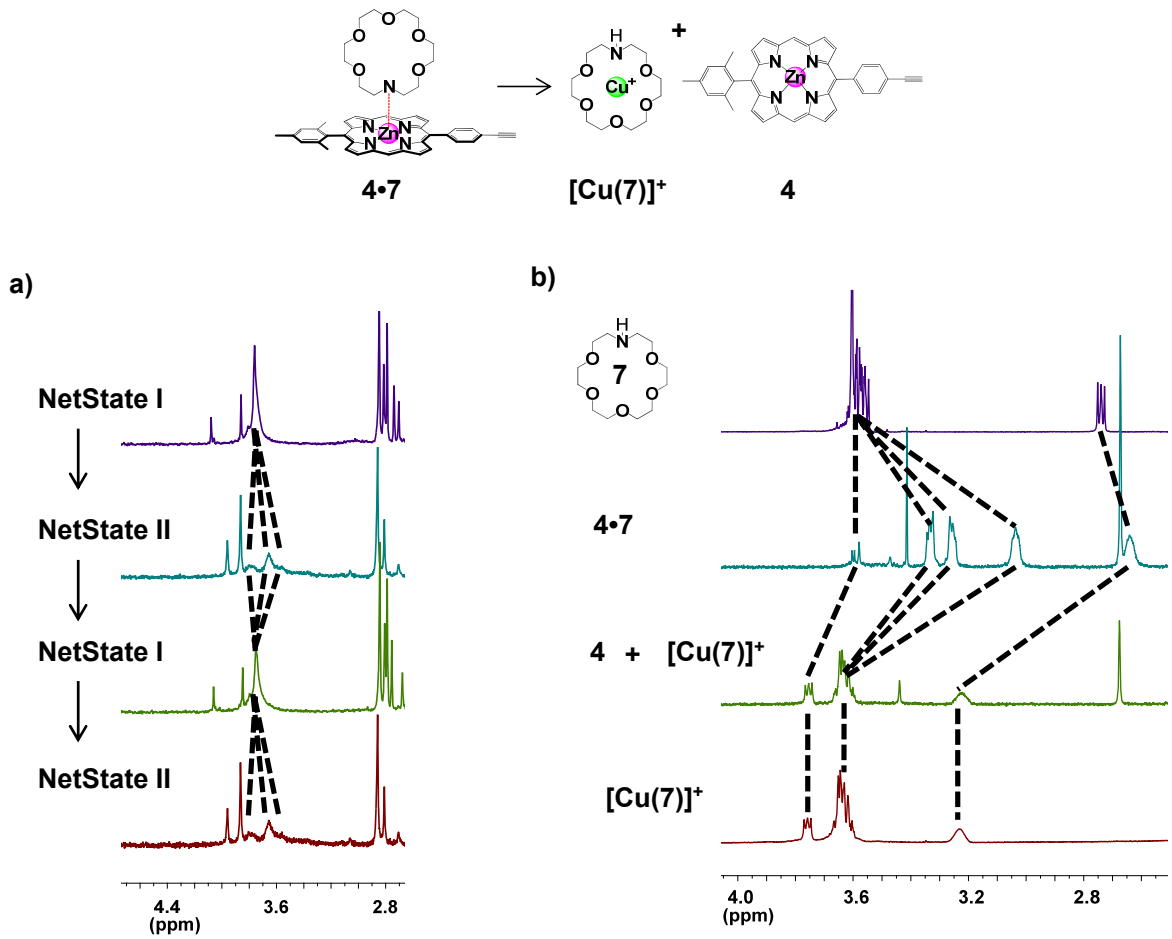

Figure S39. Changes in the ^{1}H NMR (400 MHz, 298 K) (a) during switching between NetState I and NetState II (see Figure S38) showing the capture and release of Cu^{+} by receptor **7**. (b) ^{1}H NMR signatures (from top to bottom) of **7**; of [(**4**)•(**7**)], of mixture of **4** and [Cu(**7**)]$^{+}$ (obtained upon addition of 1.0 equiv of $[Cu(CH_3CN)_4PF_6$ to [(**4**)•(**7**)]), and of [Cu(**7**)]$^{+}$ in CD_2Cl_2.

5. DOSY NMR spectra

Calculation of hydrodynamic radius from:

a) **DOSY**: The diffusion coefficient *D* for **[**Zn**(S)(R)**$]^{2+}$ and **[**Cu**(S)(R)**$]^{+}$ was obtained from their DOSY spectrum. The corresponding hydrodynamic radius was calculated by using the Stokes-Einstein equation

$$r = k_B T/6\pi\eta D$$

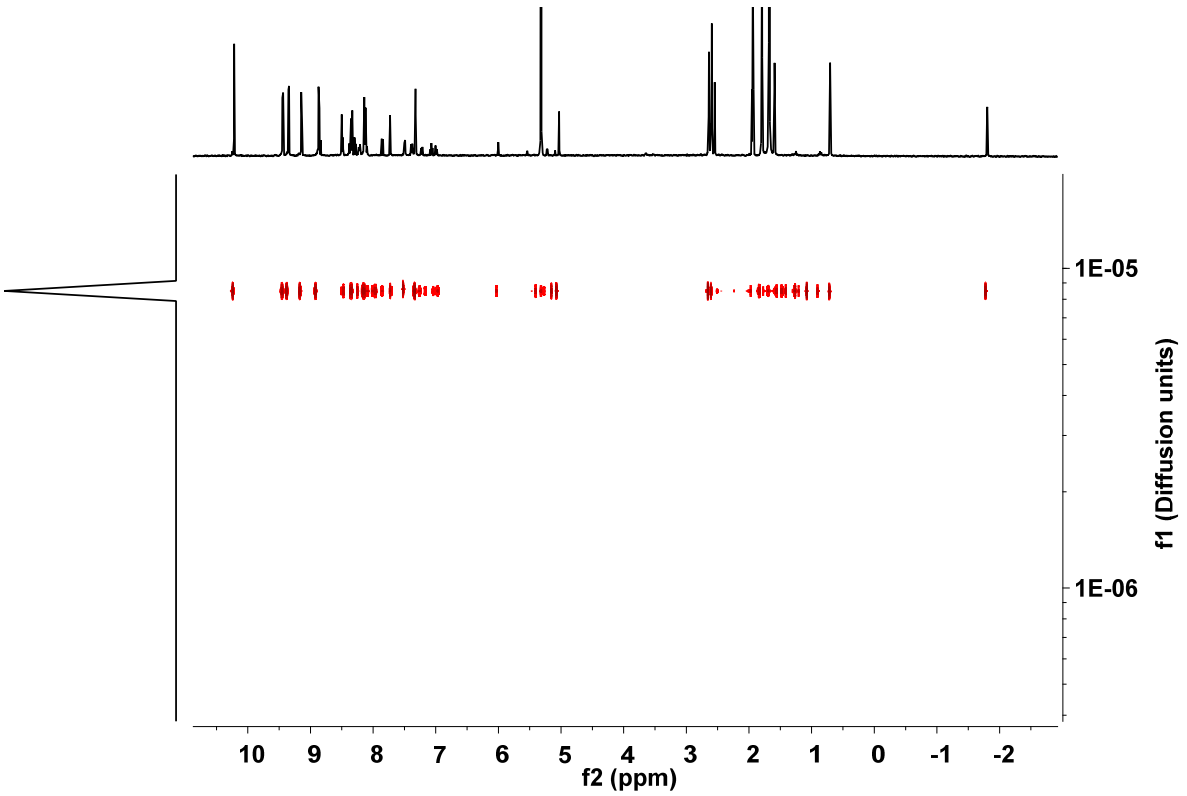

Figure S40. ^{1}H-DOSY NMR of [Zn(**S**)(**R1)**$]^{2+}$ in CD_2Cl_2:CD3CN (5:1) (600 MHz, 298 K). Diffusion coefficient D = 5.32×10^{-10} m^2 s^{-1}, hydrodynamic radius r = 9.9 Å.

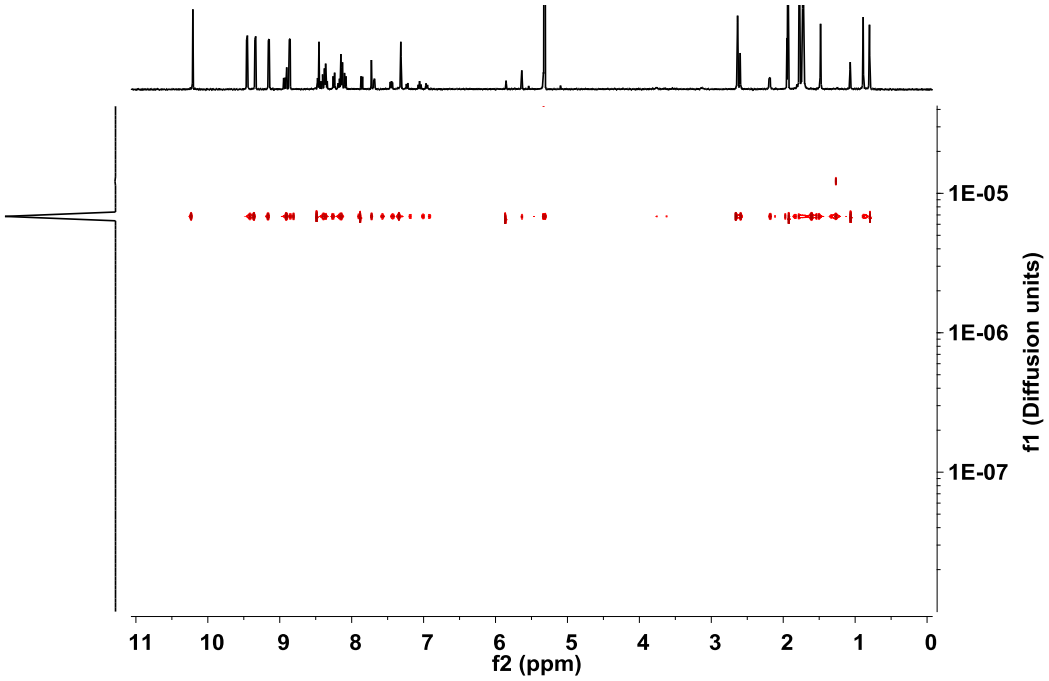

Figure S41. ^{1}H-DOSY NMR of [Zn(**S**)(**R2**)]$^{2+}$ in CD_2Cl_2:CD3CN (5:1) (600 MHz, 298 K). Diffusion coefficient D = 4.76 × 10^{-10} m^2 s^{-1}, hydrodynamic radius r = 11.1 Å.

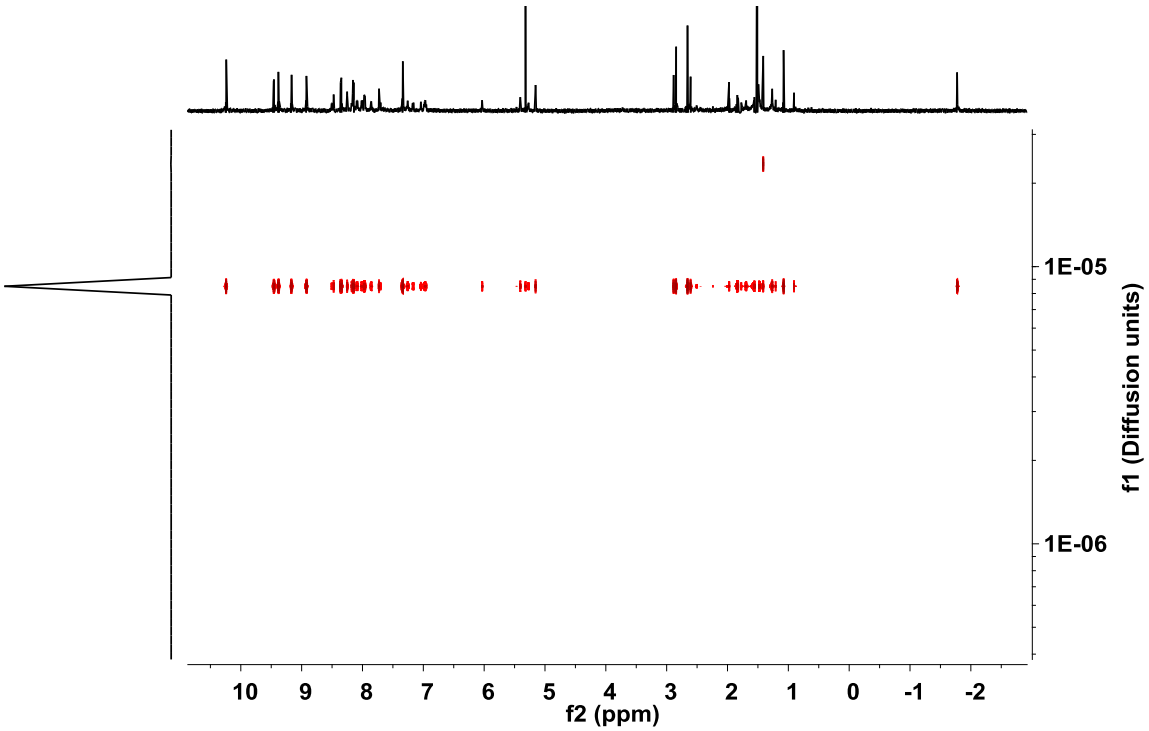

Figure S42. ^{1}H-DOSY NMR of [Cu(**S**)(**R1**)]$^{+}$ in CD_2Cl_2 (600 MHz, 298 K). Diffusion coefficient D = 5.92 × 10^{-10} m^2 s^{-1}, hydrodynamic radius r = 8.9 Å.

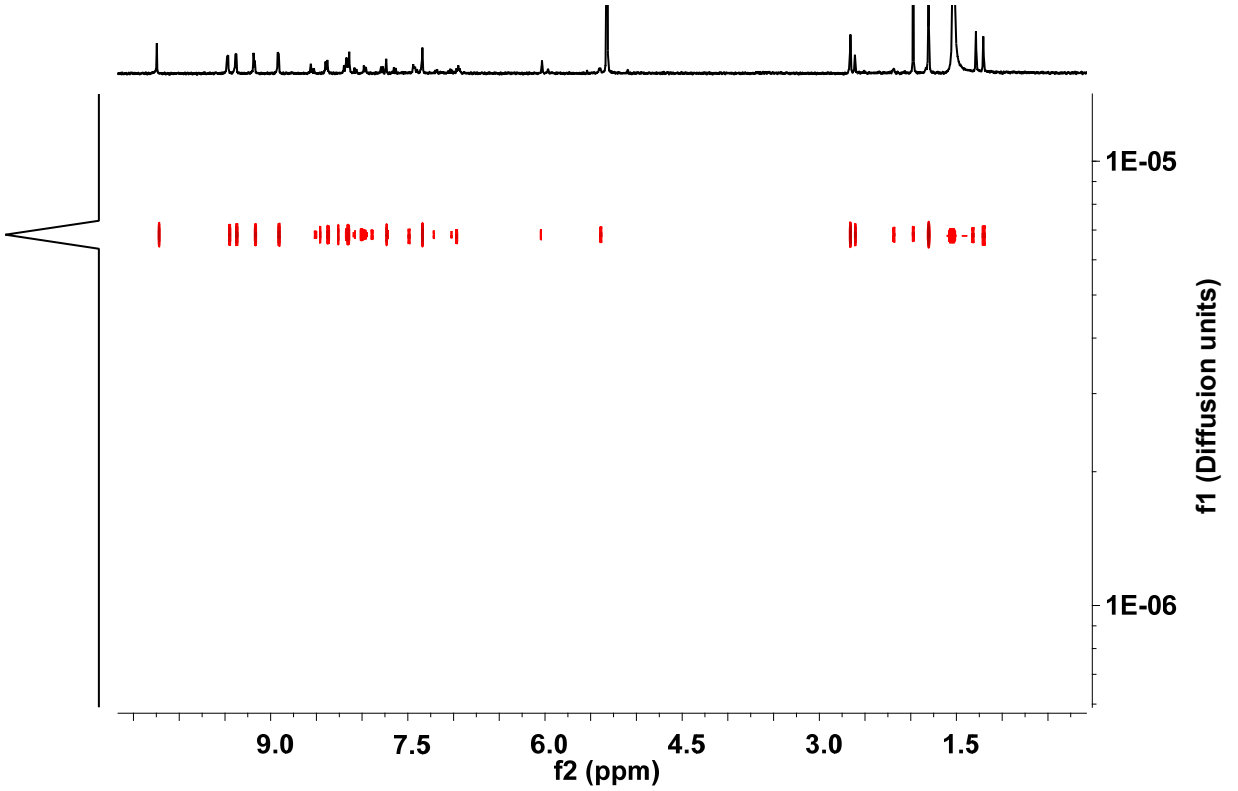

Figure S43. ^{1}H-DOSY NMR of [Cu(**S**)(**R2**)]$^{+}$ in CD_2Cl_2 (600 MHz, 298 K). Diffusion coefficient $D = 4.87 \times 10^{-10}$ m^2 s^{-1}, hydrodynamic radius $r = 10.9$ Å.

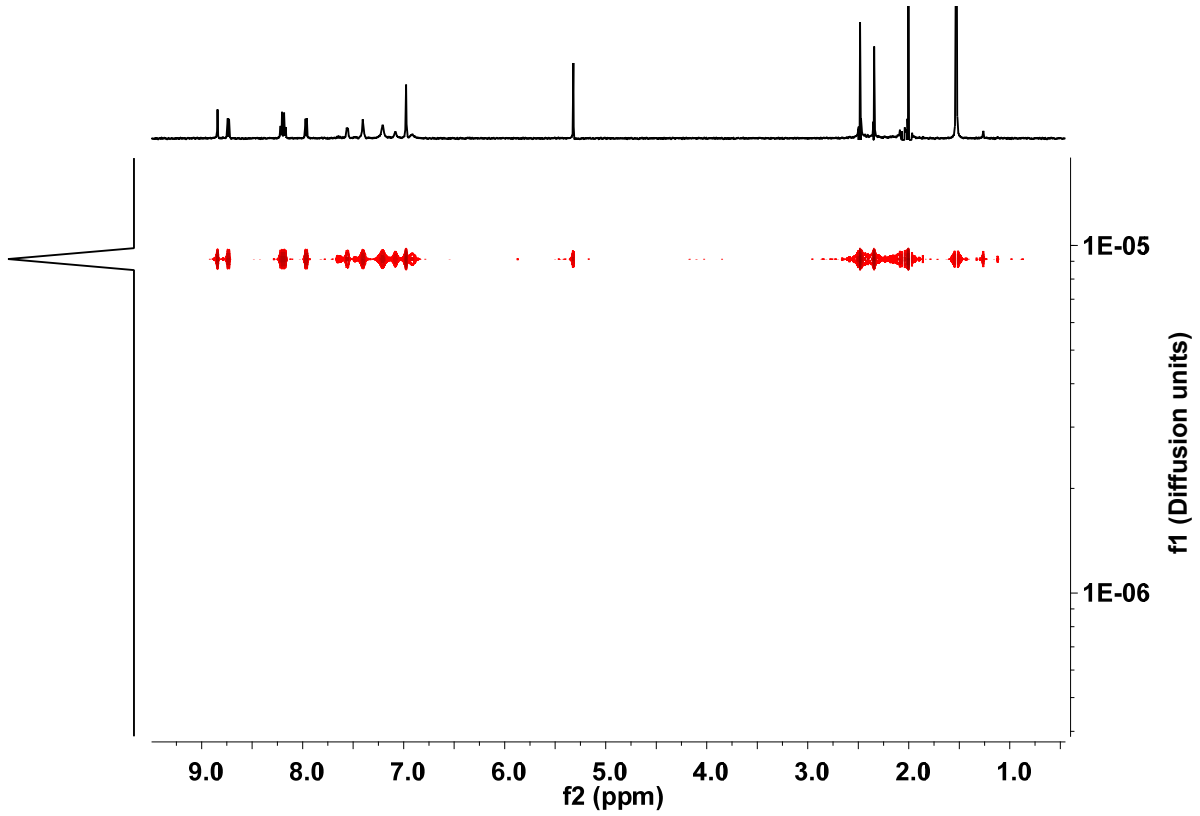

Figure S44. ^{1}H-DOSY NMR of [Cu_2(**R2**)$_2$]$^{2+}$ in CD_2Cl_2 (600 MHz, 298 K). Diffusion coefficient $D = 6.78 \times 10^{-10}$ m^2 s^{-1}, hydrodynamic radius $r = 7.8$ Å.

6. Variable temperature studies and determination of kinetic parameters

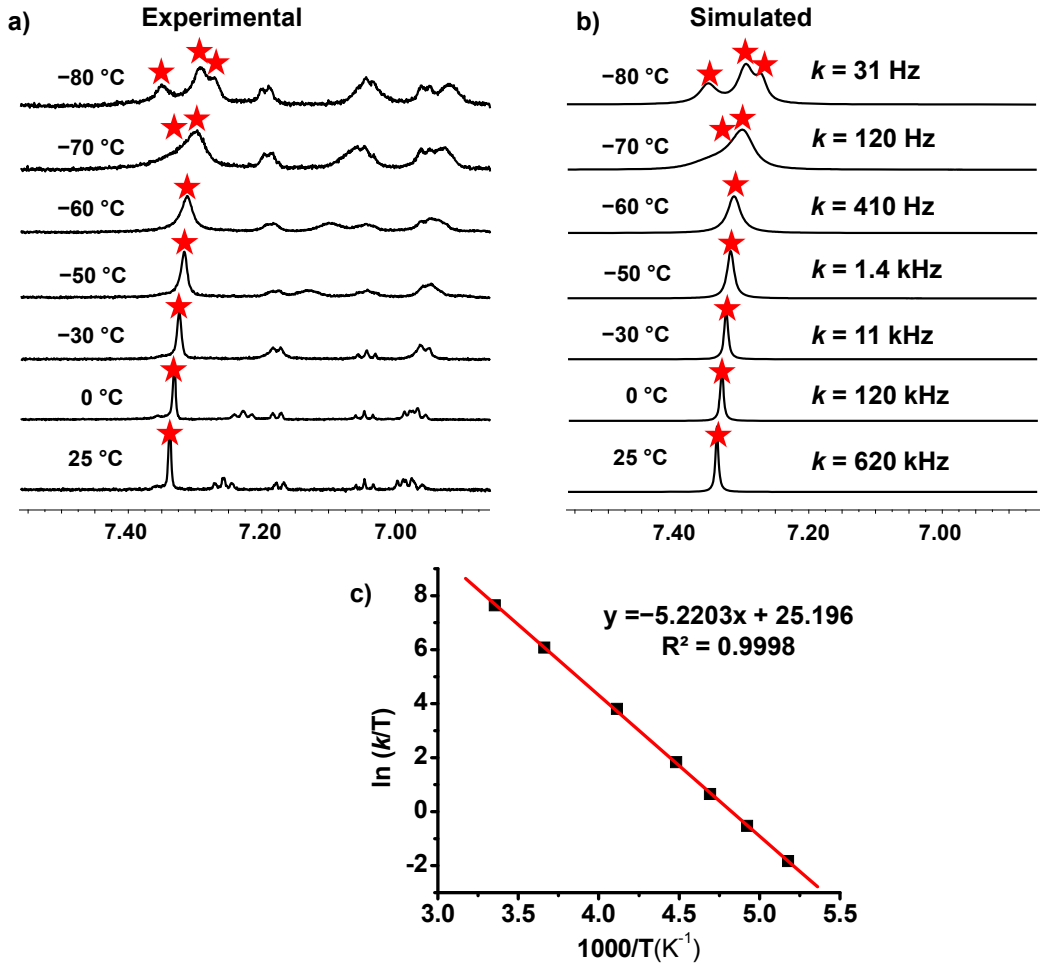

Figure S45. Partial ^{1}H VT-NMR spectra (CD_2Cl_2, 600 MHz) of [Cu(**S**)(**R1**)]$^{+}$at different temperatures showing (a) experimental, (b) theoretical splitting of m-H with corresponding rate constants. (c) Eyring plot for the rotational dynamics.

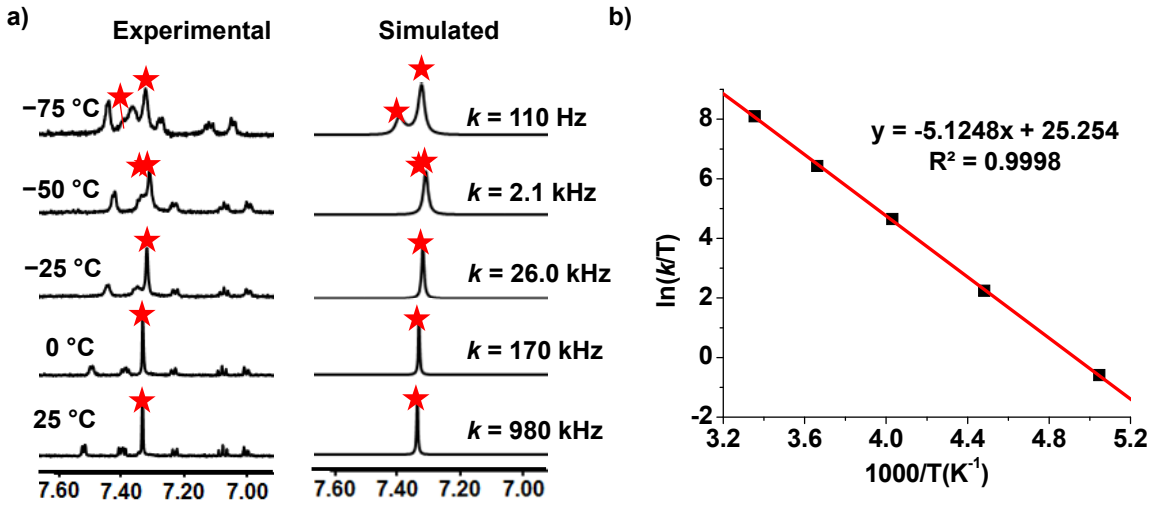

Figure S46. Partial ^{1}H VT-NMR (CD_3CN:CD_2Cl_2 (1:5), 600 MHz) of [Zn(**S**)(**R1**)]$^{2+}$ showing (a) experimental and theoretical splitting of m-H with corresponding rate constants. (b) Eyring plot for rotational dynamics in [Zn(**S**)(**R1**)]$^{2+}$.

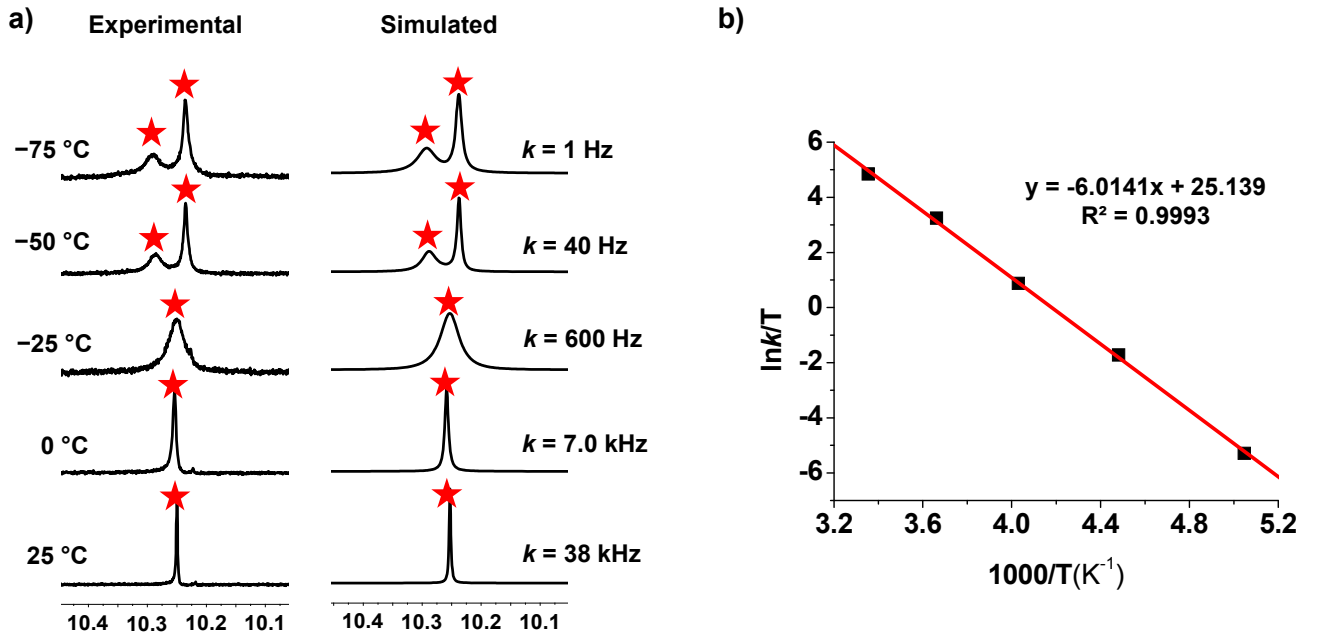

Figure S47. Partial ^{1}H VT-NMR (CD_2Cl_2, 600 MHz) of [Cu(**S**)(**R2**)]$^{+}$ showing (a) experimental and theoretical splitting of r-H with corresponding rate constants. (b) Eyring plot for rotational dynamics in [Cu (**S**)(**R2**)]$^{+}$.

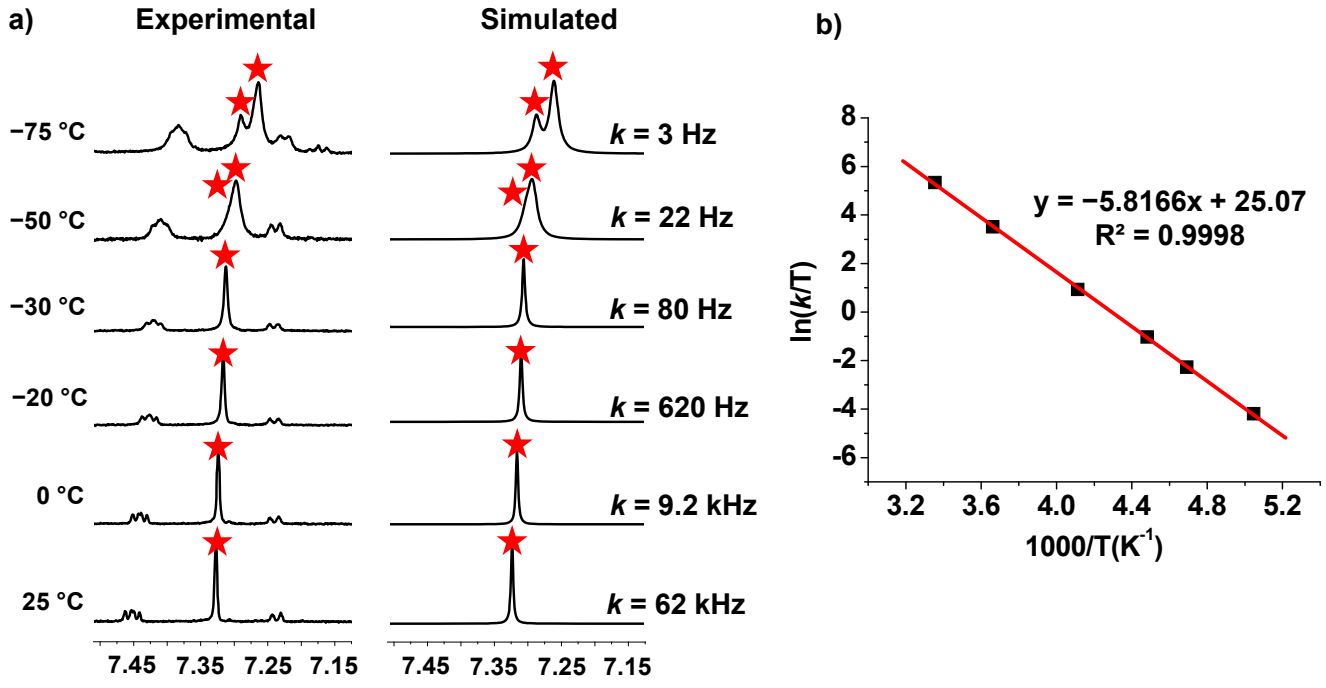

Figure S48. Partial ^{1}H VT-NMR (CD_3CN:CD_2Cl_2 (1:5), 600 MHz) of [Zn(**S**)(**R2**)]$^{2+}$ showing (a) experimental and theoretical splitting of m-H with corresponding rate constants. (b) Eyring plot for rotational dynamics in [Zn(**S**)(**R2**)]$^{2+}$.

7. Catalytic experiments

General procedure

Solid reactants were transferred to the NMR tube and dissolved in CD_2Cl_2:CD_3CN (5:1). The mixture was heated at 50 °C for 2 h and the yield of the click product (singlet at δ 5.58 ppm) and 1,4-addition product (multiplet at δ 4.86 ppm) was determined using 1,3,5-trimethoxybenzene (**14**) as an internal standard (singlet at δ 6.04 ppm).

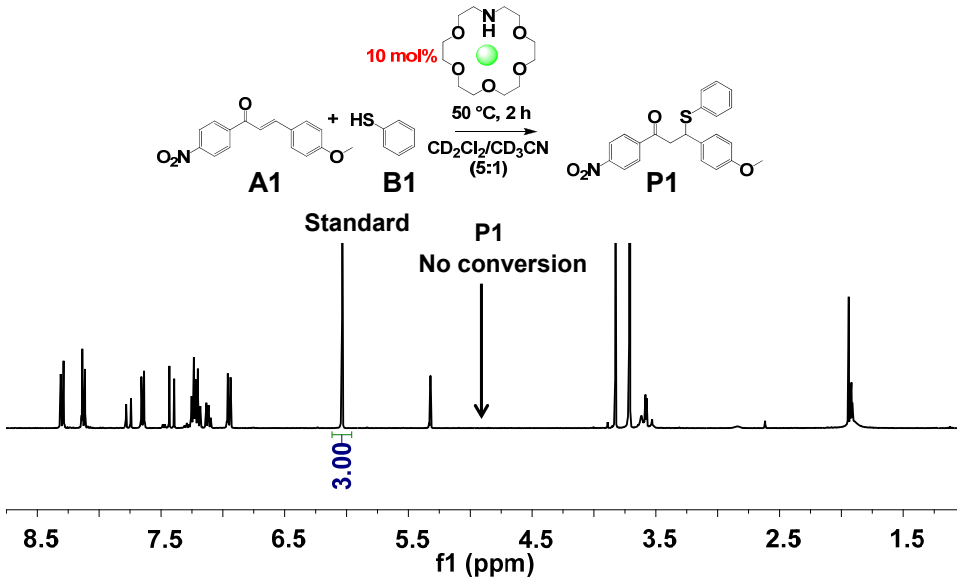

Figure S49. ^{1}H NMR (400 MHz, CD_2Cl_2:CD_3CN = 5:1, 298 K) spectrum obtained after heating the reaction mixture of **A1**, **B1**, **7** (≈ 1.92 mM), $[Cu(CH_3CN)_4]PF_6$ and standard **14** in 10:10:1:1:10 ratio at 50 °C for 2 h. No product **P1** was observed in ^{1}H NMR.

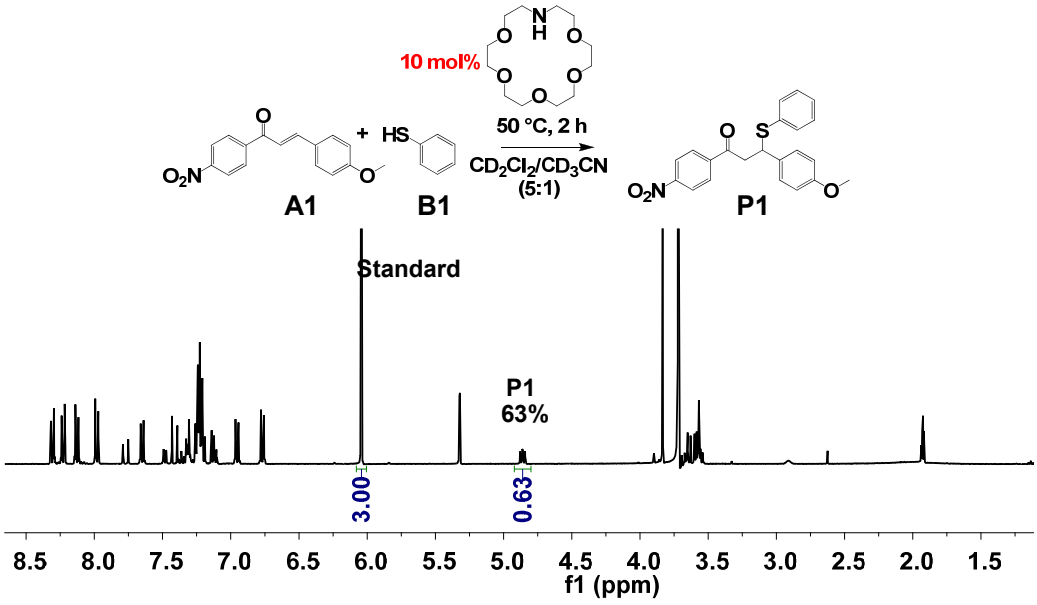

Figure S50. ^{1}H NMR (400 MHz, CD_2Cl_2:CD_3CN = 5:1, 298 K) spectrum obtained after heating the reaction mixture of **A1**, **B1**, **7** (≈ 1.92 mM), and standard **14** in 10:10:1:10 ratio at 50 °C for 2 h. The integration demonstrated that **P1** was formed in 63% yield.

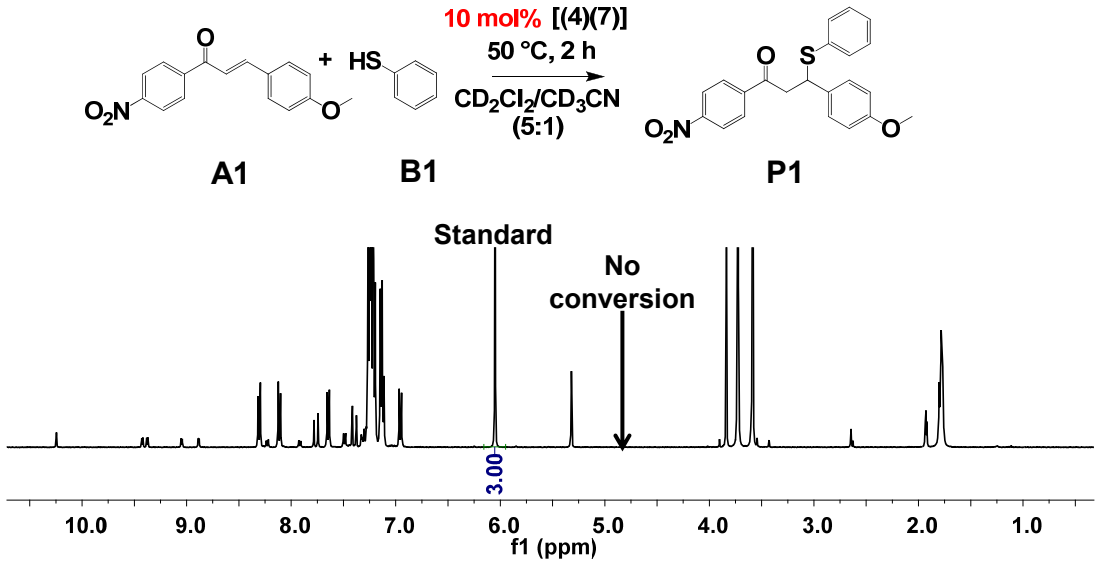

Figure S51. ^{1}H NMR (400 MHz, CD_2Cl_2:CD_3CN = 5:1, 298 K) spectrum obtained after heating the reaction mixture of **A1**, **B1**, **4**, **7** (≈ 1.92 mM), and standard **14** in 10:10:1:1:10 ratio at 50 °C for 2 h. No product was observed in ^{1}H NMR.

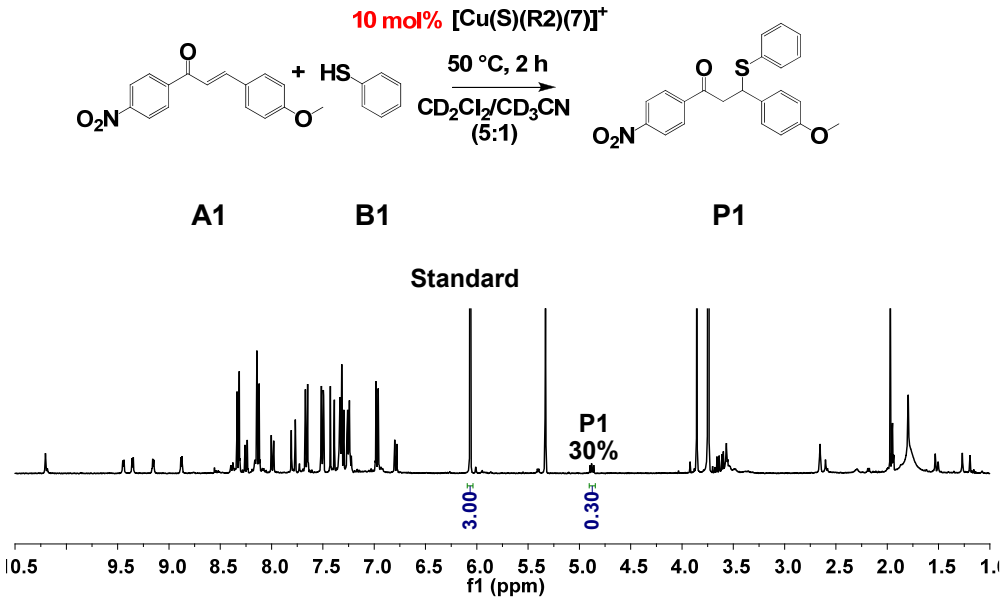

Figure S52. ^{1}H NMR (400 MHz, CD_2Cl_2:CD_3CN = 5:1, 298 K) spectrum obtained after heating the reaction mixture of **A1**, **B1**, **7** (≈ 1.92 mM), [Cu(**S**)(**R2**)]$^{+}$and standard **14** in 10:10:1:1:10 ratio at 50 °C for 2 h. The integration demonstrated that **P1** was formed in 30% yield.

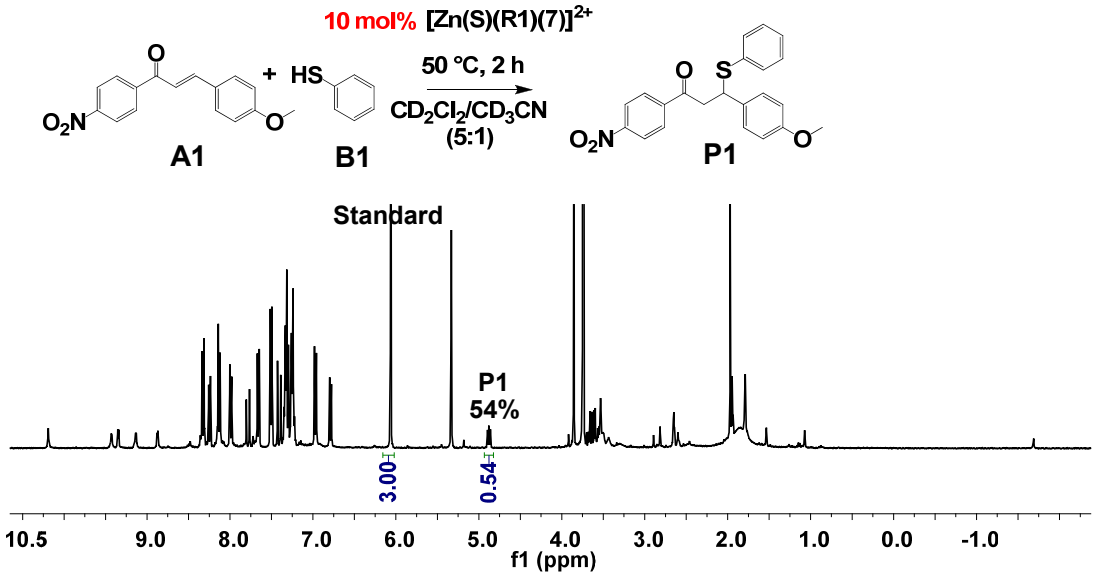

Figure S53. ^{1}H NMR (400 MHz, CD_2Cl_2:CD_3CN = 5:1, 298 K) spectrum obtained after heating the reaction mixture of **A1**, **B1**, **7** (≈ 1.92 mM), [Zn(**S**)(**R1**)]$^{2+}$and standard **14** in 10:10:1:1:10 ratio at 50 °C for 2 h. The integration demonstrated that **P1** was formed in 54% yield.

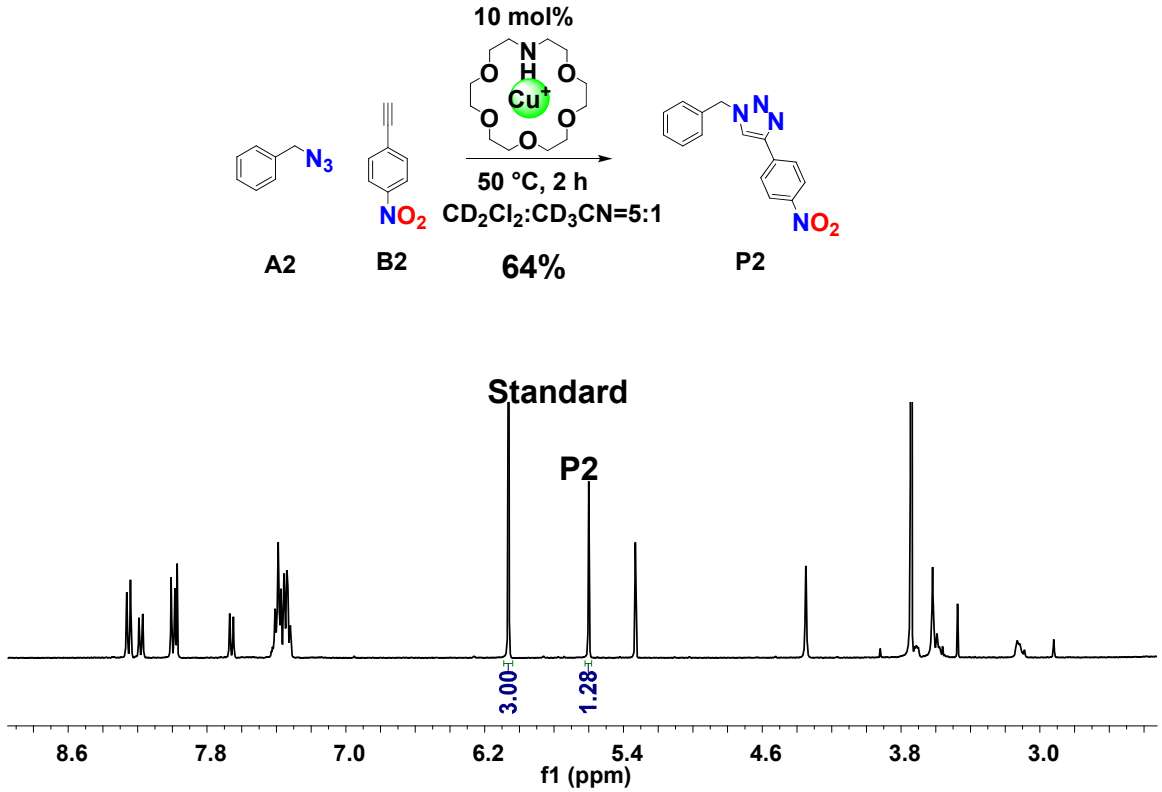

Figure S54. ^{1}H NMR (400 MHz, CD_2Cl_2:CD_3CN = 5:1, 298 K) spectrum obtained after heating the reaction mixture of **A2**, **B2**, **7** (≈ 1.92 mM), $[Cu(CH_3CN)_4]PF_6$ and standard **14** in 10:10:1:1:10 ratio at 50 °C for 2 h. The integration demonstrated that **P2** was formed in 64% yield.

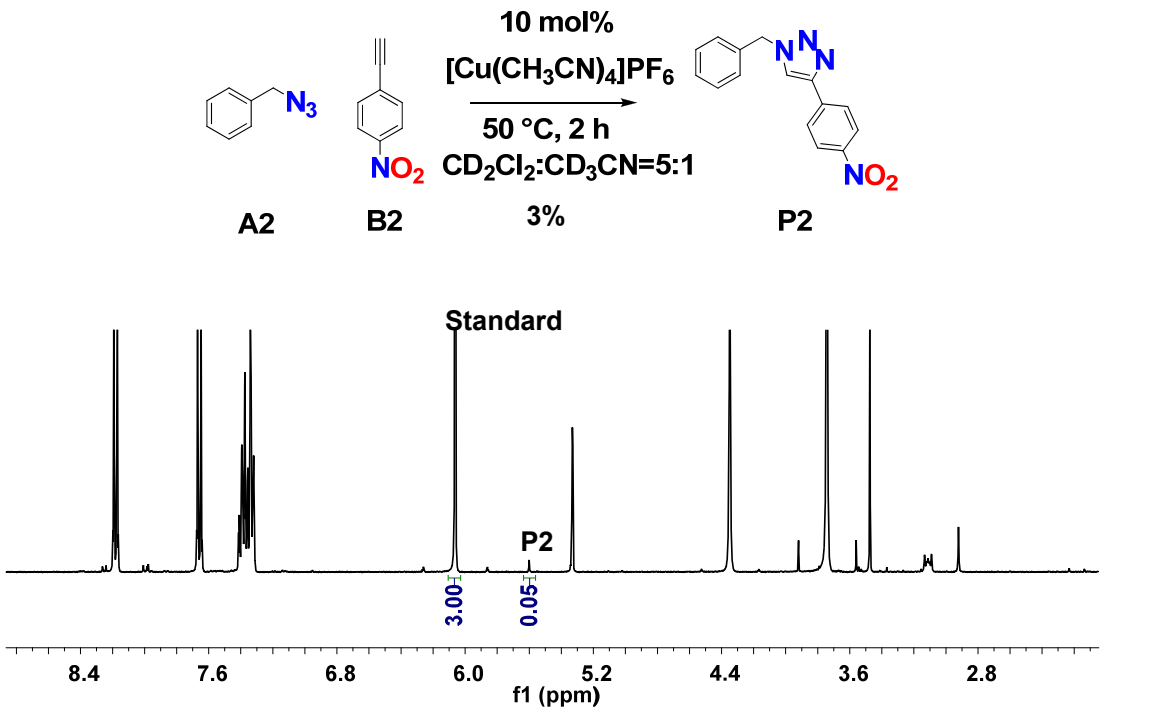

Figure S55. ^{1}H NMR (400 MHz, CD_2Cl_2:CD_3CN = 5:1, 298 K) spectrum obtained after heating the reaction mixture of **A2**, **B2**, $[Cu(CH_3CN)_4]PF_6$ (≈ 1.92 mM) and standard **14** in 10:10:1:10 ratio at 50 °C for 2 h. The integration demonstrated that only **P2** was formed in 3% yield.

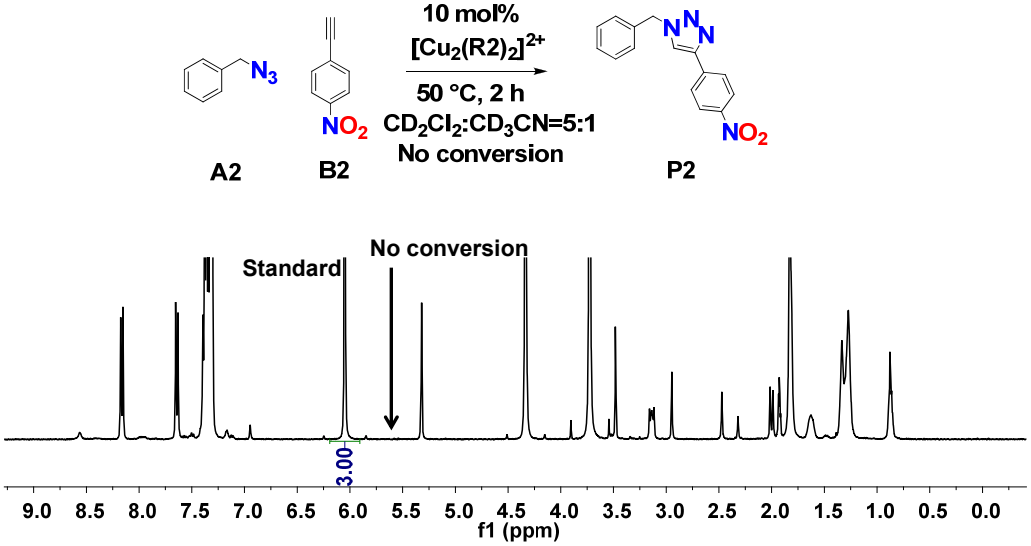

Figure S56. ^{1}H NMR (400 MHz, CD_2Cl_2:CD_3CN = 5:1, 298 K) spectrum obtained after heating the reaction mixture of **A2**, **B2**, $[Cu_2(\mathbf{R2})_2]^{2+}$ (≈ 1.92 mM) and standard **14** in 10:10:1:10 ratio at 50 °C for 2 h. No conversion was detected in ^{1}H NMR.

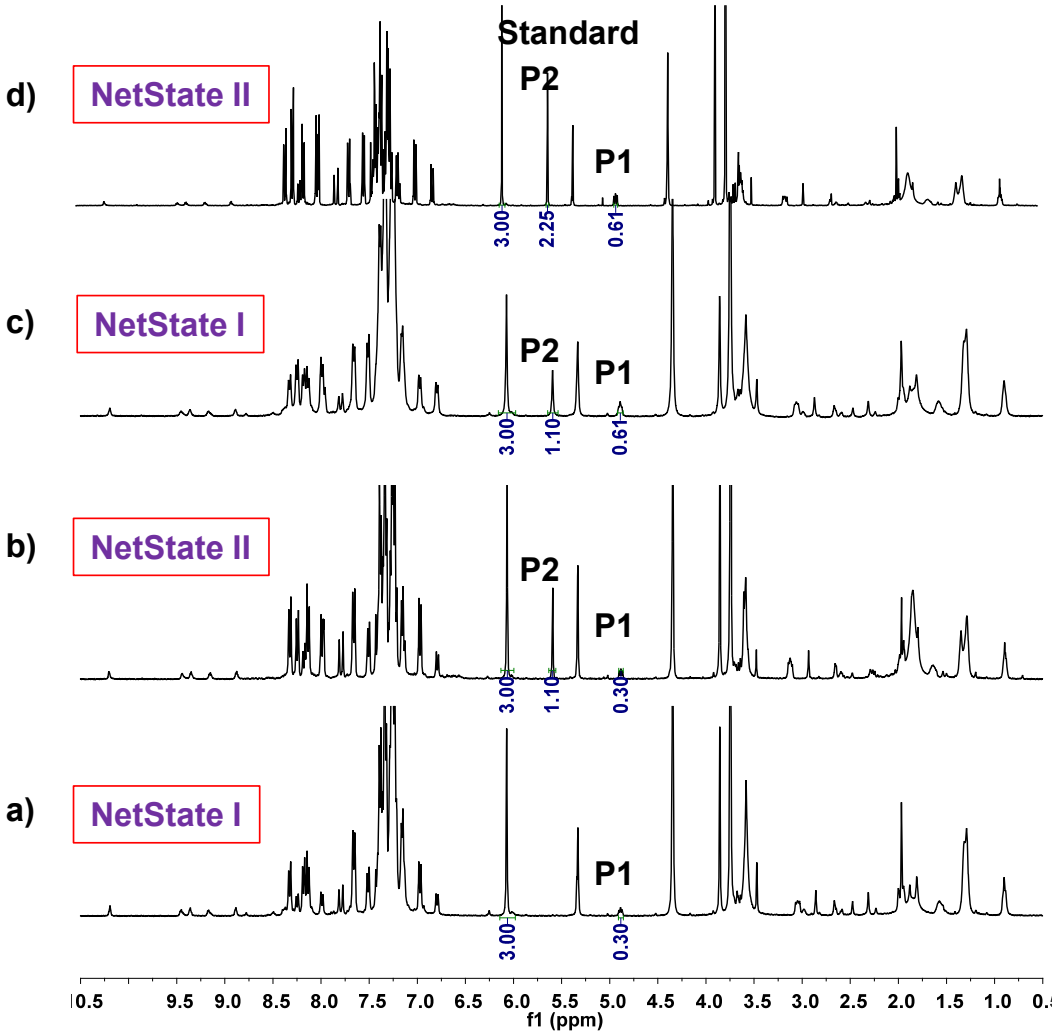

Figure S57. ^{1}H NMR (400 MHz, CD_2Cl_2:CD_3CN = 5:1, 298 K) spectrum obtained after (a) heating the reaction mixture of **A1**, **B1**, **A2**, **B2**, **7** (≈ 1.92 mM), $[Cu_2(\mathbf{R1})_2]^{2+}$, $[Cu(\mathbf{S})(\mathbf{R2})]^{+}$ and standard **14** in 20:20:20:20:2:1:2:20 ratio at 50 °C for 2 h in an NMR tube revealed 30% of 1,4 addition product **P1** was formed. (b) After addition of 1.0 equiv. of $Zn(OTf)_2$ with respect to nanorotor $[Cu(\mathbf{S})(\mathbf{R2})]^{+}$ and subsequent heating at 50 °C for 2 h, the click product **P2** was formed (yield = 55% calculated with respect to internal standard **14**). In contrast, there is no increment in the yield of **P1** observed (30%). (c) After adding 2.0 equiv. of hexacyclen with respect to nanorotor and heating at 50 °C for 2 h, 31% increase in the amount of **P1** was observed (yield = 61%), whereas no further conversion of **P2** was observed. (d) Addition of another 2.0 equiv. of $Zn(OTf)_2$ with respect to nanorotor and heating at 50 °C for 2 h resulted in an increase of the click product **P2** by 57% (total yield = 112%); no further conversion of **P1** was detected.

8. ESI-MS Spectra

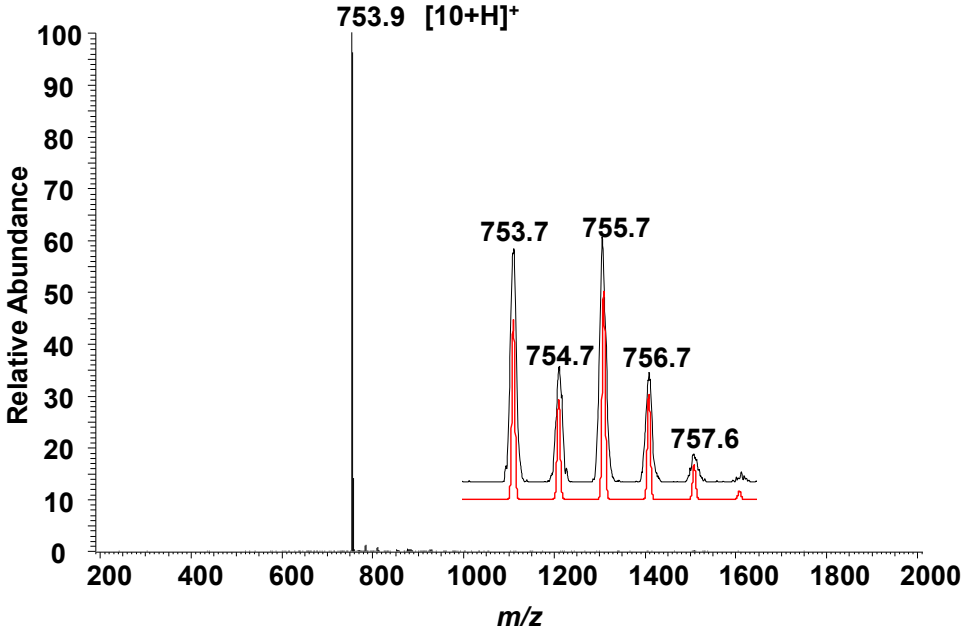

Figure S58. ESI-MS of compound **10** after protonation.

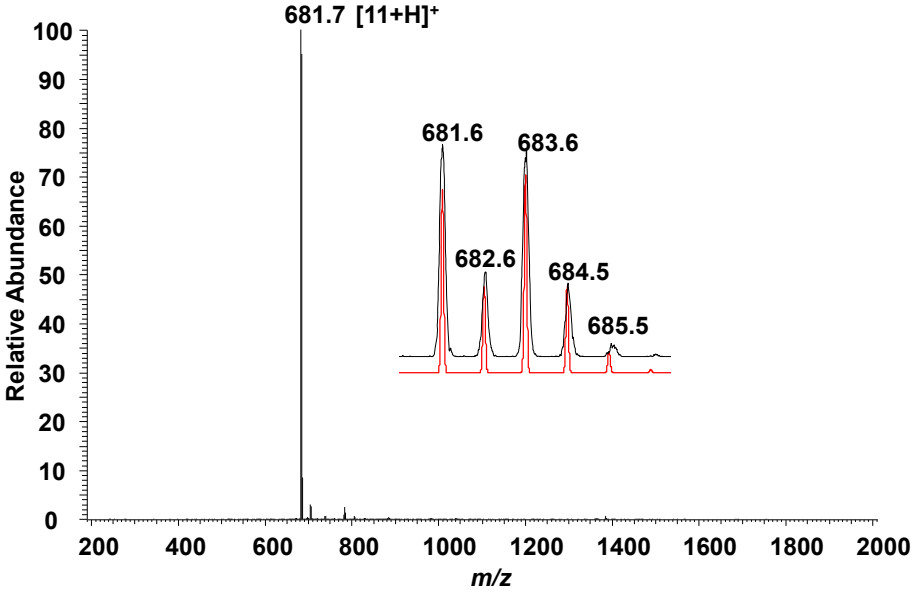

Figure S59. ESI-MS of **11** after protonation.

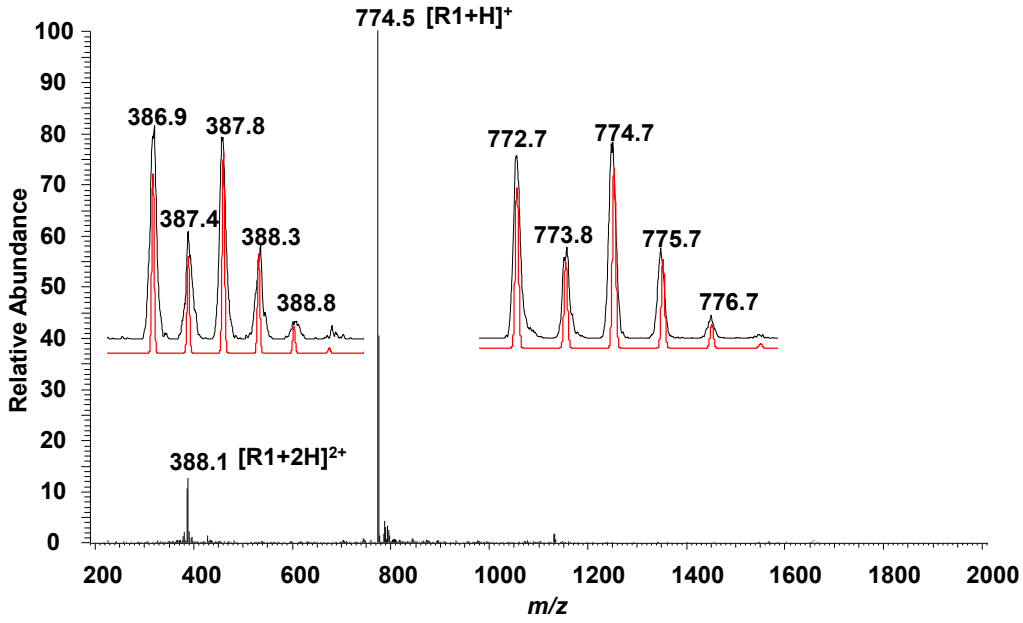

Figure S60. ESI-MS of **R1** after protonation.

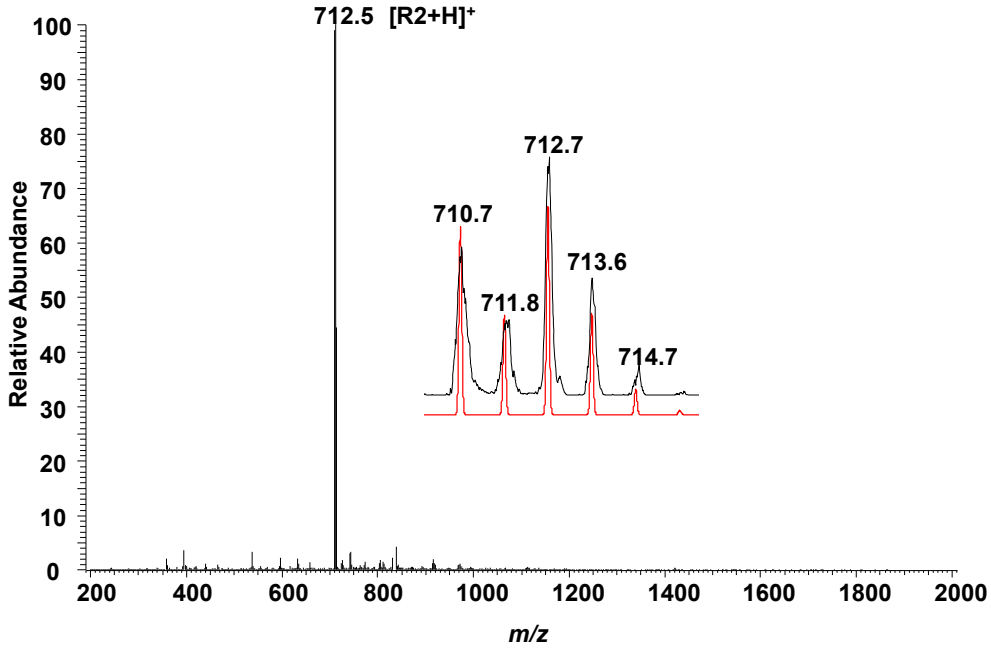

Figure S61. ESI-MS of **R2** after protonation.

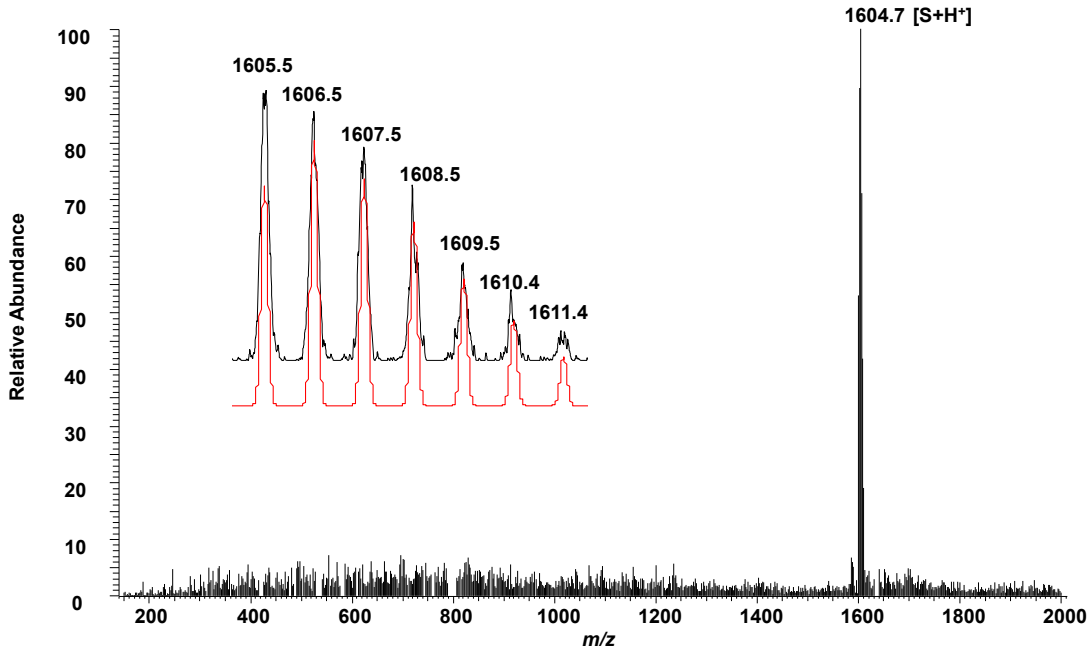

Figure S62. ESI-MS of compound **S** after protonation.

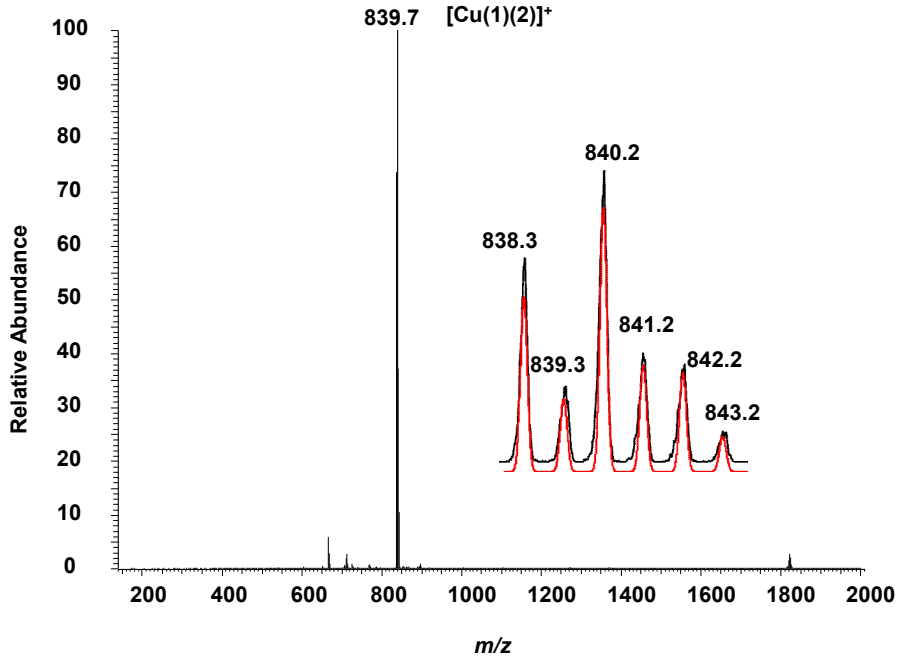

Figure S63. ESI-MS of [Cu(**1**)(**2**)]$^{+}$.

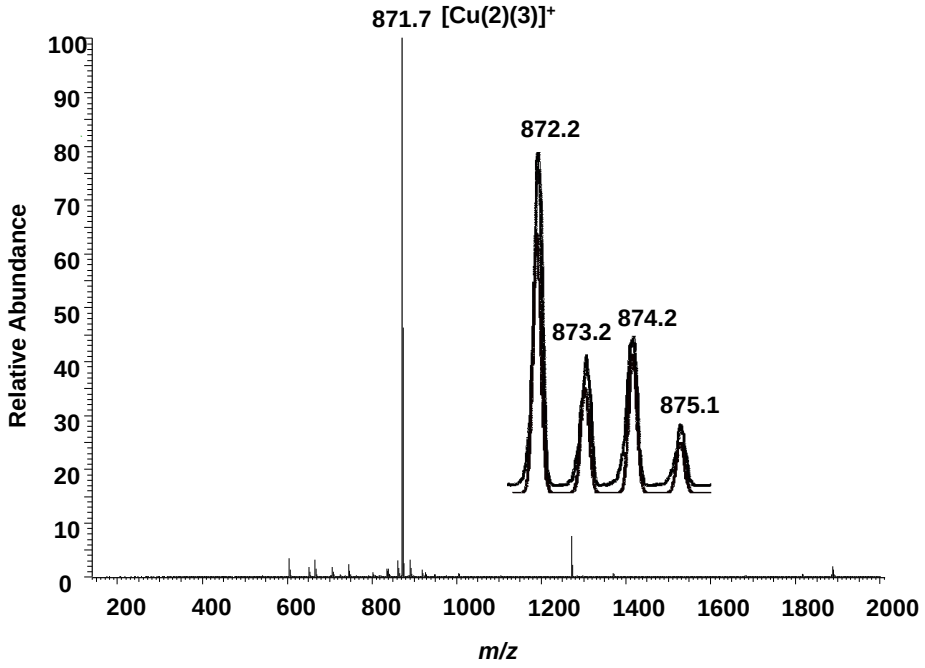

Figure S64. ESI-MS of [Cu(**2**)(**3**)]$^{+}$.

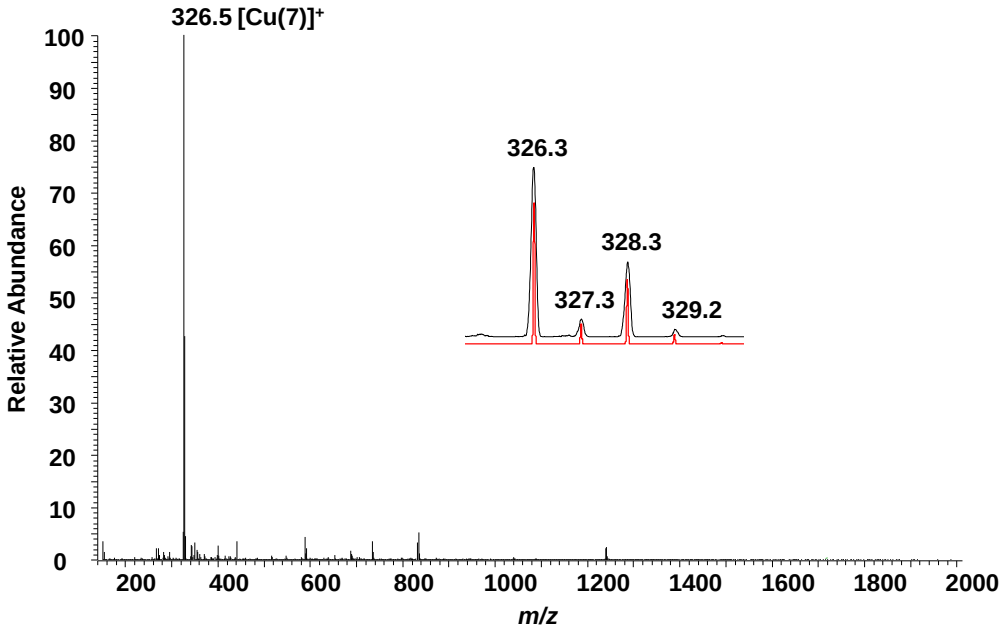

Figure S65. ESI-MS of [Cu(**7**)]$^{+}$.

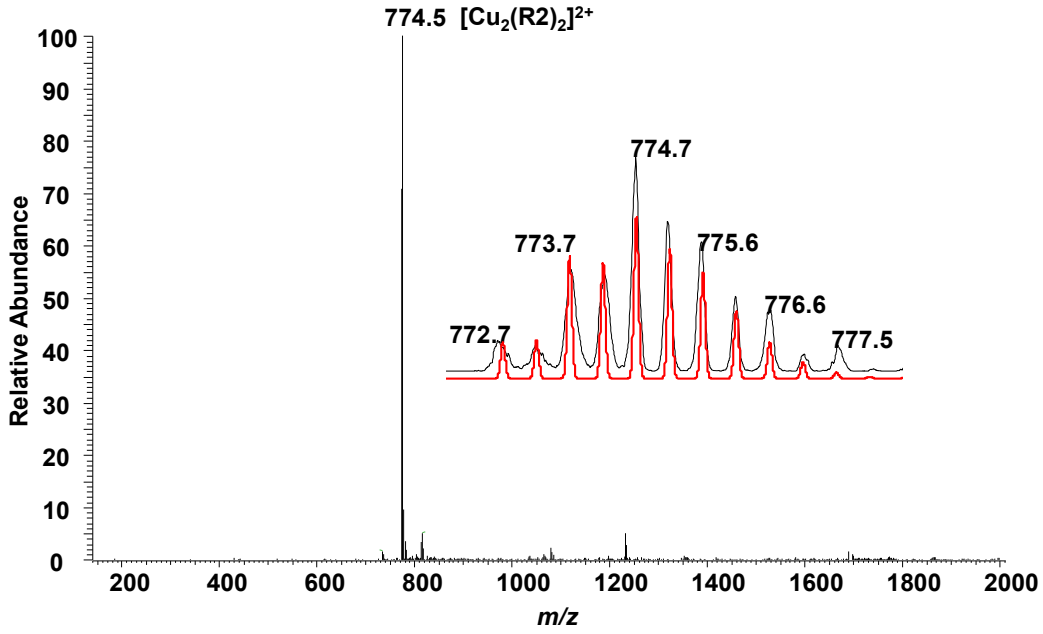

Figure S66. ESI-MS of $[Cu_2(\mathbf{R2})_2]^{2+}$.

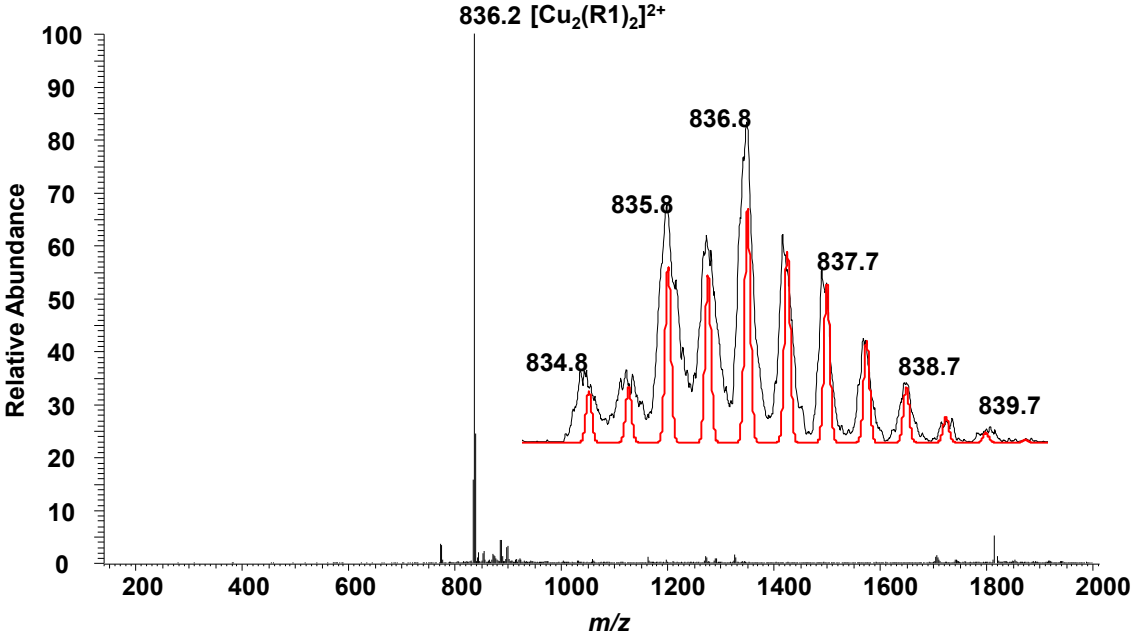

Figure S67. ESI-MS of $[Cu_2(\mathbf{R1})_2]^{2+}$.

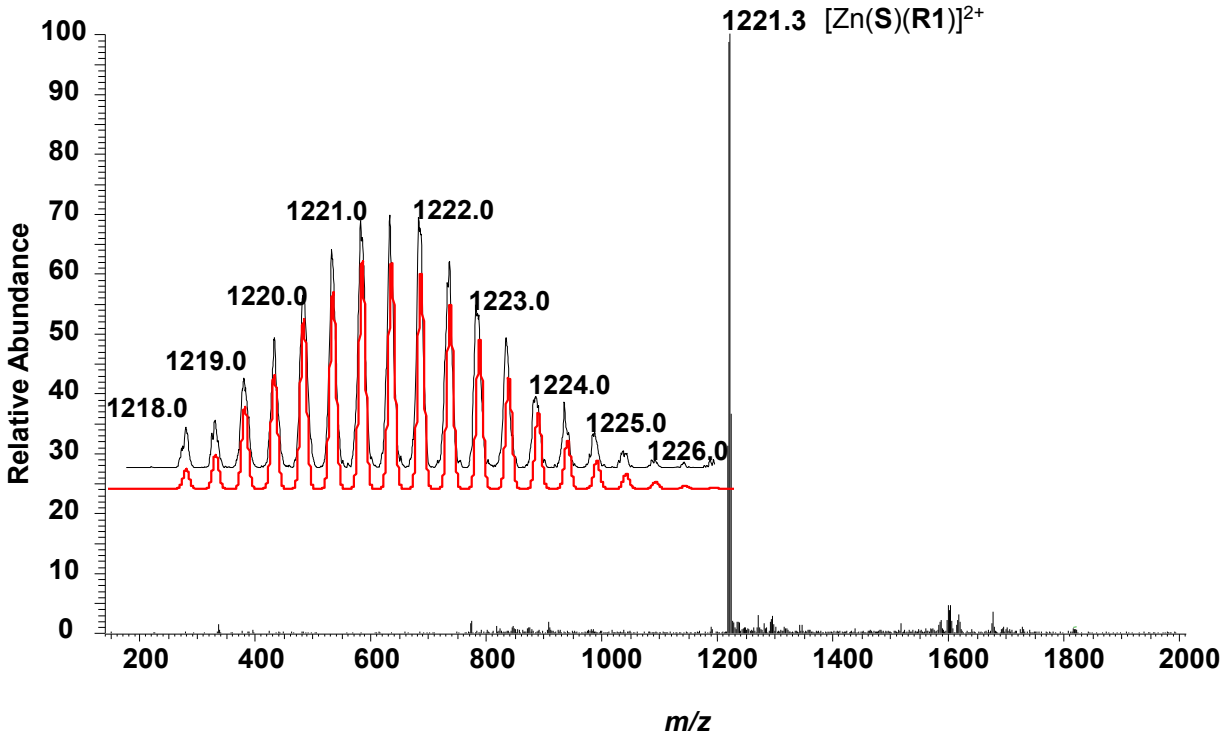

Figure S68. ESI-MS of nanorotor $[Zn(\mathbf{S})(\mathbf{R1})]^{2+}$.

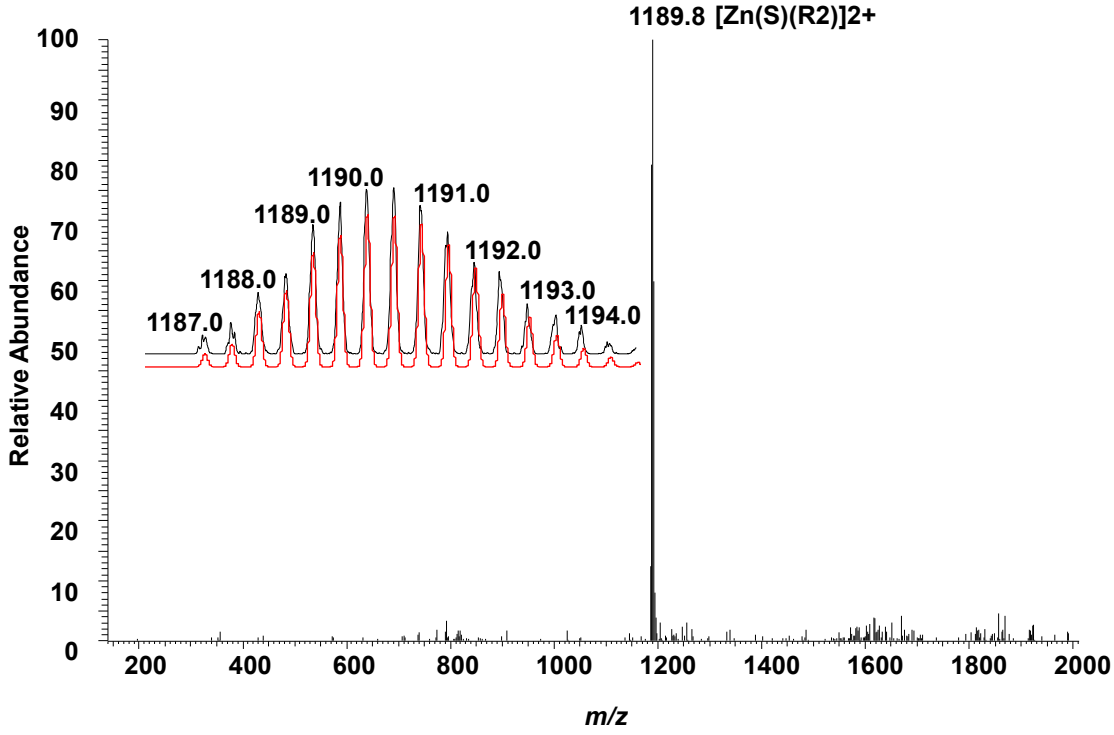

Figure S69. ESI-MS of nanorotor $[Zn(\mathbf{S})(\mathbf{R2})]^{+}$.

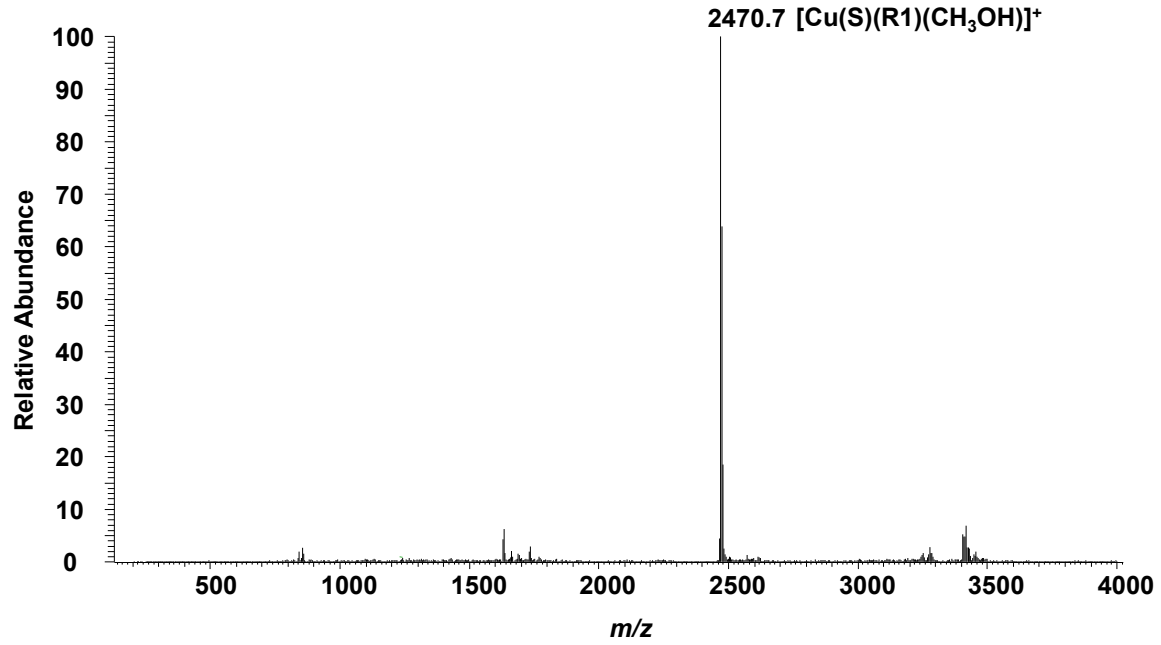

Figure S70. ESI-MS of nanorotor [Cu(**S**)(**R1**)(CH_3OH)]$^+$.

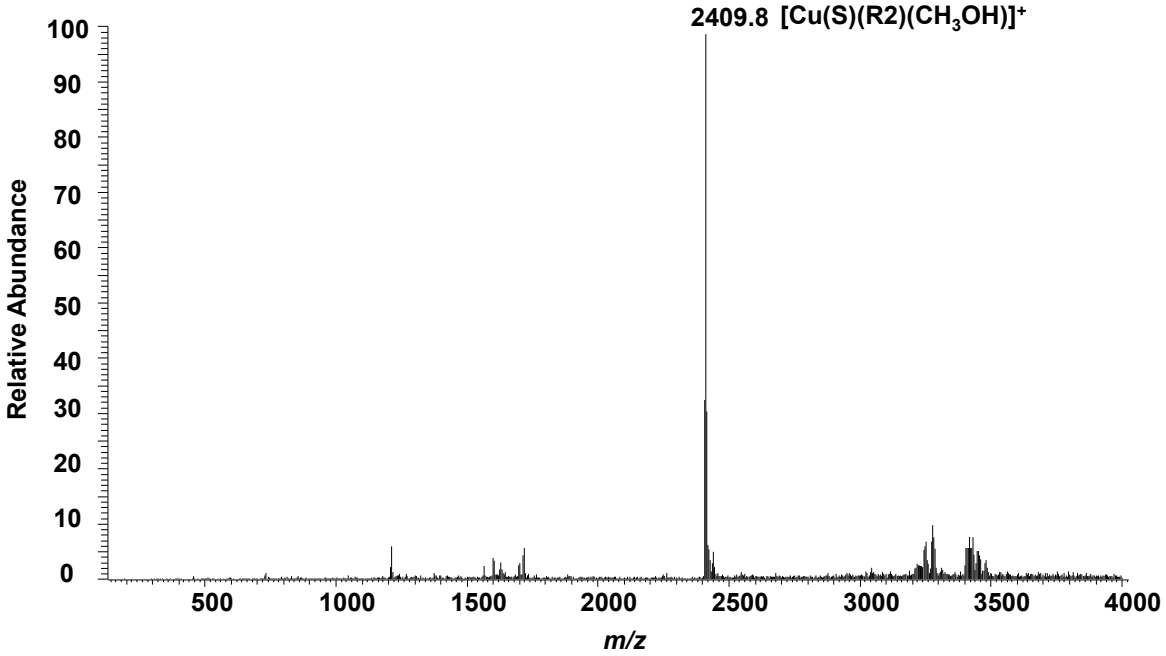

Figure S71. ESI-MS of nanorotor [Cu(**S**)(**R2**)(CH_3OH)]$^+$.

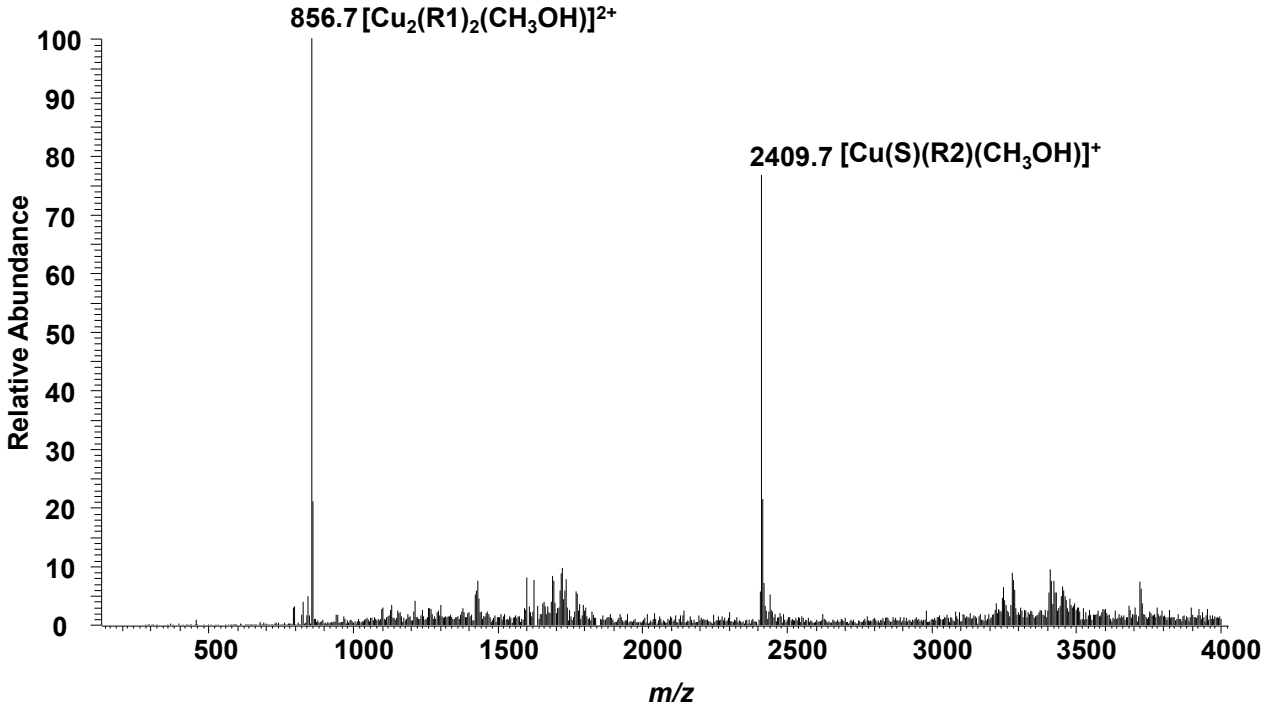

Figure S72. ESI-MS of NetState I, i.e. mixture of nanorotor [Cu(**S**)(**R2**)(CH_3OH)]$^+$ and dimer [Cu_2(**R1**)$_2$(CH_3OH)]$^{2+}$.

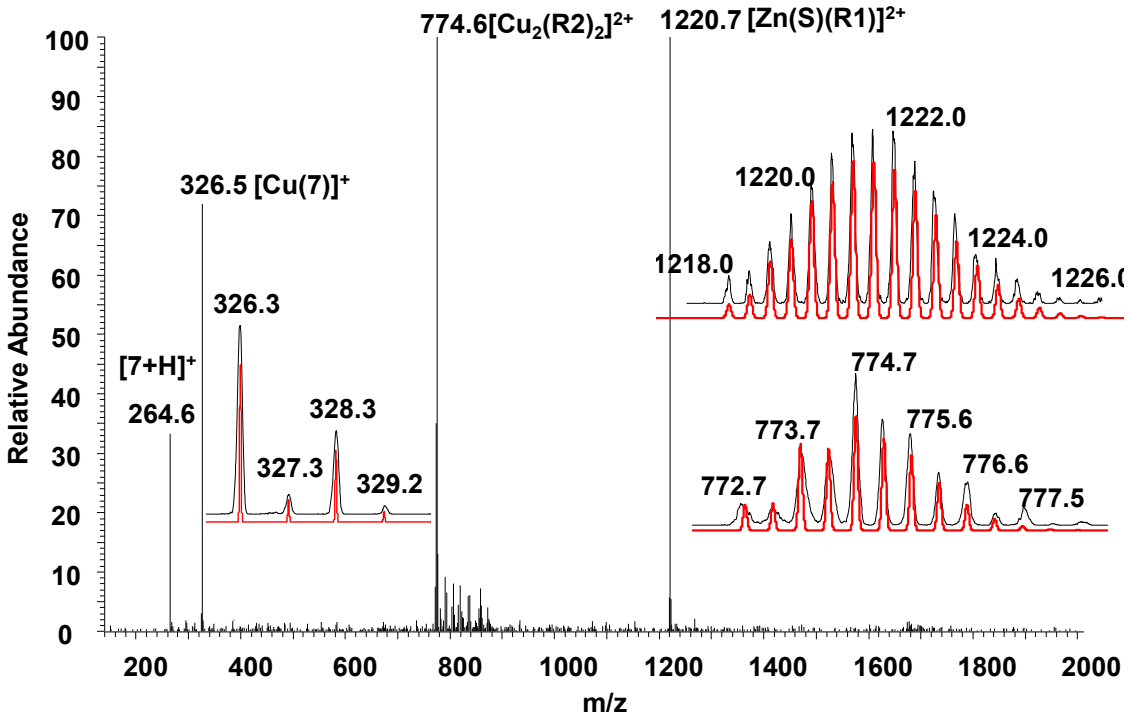

Figure S73. ESI-MS of NetState II, i.e. mixture of nanorotor [Zn(**S**)(**R1**)]$^{2+}$ and dimer [Cu_2(**R2**)$_2$]$^{2+}$.

9. UV-vis data

Measurement of binding constants

A UV-vis titration was used to measure binding constant of complex **7**→**4**

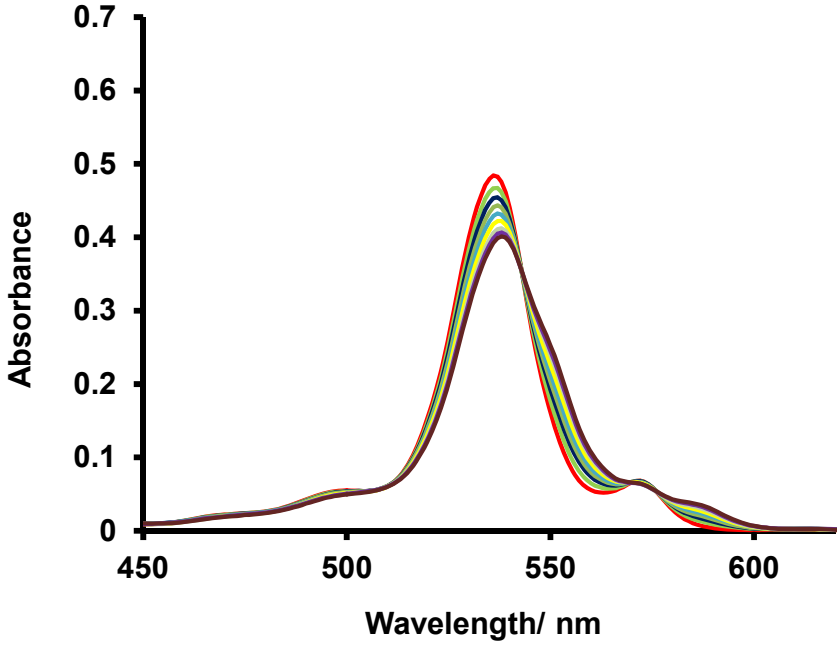

Figure S74. UV-vis titration of complex **4** (1.2×10^{-5} M) vs. **7** (1.1×10^{-3} M) in CH_2Cl_2 at 298 K. Binding constant was determined to be log $K = 5.89 \pm 0.21$ using SPECFIT software

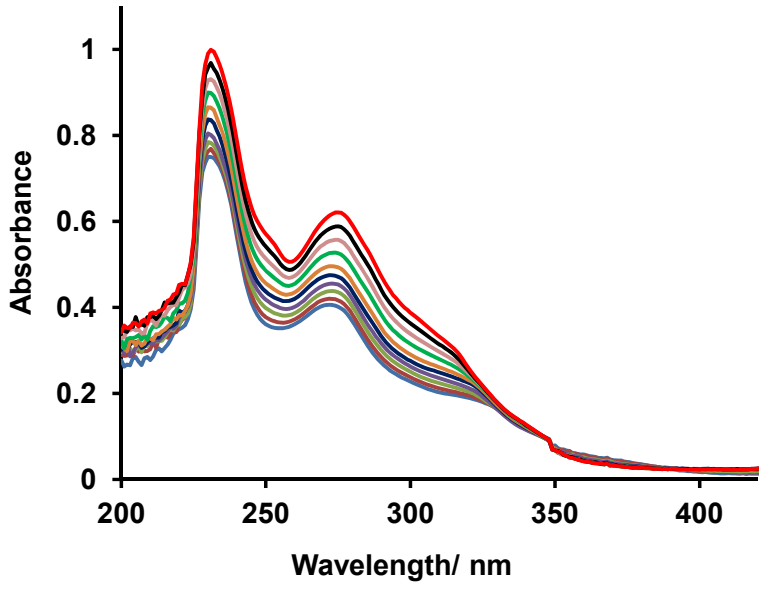

Figure S75. UV-vis titration of complex $[Cu(\mathbf{2})]^+$ (4.2×10^{-5} M) vs. **6** (2.2×10^{-3} M) in CH_2Cl_2 at 298 K. Binding constant was determined to be log $K = 4.63 \pm 0.27$ using SPECFIT software.

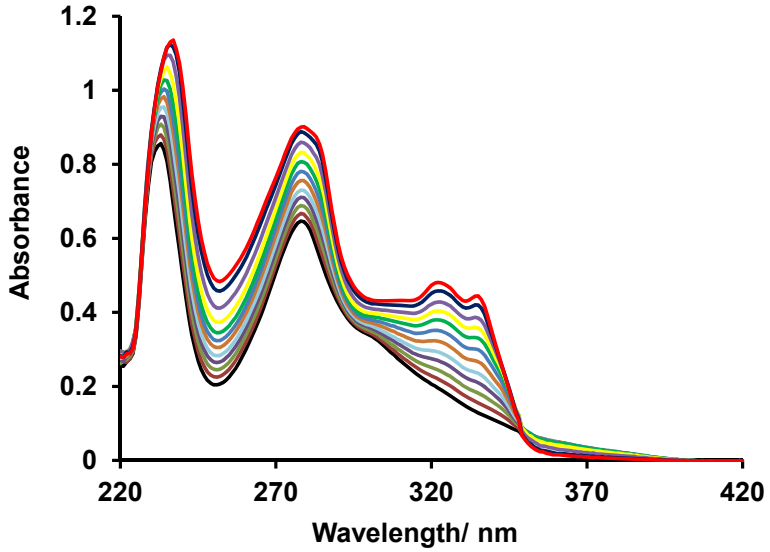

Figure S76. UV-vis titration of complex $[Zn(\mathbf{5})]^{2+}$ (7.8×10^{-5} M) vs. **6** (3.1×10^{-3} M) in CH_2Cl_2:CH_3CN (98:2) at 298 K. Binding constant was determined to be log $K = 5.26 \pm 0.18$ using SPECFIT software.

Table S1. Thermodynamic preference for NetState I

NetState I		Possible Alternate Combination I (PAC I)		Overall thermodynamic stabilization ($\Delta\log\beta$) (NetState I−PAC I)
Isolated complexation units	Thermodynamic parameters (log (β or K))	Isolated complexation units	Thermodynamic parameters (log (β or K))	
$[Cu(\mathbf{5})(\mathbf{6})]^{+}$	9.30^{6}	$[Cu(\mathbf{2})(\mathbf{6})]^{+}$	$5.64^{8}+4.63^{a}=10.27$	$2^{b} \times (17.79-16.19)$
3•4	4.31^{4}	**1•4**	2.72^{4}	$= 2 \times (1.6) = 3.2$
$[Cu(\mathbf{1})(\mathbf{2})]^{+}$	4.18^{7}	$[Cu(\mathbf{3})(\mathbf{5})]^{+}$	3.20^{9}	

a) see Figure S74. b) The factor 2 is dictated by the stoichiometric use of $[Cu_2(\mathbf{R1},\mathbf{R2})]^{2+}$.

Table S2. Thermodynamic preference for NetState II

NetState II		Possible alternate combination II (PAC II)		Overall thermodynamic stabilization ($\Delta\log\beta$) (NetState II−PAC II)
Isolated complexation units	Thermodynamic parameters (log (β or K))	Isolated complexation units	Thermodynamic parameters (log (β or K))	
$[Zn(\mathbf{2})(\mathbf{6})]^{2+}$	15.1^{10}	$[Zn(\mathbf{5})(\mathbf{6})]^{2+}$	$4.58^{11}+5.26^{b}=9.84$	$2^{b} \times (21.02-18.33)$
1•4	2.72^{4}	**3•4**	4.31^{4}	$= 2 \times (2.69) = 5.38$
$[Cu(\mathbf{3})(\mathbf{5})]^{+}$	3.20^{9}	$[Cu(\mathbf{1})(\mathbf{2})]^{+}$	4.18^{6}	

b) see Figure S75. b) The factor 2 is dictated by the stoichiometric use of $[Cu_2(\mathbf{R1},\mathbf{R2})]^{2+}$.

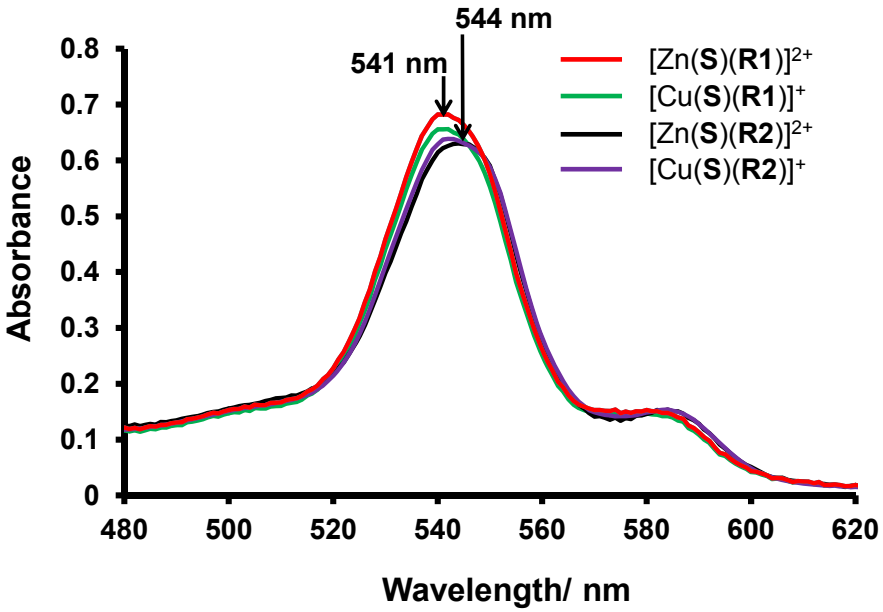

Figure S77. UV-vis spectra of nanorotor $[Zn(\mathbf{S})(\mathbf{R1})]^{2+}$, $[Cu(\mathbf{S})(\mathbf{R1})]^{+}$, $[Zn(\mathbf{S})(\mathbf{R2})]^{2+}$ and $[Cu(\mathbf{S})(\mathbf{R2})]^{+}$ (10^{-5} M).

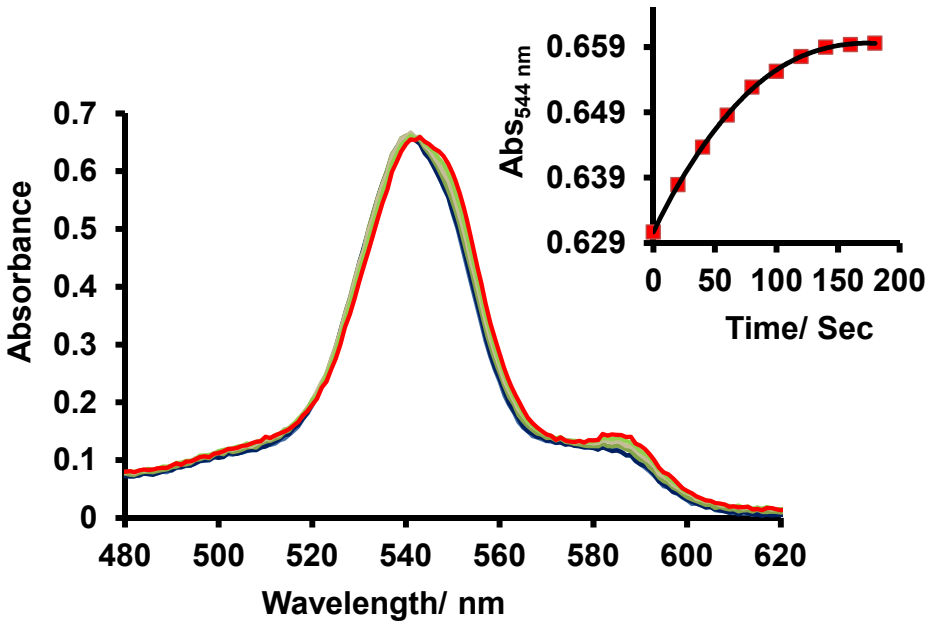

Figure S78. UV−vis spectra of the reaction between $[Cu(\mathbf{S})(\mathbf{R1})]^{+}$ and $[Cu_2(\mathbf{R2})_2]^{2+}$ (1.2×10^{-5} M) at 298 K in CH2Cl2 indicating formation of $[Cu(\mathbf{S})(\mathbf{R2})]^{+}$ (and indirectly of $[Cu_2(\mathbf{R1})_2]^{2+}$) with time. Inset: Change of absorbance at λ = 544 nm with time.

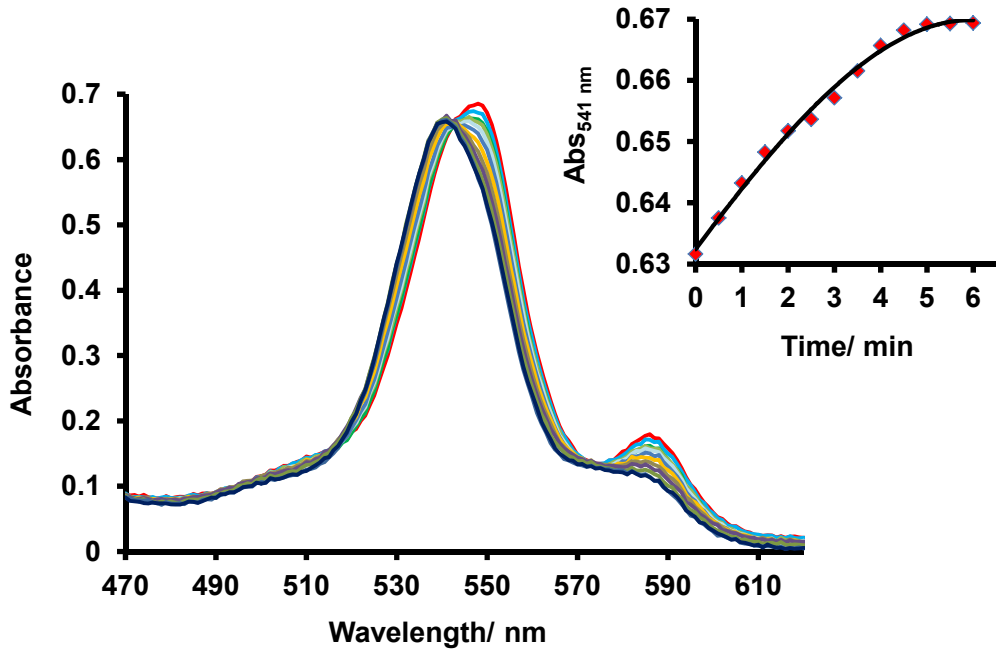

Figure S79. UV-vis spectra after addition of zinc(II) ions to the NetState I ($[Cu(\mathbf{S})(\mathbf{R2})]^{+}$ and $[Cu_2(\mathbf{R1})_2]^{2+}$) ($1.2 \times 10^{-5}$ M) at 298 K in CH_2Cl_2 indicating formation of $[Zn(\mathbf{S})(\mathbf{R1})]^{2+}$ (and indirectly of NetState II) with time. Inset: Change of absorbance at λ = 541 nm with time.

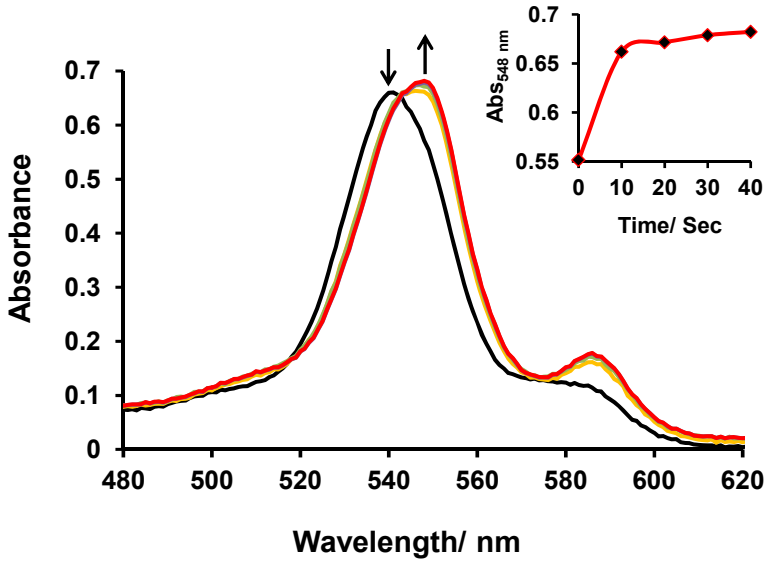

Figure S80. UV-vis spectra after addition of one equivalent of hexacyclen to NetState II (= $[Zn(\mathbf{S})(\mathbf{R1})]^{2+}$ and $[Cu_2(\mathbf{R2})_2]^{2+}$) ($1.2 \times 10^{-5}$ M) at 298 K in CH_2Cl_2 indicating formation of $[Cu(\mathbf{S})(\mathbf{R2})]^{+}$ (and indirectly of NetState I) with time. Inset: Change of absorbance at λ = 548 nm with time.

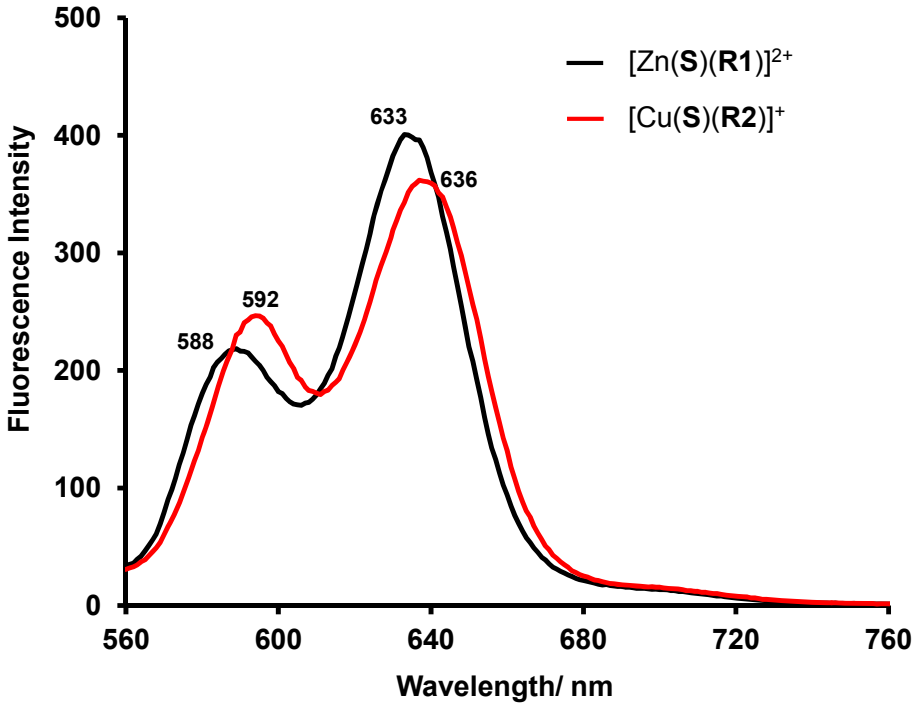

Figure S81. Fluorescence spectra of $[Zn(\mathbf{S})(\mathbf{R1})]^{2+}$ and $[Cu(\mathbf{S})(\mathbf{R2})]^{+}$ (2.3×10^{-5} M in CD_2Cl_2: CD_3CN (5:1), excitation wavelength: 540 nm).

10. References

(1) Goswami, A.; Paul, I.; Schmittel, M. *Chem. Commun.* **2017**, *53*, 5186−5189.

(2) Gaikwad, S.; Goswami, A.; De, S.; Schmittel, M. *Angew. Chem. Int. Ed.* **2016**, *55*, 10512 – 10517.

(3) Walter, K. A.; Kim, Y. J.; Hupp, J. T. *Inorg. Chem.* **2002**, *41*, 2909.

(4) Paul, I.; Goswami, A.; Mittal, N.; Schmittel, M. *Angew. Chem., Int. Ed.* **2018**, *57*, 354−358.

(59 Schmittel, M.; Michel, C.; Wiegrefe, A.; Kalsani, V. *Synthesis,* **2001**, 1561 – 1567.

(6) Schmittel, M.; Kalsani, V.; Kishore, R. S. K.; Cölfen, H.; Bats, J. W. *J. Am. Chem. Soc.* **2005**, *127*, 11544−11545.

(7) Ghosh, A.; Paul, I.; Saha, S.; Paululat, T.; Schmittel M. *Org. Lett.* **2018**, *20*, 7973−7976.

(8) Paul, I.; Samanta, D.; Gaikwad, S.; Schmittel, M. *Beilstein J. Org. Chem.* **2019**, *15*, 1371–1378.

(9) Samanta, S. K.; Schmittel, M. *J. Am. Chem. Soc.* **2013**, *135*, 18794−18797.

(10) Samanta, D.; Paul, I.; Schmittel, M. *Chem. Commun*. **2017**, *53*, 9709−9712.

(11) Özer, M. S.; Paul, I.; Goswami, A.; Schmittel, M. *Dalton Trans*., **2019**,*48*, 9043-9047.